

A standard protocol for describing individual-based and agent-based models

Online Appendix

Volker Grimm, Uta Berger, Finn Bastiansen, Sigrunn Eliassen, Vincent Ginot, Jarl Giske, John Goss-Custard, Tamara Grand, Simone K. Heinz, Geir Huse, Andreas Huth, Jane U. Jepsen, Christian Jørgensen, Wolf M. Mooij, Birgit Müller, Guy Pe'er, Cyril Piou, Steven F. Railsback, Andrew M. Robbins, Martha M. Robbins, Eva Rossmannith, Nadja Rüger, Espen Strand, Sami Souissi, Richard Stillman, Rune Vabø, Ute Visser, Donald L. DeAngelis

This document contains test applications of the ODD protocol. Most tests are based on existing published model descriptions, but some are part of work-in-progress. The examples demonstrate both, the power of the protocol to make model descriptions more similar, and the fact that at the level of the single elements of the protocol still a large variety of styles exists.

At this stage we do not want to suggest specific and detailed formats for describing the elements themselves, but some of the solutions presented in this document seem more appropriate than others. We therefore briefly comment some of the applications.

Please note also that none of the test applications provides the dual representation of the element “Submodels”, i.e. first a mathematical “skeleton”, and then a full description including detailed comments and background information.

If you want to cite any material in this Appendix, please cite both the article about ODD, and the original work listed at the beginning of each example. For the examples presenting work in progress, please contact the corresponding authors. To save space, the references cited in the examples are not included in this appendix; they can be found in the original work for each model.

April 15, 2006

Contents

Overview of Figures.....	III
Overview of Tables.....	III
Example Gorillas.....	5
Example Fish Life History	13
Example Florida Snail Kite	23
Example Vertical Migration of Cod.....	28
Example Migration of Fish	36
Example Shore Birds I	46
Example Shore Birds II.....	55
Example Search Behaviour of Fish.....	69
Example Copepods.....	75
Example Colorado pikeminnow	82
Example Mangroves.....	97
Example Mangrove Crab Movement	103
Example Mosquitofish	110
Example Biological Control.....	117
Example Species-rich Forest I.....	123
Example Species-rich Forest II	133
Example Range Management.....	136
Example Epidemiology	148
Example Lesser Spotted Woodpecker.....	155

Overview of Figures

Gorillas: Flowchart for the agent-based model.	12
Fish life history: Schematic overview over a life-history energy allocation	22
Vertical migration of cod: Flowchart.	34
Vertical migration of cod: The neural network design.....	35
Migration of fish: Flowchart of the daily activities of the fish.....	42
Migration of fish: Temperature (°C) distribution.....	43
Migration of fish: Zooplankton distribution (x10 ¹³ cell-1).....	43
Migration of fish: Distribution of daily predation risk.....	44
Migration of fish: Description of the Artificial Neural Network..	44
Migration of fish: Example of recombination and creation of new individuals.....	45
Shore birds I: Flowchart.....	54
Shore birds II: The sequence of events during each time step.....	60
Shore birds II: How uncertainty is incorporated into the model.....	65
Copepods: Schematic representation of life cycle.	76
Copepods: An example of building a task with primitives.	79
Colorado pikeminnow: Flow diagram of model processes.	86
Mangroves: Scheme of the KiWi model.....	98
Mosquitofish: Relationship between water temperature and growth.	116
Biological control: Population density of adult hosts and parasitoids.....	121
Biological control: Snapshot of a virtual landscape..	121
Range management: Causal diagram.....	139
Epidemiology: Model area.....	150

Overview of Tables

Gorillas: Summary of the input parameters..	10
Gorillas: Summary of input probabilities.....	11
Fish life history: Parameters used for Northeast Arctic cod (<i>Gadus morhua</i>).....	21
Vertical migration of cod: Bioenergetic equations used in the model.	33
Migration of fish: Parameters.....	42
Shore birds II: State variables.	56
Shore birds II: Basic set of parameter values and submodels.....	61
Seach behaviour of fish: Simulation settings and general parameters.....	74

Copepods: List of attributes used to define the life cycle.	77
Copepods: List of the tasks used to develop the life cycle.	77
Copepods: Definition of the tasks used to develop the life cycle.	80
Colorado pikeminnow: Habitat and fish state variables.	84
Colorado pikeminnow: Initial values of variables and initialization dates.	88
Colorado pikeminnow: Parameter values and descriptions.	95
Colorado pikeminnow: Internal model variables and descriptions.	95
Mangroves: Species-specific parameters used in the KiWi model.	101
Mangrove crab movement: Parameters.	107
Mangrove crab movement: Input parameters to test the Null sub-models	108
Mangrove crab movement: Input parameters to test the FRN and FON sub-models	108
Mosquitofish: State variables and processes.	114
Mosquitofish: Parameter values.	115
Biological control: Parameters for the first and the second landscape scenario.	120
Biological control: Values of population model parameters.	121
Species-rich forest I: Variables of FORMIND2.3.	Fehler! Textmarke nicht definiert.
Species-rich forest I: Parameters of FORMIND2.3	Fehler! Textmarke nicht definiert.
Range management: Full set of state variables in the model.	137
Range management: Rainfall classes.	140
Range management: Rain use efficiencies.	140
Range management: Classification of perennial ground cover.	140
Range management: Overview about the four compared strategies.	142
Range management: Actions for insufficient biomass.	142
Range management: Formulas to calculate the portion of fodder required.	144
Range management: Adjustment of perennial ground cover.	146
Range management: List of parameters for sensitivity analysis.	147
Epidemiology: Average temperatures from the city of Zürich.	152
Lesser spotted woodpecker: Default parameter set.	158

Example Gorillas

The original model description, including the full references, is in:

Robbins MM, Robbins AM (2004) Model of population dynamics and social structure of the Virunga mountain gorillas. American Journal of Primatology 63:201-233

Abstract: An agent-based model was developed to simulate the growth rate, age structure, and social system of the endangered mountain gorillas (*Gorilla beringei beringei*) in the Virunga Volcanoes region. The model was used to compare two types of data: 1) estimates of the overall population size, age structure, and social structure, as measured by six censuses of the entire region that were conducted in 1971–2000; and 2) information about birth rates, mortality rates, dispersal patterns, and other life history events, as measured from three to five habituated research groups since 1967. On the basis of the research-group data, the “base simulation” predicted a higher growth rate than that observed from the census data (3% vs. 1%). This was as expected, because the research groups have indeed grown faster than the overall population. Additional simulations suggested that the research groups primarily have a lower mortality rate, rather than higher birth rates, compared to the overall population. Predictions from the base simulation generally fell within the range of census values for the average group size, the percentage of multimale groups, and the distribution of females among groups. However, other discrepancies predicted from the research-group data were a higher percentage of adult males than observed, an overestimation of the number of multimale groups with more than two silverbacks, and an overestimated number of groups with only two or three members. Possible causes for such discrepancies include inaccuracies in the census techniques used, and/or limitations with the long-term demographic data set obtained from only a few research groups of a long-lived species. In particular, estimates of mortality and male dispersal obtained from the research groups may not be representative of the entire population. Our final simulation addressed these discrepancies, and provided a better basis for further studies on the complex relationships among individual life history events, group composition, population age structure, and growth rate patterns

Modified model description written by: **Andrew M. Robbins and Martha M. Robbins**

Notes: The Submodels are not included here; please refer to the original publication.

Purpose

The main purpose of this initial model is to compare two sets of data from studies of the critically endangered mountain gorillas (*Gorilla beringei beringei*) of the Virunga Volcano region:

- Six censuses of the entire region have been conducted between 1971 and 2000, providing estimations of the overall population size, age structure, and the distribution of gorillas into social groups (Harcourt & Groom 1972; Groom 1973; Weber & Vedder 1983; Aveling & Harcourt 1984; Vedder & Aveling 1986; Sholley 1991; Kalpers et al. 2003).

- Concurrently, three to five groups of gorillas have been habituated for more detailed research, providing information about birth rates, mortality rates, dispersal patterns, and other life history events (e.g. Gerald 1995; Watts 1990a, 1991, 2000; Robbins 1995, 2001; Sicotte 2001).

By using the research group data to model the population, and then comparing the results with actual population estimates obtained from the census data, we are then able to discuss possible explanations for discrepancies between the two data sets. The comparisons can help to reconcile the strengths and weaknesses of each data set, and to develop a more consistent interpretation of all the data collectively.

State variables and scales

In the agent-based model, each individual and its traits is followed over successive time intervals, while also keeping track of groups and overall population structure. Traits of each individual include its age, sex, group affiliation. Additional traits for each female are whether she is still in her natal group, the years since she last gave birth, and whether that last offspring is still alive. The traits for each group are the numbers of total members, adult males (silverbacks), and adult females. Traits for the overall population include its age structure, group size distribution, the proportion of groups with more than one silverback, and the distribution of females among one-male versus multi-male groups.

Process overview and scheduling

Individual processes include aging, death, female transfers, births, and male emigration. Both males and females may be philopatric or disperse (Harcourt et al. 1976). Subordinate silverbacks emigrate to become solitary males. Females transfer directly to a solitary male or to another group. Females may transfer multiple times in their lives, but usually not with an unweaned offspring because unrelated males typically kill the infants (Watts 1989; but see Sicotte 2000).

Variability in the social system of mountain gorillas is due to the following transitions (Robbins 1995, 2001; Yamagiwa 1987, 2001). New social groups form when females transfer to lone silverbacks. Such groups remain one-male until male offspring mature into silverbacks and the group is then multimale. Multimale groups can return to a one-male structure if an adult male emigrates or dies, or if the group fissions. When the silverback of a one-male group dies, the group disintegrates. If a breeding group loses all of its adult females, it becomes an all-male group. If a dominant male loses all of his group members, he becomes a lone silverback. Outsider males have not been observed to take over existing groups.

To begin a simulation, the model selects the first gorilla from the initial population, adds a year to its age, and applies input probabilities for each life history event (Figure 1). The model first evaluates death, then female transfers, births, and male emigration. After the model has considered all of the potential life history events for one gorilla, it repeats the process for each gorilla in the population. After processing each gorilla, the model then evaluates whether any groups with more than one silverback will split into two separate groups. After evaluating potential fissions, the model steps forward one year, and continues iterations for a total of 30 simulation-years.

Whenever the silverback dies in a one-male group, the model immediately processes the group disintegration. The remaining members are randomly assigned to another group or to a lone silverback. The new silverback evicts all males between ages 3-11, who are randomly assigned to an all-male group or to another lone silverback (Robbins 1995). The new silverback also kills all infants less than 3 years old (Fossey 1984; Watts 1989; Harcourt & Greenberg 2001). Infanticide is one of two types of deterministic death that the model treats

separately from mortality probabilities. In addition, when infants are less than 2 years old, they automatically die if their mother dies (orphan co-mortality).

Design concepts

Emergence. –Results from the base simulation closely match the values for demographic data obtained from the research groups (Table 4). In the model, most of those values are directly related to specific input parameters, so while the accurate results may support the general validity of the model, they mostly confirm that we set the input parameters appropriately. For example, the predictions confirm that we set the mortality probabilities to match the reported values for survivorship (Figure 2), and that we set the parameters in Equation 1 to match the distribution of ages for first parturition, and the intervals for subsequent births (Figure 3).

Other results from the model emerge from the more complex inter-relationships between individual life history events, group compositions, and the population age structure. For example, the growth rate is influenced by group disintegrations and infanticide, which depend upon male mortality and the percentage of multimale groups, which in turn are related to patterns of male emigration and group fissions.

Fitness. – This initial model made no attempt to quantify the fitness consequences of individual behaviors, nor did it assume that those behaviors would optimize individual fitness. A subsequent model has examined the fitness consequences of dispersal decisions for male mountain gorillas, and the results suggest that the species may be at an evolutionary disequilibrium because some observed behaviors do not seem to improve individual fitness (Robbins and Robbins, 2005).

Interaction. – Individuals interact mainly when a silverback kills or evicts immature offspring, and when a deceased mother fails to preserve the life of her most recent offspring. Group compositions also influence dispersal decisions of both males and females, but those influences are not represented as explicit interactions between particular individuals. Nonetheless, some real interactions may contribute to those relationships, such as when silverbacks “herd” adult females to prevent them from leaving a group (Sicotte 2001).

Sensing. –Transferring females are assumed to know whether they are still in their natal group, and the number of silverbacks in their group, and the number of silverbacks in a potential destination. Emigrating silverbacks are expected to know whether their group contains any females. Infanticidal silverbacks are expected to know which offspring are still nursing. Individual knowledge of these factors should be fairly accurate, although years of memory could be needed for some females to know whether they are still in their natal group.

Stochasticity. – The model compares the input probabilities for each life history event with output from a randomly generated number between 0-1. For example, if a female gorilla has 5% probability of dying, then she survives only if the random number is more than 0.05. If she dies, the model reduces the total population size, and her group size, and the number of adult females. In order to obtain more precise prediction values and a measure of variance from this stochasticity, each simulation involved 500 replicate “runs” from which we calculated the respective means and standard deviations.

Collectives. – Collectives are represented in the IBM as social groups of gorillas. Collectives occur as phenomena emerging from individual behavior, specifically the universal tendency of adult females to associate with a silverback (who protects their offspring from infanticide). Collectives are represented as explicit entities with their own state variables and traits (see State variables and scales), and they undergo their own processes such as fissions and disintegrations (see Process overview and scheduling).

Observation. –The IBM and its objectives were testing using model results that match the information gathered by field biologists through the periodic censuses and the ongoing studies of habituated groups.

Initialization

The initial population (Table 1) was based upon the results of the 1971-72 census (Groom 1973; Harcourt & Groom 1972; Weber & Vedder 1983). Immature gorillas are classified as infants (0-3.5 years), juveniles (3.5-6 years), and subadults (6-8 years). Adult females are >8 years. Males between 8-12 years are called blackbacks, and those >12 years are called adult males or silverbacks. Within those age classifications, the specific age assigned to each individual was based upon a stable age structure from published mortality and birth rates. Each infant was arbitrarily assigned to a particular mother, which thereby specified the time since the adult female had last given birth to a surviving offspring. Individuals were arbitrarily assigned to groups, to match the social structure shown in Table 1, and the typical group size distribution from the initial censuses.

Input

For the base simulation, the input probabilities were set so that the model fits previously reported data from the research groups. The model uses separate mortality probabilities for both sexes at all ages. The input parameters were based upon age-specific life tables for ages 0-11, and time-specific life tables for ages 12-40 (Gerald 1995). The model treats some infant mortality deterministically (see above), so we reduced their input probabilities until the model matched the reported values for overall survivorship through those ages. We also added mortality probabilities for ages above 40, until no gorillas survive past age 45. Table 2a reflects those adjustments to the previously reported parameters.

Birth probabilities were calculated with Equation (1), where “P” is the cumulative probability that a female will have given birth by the time “t” (years); and a, b, & c are constants shown in Table 2b.

$$(1) \quad P = 1 / (1 + \exp(a - b \cdot (t - c)))$$

This equation produces an s-shaped (or sigmoid) curve that is characteristic of many cumulative probability distributions. When $c=0$, the ratio a/b represents the (median) time at which the cumulative probability reaches 50%. The steepness of the curves depend upon the magnitude of a & b, relative to “t”. The constant “c” shifts the cumulative probability curve forward or backward in time, without changing its steepness. When the model applies Equation (1) to nulliparous females, “t” refers to the age of the female. For parous females whose previous offspring has survived, “t” refers to the years since their last birth. For parous females whose previous offspring has died, “t” refers to the years since the offspring died.

The values for a, b, & c were set so the model would match previously reported distributions for a female’s age of first parturition, and for the interval between subsequent births. The age of first parturition is earlier for females in multimale groups; subsequent birth intervals are shorter when the previous offspring dies (Gerald 1995). No significant relationship has been reported between birth rate and female group size (Watts 1990b). Births in the research groups have not differed significantly from an equal sex ratio (56 males, 41 females, chi-squared = 1.2, $p = 0.28$), (Gerald 1995), so the model randomly assigns the sex of offspring with a 50% probability of either male or female.

Subordinate silverbacks in breeding groups are given a 50% emigration probability, at one randomly assigned age between 12 and 18, to match the observed proportion of such silverbacks who emigrate (Robbins 1995). For all-male groups, the model gives subordinates

a 50% probability of emigrating *each year*, because when the research groups have been all-male, nine emigrations occurred in 18 subordinate-years (Robbins 1995).

The model gives an annual transfer probability to females above age 6, whenever they do not have a surviving offspring below 3 years of age (Sicotte 2001; Watts 2000). The model uses two different annual probabilities, depending upon whether the female is still in her natal group (Table 2c). Whenever the probabilities indicate that a female will transfer, the model uses a simple weighting function to decide what type of social unit she will enter. For example, the probability that a transferring female will choose a one-male group is:

$$(2) \quad \frac{N_{OMG} * FTW_{OMG}}{(N_{OMG} * FTW_{OMG}) + (N_{MMG} * FTW_{MMG}) + (N_{LSB} * FTW_{LSB})}$$

where N_{LSB} , N_{MMG} , and N_{OMG} are the number of lone silverbacks, multimale groups, and one-male groups, respectively; and FTW_{LSB} , FTW_{MMG} , and FTW_{OMG} are the weighting factors (transfer preferences) for female transfers to each potential destination. (Table 2c). The weighting factors were set so the base simulation model would match previously reported proportions for the destinations of female transfers (Watts 2000).

Five group fissions have been reported for approximately 100 multimale-group years that habituated groups have been followed (Robbins 1995, Kalpers 2003), so the model uses a 5% probability that a multimale group will fission in a given year. A multimale group must have at least 5 members before the model will apply that probability. For purposes of computation expediency, fission automatically occurs in the very rare cases when a multimale group has more than 90 members at the end of a year. During fissions, the model randomly gives the resulting new group between 10-50% of the members from the parent group. At ages 0-4, gorillas stay with their mothers during fissions.

Submodels

[Not included here; please refer to the original publication.]

Table 1. Summary of the input parameters for the starting population in the simulations. The parameters are mainly based upon the 1971-73 censuses (Groom 1973; Harcourt & Groom 1972; Weber & Vedder 1983).

Age Structure	Number of Individuals
Infant	33
Juvenile	27
Young Adult	38
Blackback	16
Silverback	58
Adult Female	89
Total	261
Social Structure	Initial value
Social Groups	31
Mean Group Size	7.9
Solitary Males	15
% Multimale groups	42%
% Immatures in groups	39.8%

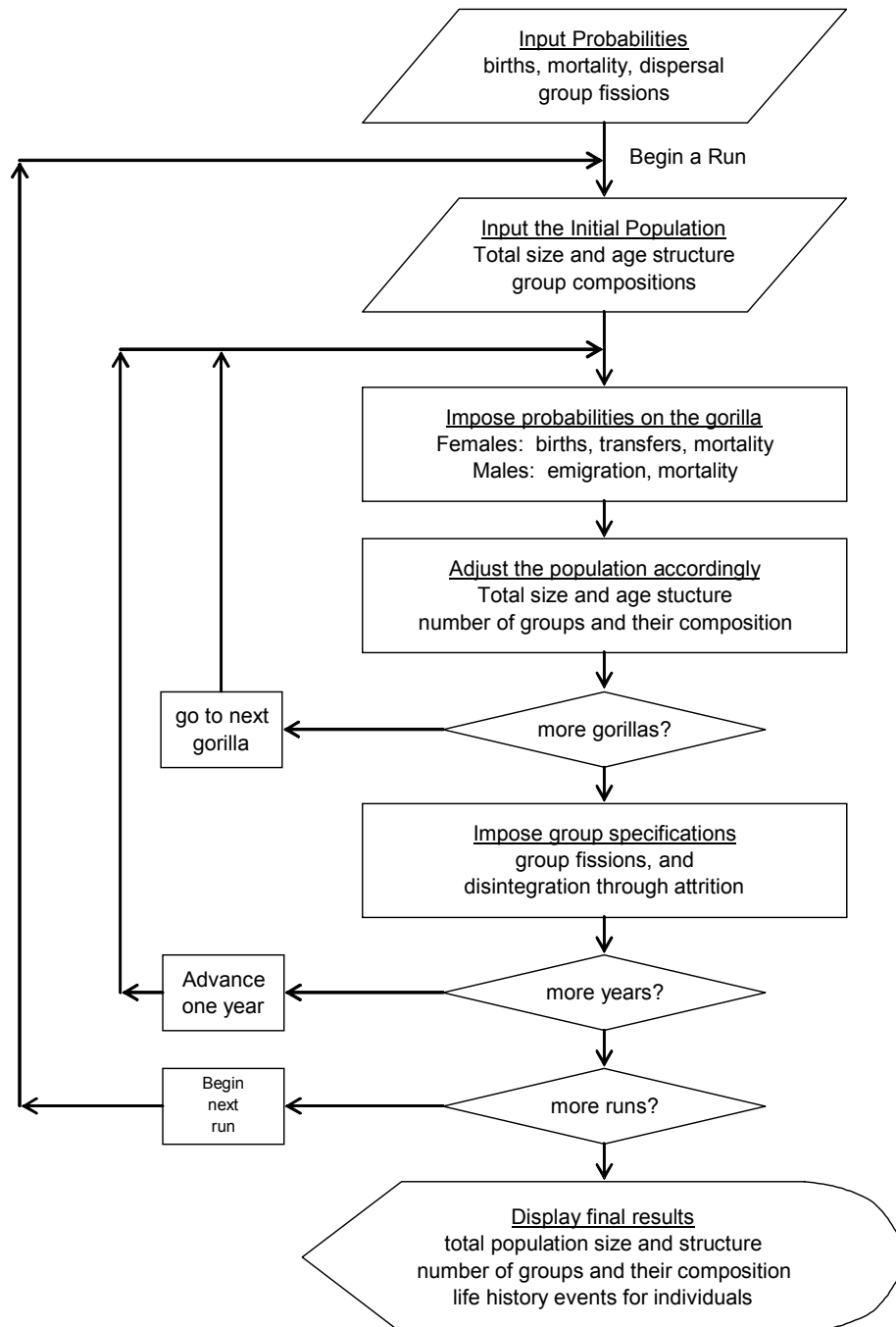
Table 2. Summary of input probabilities for the base simulation. Input parameters were set so the simulation would match reported values from the research groups. A. Annual mortality probabilities for each sex at each age (with sample sizes in parentheses when available from the age-specific life table in Gerald 1995). B. Birth probabilities (Gerald 1995). C. Female transfer probabilities. Transferring females must be at least age 6, with no offspring below age three (Sicotte 2001; Watts 2000).

2A: Annual mortality probabilities		
Age	Males	Females
0	0.104 (83)	0.115 (78)
1	0.008 (53)	0.058 (53)
2	0.024 (45)	0.001 (45)
3	0.064 (42)	0.073 (42)
4-5	0.024 (36)	0.029 (36)
6-7	0.000 (29)	0.000 (29)
8-11	0.000 (23)	0.014 (23)
12-17	0.025	0.017
18-23	0.022	0.018
24-29	0.157	0.029
30-39	0.104	0.083
40-43	0.400	0.400
44	1.000	1.000

Table 2B: Constants for the cumulative birth probability equation (1)			
<u>Age of first parturition</u>	<u>A</u>	<u>b</u>	<u>c</u>
One-male groups	14.0	1.2	0.0
Multimale groups	16.0	1.7	0.0
<u>Subsequent birth intervals</u>			
Previous offspring survived	10.0	2.5	0.0
Previous offspring died	15.0	18.0	0.0

Table 2C: Female transfer probabilities and destination preferences			
Transfer Probabilities		Destination Preferences	
		<u>Transfer from:</u>	
		<u>Transfer to:</u>	
Natal transfer	0.300	OMG	MMG
Secondary transfer	0.062	Lone silverback	0.22 0.10
		One-male group (OMG)	0.22 0.10
		Multimale group (MMG)	0.56 0.80

Figure 1. Flowchart for the agent-based model. The simulations are based on 500 runs of 30 years with 200-700 gorillas.



Example Fish Life History

The original model description, including all full references, is presented in:

Jørgensen, C. and Fiksen, Ø. In press. State-dependent energy allocation in cod (*Gadus morhua*). Can. J. Fish. Aquat. Sci.

Abstract: Growth and maturation are processes that are tuned to the external environment an individual is likely to experience, where food availability, the mortality regime, and events necessary to complete the life cycle are of special importance. Understanding what influences life history strategies and how changes in life history in turn influence population dynamics and ecological interactions are crucial to our understanding of marine ecology and contemporary anthropogenic induced change. We present a state-dependent model that optimises life-long energy allocation in iteroparous fish. Energy can be allocated to growth or reproduction, and depends in the individual's age, body length, stored energy, and the state of the environment. Allocation and the physiological processes of growth, storing energy, and reproduction are modelled mechanistically. The model is parameterised for Atlantic cod (*Gadus morhua*); more specifically for the Northeast Arctic cod stock. Growth and maturation predicted by the model fit well with field observations, and based on a further investigation of cod reproduction in the model we conclude that the model has the ability to recapture complex life history phenomena, e.g. indeterminate growth and skipped spawning, and therefore provides an important tool that can improve our understanding of life history strategies in fish.

Modified model description written by: **Christian Jørgensen**

Notes: This model description includes, in the element “Submodels”, an extra section describing parameterization for the Atlantic cod. In addition, an Appendix is provided discussing the range of environmental conditions considered in the model.

Purpose

We develop a state-dependent model that mechanistically describes energy allocation to growth and reproduction in fish. Since energy is a restricted resource, the life-long pattern in this allocation embodies many of the trade-offs that shape life history. The focus on energy allocation therefore fulfils the purpose of this model, which is to find the optimal life-history under varying external forcing (e.g., fishing mortality, migration, and food availability). Throughout, we model the energy allocation processes as mechanistically correct as feasible, while retaining flexibility in how allocation can change with time and state. In this way we can use dynamic programming algorithms to find the optimal allocation pattern under the constraints given by the realistic and detailed description of physiology and ecology.

State variables and scales

The optimal allocation is found by dynamic programming (Houston and McNamara 1999; Clark and Mangel 2000) and depends on four individual states: age (in months, thus including season); body length (cm); size of energy stores (relative scale); and current feeding conditions. The result is a state-dependent energy allocation rule that is a life history strategy. In the model, we consider only female cod. With the optimal life history strategy, we run

population dynamics; these simulations are cohort-based, and in addition to the individual states mentioned above each cohort also has a number of individuals attached to it. The model is parameterised for the Northeast Arctic cod stock, which is a long-lived species with iteroparous reproduction. From their feeding grounds in the Barents Sea, the spawners migrate in spring to the Lofoten area where spawning takes place. The temporal resolution is months (discrete steps), and space only enters the model as individuals are separated between the feeding grounds and the spawning grounds.

Process overview and scheduling

Each month the following processes take place: feeding, energy allocation (leading to growth and increase of energy stores), and mortality. Fish that will spawn migrate in January, spawn their stored energy as one batch of eggs in March, and migrate back in May; the remainder of the year is used for growth and to rebuild energy stores.. During this period their feeding intake is so low that no allocation takes place. Energy allocated to growth irreversibly increases body length, while stored energy can be used for spawning (migration and egg production) or for metabolism during times when feeding conditions are poor (Fig. 1). Density-dependence is not included in the model.

Design concepts

Optimal energy allocation is determined for each state combination with expected reproductive value as fitness measure. The result is a highly flexible multi-dimensional hypersurface that defines a life-history strategy, described by 6.4 million independent points (each point corresponding to the allocation value conditional on a particular combination of the four states). Because rewarding analyses are virtually impossible on such amounts of data directly, we simulated populations of fish realising such life-history allocation strategies to let age-, size-, and condition-dependent patterns emerge at the individual and population level. A series of monthly energy allocations results in e.g. a time-series of growth, an age at sexual maturation, reproductive episodes with specific fecundities, and skipped spawning seasons (analysed separately in Jørgensen et al. this issue). There is no interaction between individuals in the simulated population, and individuals only have information about their four individual states. Food availability is auto-correlated in time to allow for more extended periods of advantageous/unfavourable environment. In the forward population simulation, this is modelled as a stochastic process. Since optimal strategies may use the predictive power of an auto-correlated environment to fine-tune allocation strategies (e.g., that a favourable environment is likely to persist for some time), current food availability was included as an extra state.

Initialization

Juvenile fish were introduced in the model at age 2 years and body length 25 cm. Maximum age was set to 25 years, and the model was solved for body lengths up to 250 cm to avoid artificial boundary effects.

Input

Growth and maturation data from the literature were used to test parameter values and general properties.

Submodels

Details of the relationships defining the model are given below, followed by specific parameter values chosen to represent the Northeast Arctic cod stock.

Individual physiology

Body mass is divided into two compartments: soma and energy stores. Soma $W_{\text{soma}}(L)$ (g wet weight) includes systematic structures such as skeleton, internal organs, the neural system, a minimum amount of muscle mass, and for which growth is irreversible. Additional energy may be stored above this level for reproduction or to enhance survival during periods of food shortage. Because weight usually increases with length with an exponent slightly above 3, the length-specific somatic weight (with no energy stores) can be written as function of $W \propto L^{3+\varepsilon}$ where ε for many species falls between 0.1 and 0.4 (Ware 1978):

$$(1) W_{\text{soma}}(L) = \frac{K_{\min} \cdot L^{3+\varepsilon}}{100 \cdot L_{\text{std}}^{\varepsilon}},$$

where K_{\min} is the minimum Fulton's condition factor $K = W \cdot 100 \cdot L^{-3}$, where weight is measured in g wet weight and length in cm (the resulting number varies around 1.0 and describes the fatness or body condition of an individual). For a given length, K_{\min} represents the minimum body mass required for structures; death by starvation can be incorporated to occur at K_{\min} or with increasing probability as K_{\min} is approached. Similarly, there is a limit for how spherical the shape of an individual can be, and K_{\max} is the maximum Fulton's condition factor that includes W_{soma} and full energy stores. This maximum reflects the physical limitations imposed by anatomy and the need to maintain other body functions while carrying stores, and in this model stores cannot be increased above the level set by K_{\max} . For $\varepsilon \neq 0$, K_{\min} and K_{\max} must be specified for a given length L_{std} (cm).

Energy is normally stored partly as proteins by increasing muscle mass, and partly as lipids either embedded in the muscles (common for salmonids) or stored separately in the liver (typical for gadoids). The average energy density of these energy stores combined, ρ_E ($\text{J} \cdot \text{g}^{-1}$), has to be known. We assume that this density is constant, meaning that muscle proteins and lipids are stored at a constant ratio above the minimum muscle mass included in W_{soma} . When the amount of stored energy E (J) is known, total body mass W (g wet weight) can be calculated as:

$$(2a) \quad W(L, E) = W_{\text{soma}}(L) + \frac{E}{\rho_E},$$

where E has to be less than or equal to the maximum energy that can be stored, E_{\max} (J):

$$(2b) \quad E_{\max}(L) = (K_{\max} - K_{\min}) \cdot \frac{\rho_E \cdot L^{3+\varepsilon}}{100 \cdot L_{\text{std}}^{\varepsilon}}.$$

Energy expenditure is calculated according to the bioenergetics model by Hewett and Johnson (1992). Metabolic rate (MR ; $\text{J} \cdot \text{t}^{-1}$) is the product of the standard metabolic rate (SMR ; $\text{J} \cdot \text{t}^{-1}$) and an activity parameter Act_{Std} to include a routine level of activity:

$$(3) MR = SMR \cdot Act_{\text{Std}} = \kappa_1 \cdot W(L, E)^{\beta_1} \cdot Act_{\text{Std}}, \quad Act_{\text{Std}} > 1.$$

Here, κ_1 ($\text{J} \cdot \text{g}^{-\beta_1} \cdot \text{t}^{-1}$) is the coefficient and β_1 mass exponent of the allometric function.

Environment

Food intake ϕ ($\text{J} \cdot \text{t}^{-1}$) is determined by food availability in the environment and a measure of body size (body mass W (g) or body length L (cm)). A stochastic function χ and seasonal

cycles $C(t)$ can be incorporated to account for environmental variability in food availability. Feeding intake would thus be

$$(4a) \quad \phi(W) = \chi \cdot C(t) \cdot \kappa_2 \cdot W(L, E)^{\beta_2} \quad , \quad \text{or}$$

$$(4b) \quad \phi(L) = \chi \cdot C(t) \cdot \kappa_3 \cdot L^{\beta_3} \quad .$$

where $\kappa_2 \cdot W(L, E)^{\beta_2}$ and $\kappa_3 \cdot L^{\beta_3}$ are average food intake for a given body mass or body length, respectively. Typical values for the allometric exponents in fish are $\beta_2 \sim 0.8$ and $\beta_3 \sim 2.5$ (Schmidt-Nielsen 1984).

Energy allocation

For every time-step, a proportion $u(a, L, E, \phi)$ of net energy intake will be allocated to storage. The variable u is the core of this model, and when optimised over the entire life span it represents optimal life history strategies. As such, u balances the trade-off between growth and reproduction, and as such also integrates the effects of natural and fishing mortalities and the environment. Given u , the new state value of the energy stores in the next time-step is

$$(5) \quad E(t+1 | u) = E(t) + u \cdot (\phi - MR) \cdot \delta_{\text{store}} \quad , \quad E \leq E_{\text{max}} \quad .$$

Here, δ_{store} is the assimilation efficiency for the conversion of ingested energy to stores. The concept of the metabolic rate and the relationship between stored energy and spawned eggs embody energy losses at later steps; therefore this value is commonly higher than the assimilation efficiency for growth of somatic structures (δ_{growth}) below. The proportion $(1 - u)$ is allocated to somatic growth to a new length $L(t+1 | u)$

$$(6) \quad L(t+1 | u) = \left[L(t)^{3+\varepsilon} + \frac{(1-u) \cdot (\phi - MR) \cdot \delta_{\text{growth}} \cdot 100 \cdot L_{\text{std}}^{\varepsilon}}{K_{\text{min}} \cdot \rho_s} \right]^{\frac{1}{3+\varepsilon}} ,$$

$$L(t+1) - L(t) \leq \Delta L_{\text{max}} \quad ,$$

where δ_{growth} is the efficiency with which available energy is assimilated into somatic structures, and ρ_s ($\text{J} \cdot \text{g}^{-1}$) is the energy density of somatic tissues and typically lower than the energy density of stores. The equation basically states that growth is allometric with the exponent $(3+\varepsilon)$, and new tissue is laid down according to available food, assimilation efficiency and the energy density of somatic tissue. The constraint on maximum theoretical growth rate, ΔL_{max} ($\text{cm} \cdot \text{t}^{-1}$), acts as an upper physiological limit for length increment per time and can be parameterized from growth studies in food-unlimited immature fish.

Reproduction and migration

Feeding behaviour may be altered during reproduction and possibly also during the migration to and from the spawning grounds. Therefore, the duration of these events must be explicitly incorporated into the time-structure of the model. The time required for the migration $T_M(t)$ is the migration distance D_M (m) divided by the swimming speed through the water masses:

$$(7) \quad T_M = \frac{D_M}{(U_s + U_c)} \quad ,$$

where U_S ($\text{m}\cdot\text{t}^{-1}$) is the average or typical swimming speed during the migration and U_C ($\text{m}\cdot\text{t}^{-1}$) the speed of possible currents that have to be taken into consideration. If $U_C \neq 0$ or the migration route differs to and from the spawning grounds, T_M and the energetic cost of migration E_M (J) have to be calculated separately for each direction. For species migrating in groups or schools, U_S will often be identical for smaller and larger individuals.

The energetic costs of migration E_M (J) can then be found from:

$$(8) E_M(W, L) = SMR(W) \cdot \left[\left(\frac{\kappa_4 \cdot U_S^{1.5}}{L} + 1 \right) - Act_{std} \right] \cdot T_M, \quad E_M \geq 0,$$

The expression $(\kappa_4 \cdot U_S^{1.5} \cdot L^{-1} + 1)$ determines an activity parameter similar to Act_{std} from swimming speed and body size. Other formulations can be used, but a function on this form proved to capture the dynamics of both body length and swimming speed in empirical data for Atlantic cod (Strand et al. 2005) and other fish species (Nøttestad et al. 1999).

Stored energy is eventually spawned, and total egg production b is proportional to invested energy (Marshall et al. 1999). If migration takes place, energy to fuel migration from spawning grounds back to feeding areas has to be retained, although this constraint may be modified to allow for semelparous life history strategies.

$$(9) b(E) = \kappa_5 \cdot (E - E_M).$$

Mortality

A flexible mortality regime incorporating length-, size-, or age-specific natural mortality M , size- or stage-selective fisheries mortality F and additional mortality during migration and spawning M_S can be specified. Mortality rates (t^{-1}) are summed and survival probability S over a discrete time interval T (t) is then given by:

$$(10) \quad S = e^{-T(M+F+M_S)}.$$

If death by starvation is included, the above equation will apply for $E > 0$, while $S = 0$ when $E \leq 0$. Details of the mortality regime used for calculations in this paper are given below under the heading *Parameters for the Northeast Arctic cod stock*.

Optimisation algorithm

Optimal life-history strategies were optimized using dynamic programming (Houston and McNamara 1999; Clark and Mangel 2000). Models of this type optimise a fitness function by backward iteration through an individual's life history, starting at the maximum age and constantly assuming that the individual acts optimally at every decision point in its future life. A central point is that such models separate between the information available to the individual (here its states) although other factors may affect its success (for instance the development in food availability). Dynamic programming then finds the best response, conditional on the information known by the individual, and averaged over possible outcomes. The optimisation problem considered here is thus to find the allocation to reproduction $u(a, L, E, \phi)$ that maximises future expected reproductive value $V(a, L, E, \phi)$ discounted by survival probability S for every combination of the four states (age a , body length L , energy store E , and environment ϕ):

(11)

$$V(a, L, E, \phi) = \max_u \left\{ S \cdot \sum_{\phi(t+1)} P(\phi(t+1) | \phi(t)) \cdot [V(a+1, L(t+1|u), E(t+1|u), \phi(t+1)) + b(E)] \right\}$$

Here $P(\phi(t+1)|\phi(t))$ is the conditional probability of food availability in the next time step given food availability in this time step. To find mean expected fitness one has to take the sum over all possible states of food availability at time $t+1$. During the spawning season, fitness values for both migrating and non-migrating individuals were calculated, and the option yielding the highest fitness value was stored.

Parameters for the Northeast Arctic cod stock

The parameters below are selected to describe the physiology and ecology of the Northeast Arctic cod stock (summarised in Tab. 1). The time resolution is months to allow for seasonal variations in allocation patterns. Many of the parameter values below can be used also for other cod stocks. Mortalities and details regarding the spawning migration vary between stocks and have to be changed. The physiology remains the same, except for the temperature dependence of food intake (Jobling, 1988) and metabolic rate (Hansson et al., 1996).

Metabolic rate and food intake

The equations for metabolic rate have been parameterised for Atlantic cod by Hansson et al. (1996). At an ambient temperature of 5 °C, and with a standard activity level set to $Act_{Std} = 1.25$ (Hansson et al. 1996), monthly metabolic rate MR (J·month⁻¹) was:

$$(12) \quad MR = SMR \cdot Act_{Std} = 2116 \cdot W(t)^{0.828},$$

where SMR is the standard monthly metabolic rate (J·month⁻¹).

Food intake at 5 °C was calculated according to Jobling (1988):

$$(13a) \quad \phi(L) = \chi(t) \cdot 276 \cdot L^{2.408},$$

by introducing additional stochasticity of the environment $\chi(t)$, auto-correlated in time and given by:

$$(13b) \quad \chi(t) = \bar{\chi} + C_1 \cdot (\chi(t-1) - \bar{\chi}) + C_2 \cdot N \cdot \sqrt{1 - C_1^2},$$

where N is a random number drawn from a standard normal distribution $N(0,1)$, $C_1 = 0.9$ is the auto-correlation coefficient, $C_2 = 0.15$ scales the variance, and $\bar{\chi} = 0.75$ is the mean of the stochastic distribution. The feeding equation 13a was obtained in farmed cod fed to satiation (Jobling 1988) and $\bar{\chi} = 1$ would correspond to the same feeding level in the model; by setting $\bar{\chi} = 0.75$ the mean feeding intake in the model is 25% less than for the farmed cod. Cod utilise many different prey species and can switch during unfavourable periods; there is also a maximum feeding rate that sets an upper limit for energy intake; for these reasons $\chi(t)$ was constrained to fall between 0.3 and 1.5.

Growth

We used $\varepsilon = 0.065$, which was found from a log-log regression between mean length and weight for Northeast Arctic cod age-classes 1-12 measured in the field over the period 1978-

2000 (ICES 2003). Maximum and minimum condition factors were set to $K_{\min} = 0.75$ and $K_{\max} = 1.25$ for a standard length of $L_{\text{std}} = 70$ cm; see Appendix 1 for justification. Maximum length increment was set to $\Delta L_{\max} = 18 \text{ cm} \cdot \text{year}^{-1}$ and is a constant independent of length in this model, since field and experimental data show that length-growth is typically linear with time for food-unlimited immature cod, and decreases thereafter as a result of allocation to reproduction (e.g. Jørgensen 1992; Michalsen et al. 1998).

Energy stores

Together, muscle and liver stores vary between K_{\min} and K_{\max} , and the average energy density of full stores can be calculated provided that we know the energy content and relative contribution of each tissue type. Lipids are stored primarily in the liver, and the liver condition index (LCI) is liver weight expressed as percentage of total body mass. LCI reaches maximum values just prior to spawning; maximum monthly mean values for the Northeast Arctic cod stock are typically 7-8 % in early winter if food is abundant (Yaragina and Marshall 2000). A maximum value that can be obtained by the most successful individuals may exceed the average and was therefore set to $LCI_{\max} = 9\%$. Total liver energy density (LEC ; $\text{J} \cdot \text{g}^{-1}$) of full lipid stores in the liver is then given by (Lambert and Dutil 1997; Marshall et al. 1999):

$$(14) \quad LEC = 2.477 \cdot 10^4 \cdot \left(1 - e^{-0.52(LCI_{\max} - 0.48)}\right) .$$

The remainder of the weight increase due to storage is increased white muscle mass, which has an energy density of $4130 \text{ J} \cdot \text{g}^{-1}$ (Holdway and Beamish 1984, their table V). The average energy density of full stores can then be calculated to be $\rho_E = 8700 \text{ J} \cdot \text{g}^{-1}$. For comparison, whole body energy density, which includes all tissue types and not only the lipid-rich energy stores, peaked at $7000 \text{ J} \cdot \text{g}^{-1}$ in a study of the chemical composition of cod (Holdway and Beamish 1984). The energy density of somatic tissues was furthermore calculated to be $\rho_S = 4000 \text{ J} \cdot \text{g}^{-1}$ from whole body energy content minus the liver for cod reared at 5°C in a study on chemical composition analysis of Atlantic cod (Holdway and Beamish 1984, their tables II, III and VI).

It is difficult to estimate energy loss in metabolic reactions, especially when the ingested molecules are only moderately rearranged before e.g. becoming part of the animal's stores. In general, half the energy in food can be made available as ATP (adenosine triphosphate), and maximum muscle efficiency (energy in ATP versus physical work done) is around 0.45 (Alexander 2003), but we have not been able to find more exact determinations of overall metabolic pathways of relevance to this model. We set the proportion of ingested energy that was preserved when stored to $\delta_{\text{store}} = 0.4$. This value is relatively high because lipid and protein storage requires few biochemical rearrangements compared to somatic growth processes, and δ_{store} accounts only for energy lost from ingestion to storage; energy losses during metabolism and production of eggs is taken into account in the empirical relationships in eqs. 9 and 12. Assuming further that the efficiency in converting energy from stores to eggs is also 0.4, and that growing somatic structures such as bones and neural tissue is only half as efficient as the entire process from ingestion to egg production, we ended up with $\delta_{\text{growth}} = 0.08$ of the energy being preserved when used for somatic growth. These parameters were chosen also based on predicted growth patterns in terms of length and weight in the model.

Migration and spawning

Each January fish can either start migration in order to spawn, which occupies January through May, or stay at the feeding grounds. Atlantic cod eat little or nothing during the

spawning season (Fordham and Trippel 1999). This has been simplified in the model, where there is no net gain in energy for spawning fish ($\phi(W) = SMR \cdot Act_{Std}$). For calculations of energy consumption during spawning migrations, we used $\kappa_4 = 320 \text{ cm} \cdot \text{s}^{1.5} \cdot \text{m}^{-1.5}$ (Strand et al. 2005), $U_S = 0.3 \text{ m} \cdot \text{s}^{-1}$ (Brander 1994), and $U_C = 0.1 \text{ m} \cdot \text{s}^{-1}$ (Brander 1994). Because the current flows north along the Norwegian coast, $(U_S + U_C)$ was used for estimating required time for the southward migration, while $(U_S - U_C)$ was used for the migration north. The migration distance $D_M = 7.8 \cdot 10^5 \text{ m}$ was measured on a nautical map. The required energy for migration was subtracted from the balance in one month, although the migration may take longer.

Stored energy was, for simplicity, spawned in one batch in March. Although there are indications that cod may adjust their spawning intensity between years to compensate for previous reproductive investments (Kjesbu et al. 1996), all stored energy except that required for the northbound migration was used for egg production in this model. Introducing a variable spawning intensity would mean to include one more trait in the model; deemed too complicated at present it suggests a potential direction in the future. In eq. 9, κ_5 was set to $0.407 \cdot P_{\text{lipids}}$ (Marshall et al. 1999), where $P_{\text{lipids}} = 0.63$ is the proportion of total energy stored that is stored as lipids in the liver and can be derived from the considerations on energy densities in different tissues above.

Mortality

Growth and maturation in the model are very sensitive to the choice of mortality regime. The mortalities in the spawner and the feeder fisheries were chosen to lie between the historic situation (before the onset of trawling), and the current harvesting regime. In evolutionary terms, this would imply that the resulting life history is partly adapted to the new and higher fisheries mortalities (either through contemporary evolution or through phenotypic plasticity that has evolved in response to variable mortality patterns in the past). The simulations in this paper used the following mortalities (all rates per year): natural mortality $M = 0.25$, increased mortality during the spawning/migration period $M_S = 0.1$, spawner fisheries mortality $F_S = 0.22$, and feeder fisheries mortality $F_F = 0.20$. The spawning season lasts five months in this model, so annual mortality rates affecting only spawning individuals was spread evenly over these five months. The probability of surviving the next month was thus $S = e^{-[M/12 + (M_S + F_S)/5]}$ when at the spawning grounds and $S = e^{-(M + F_F)/12}$ when in the Barents Sea (from Eq. 10). The sensitivity to and effects of different mortality regimes are analysed together with skipped spawning in a companion paper (Jørgensen et al. this issue). We have not specified any size-dependent mortality.

Appendix: Justification for choice of minimum and maximum condition factors

Growth in the model was sensitive to the choice of minimum and maximum condition factors. The following reasons for choosing K_{\min} and K_{\max} were therefore tightly coupled with sensitivity tests and comparisons with growth data. In an experiment following individual cod throughout the spawning season (length 56-87 cm; only females considered here), mean pre-spawning condition factor was 1.39 (range 1.19-1.75), while the average for spent cod was 0.97 (range 0.81-1.13) (Fordham and Trippel 1999). Using these condition factors for K_{\min} and K_{\max} in the model, however, gives higher condition factors and weight-at-age than is observed for the Northeast Arctic cod stock. This can be partly because eggs swell prior to spawning by taking up water (Tyler and Sumpter 1996; Fordham and Trippel 1999), which may artificially inflate condition factors for pre-spawning cod so that they no longer reflect the true size of energy stores. The extent of water uptake can be illustrated by the fact that total volume of eggs spawned was on average 150% of post-spawning body volume in the same study (Fordham and Trippel 1999). Also, cod were fed *ad libitum* throughout the

spawning period in that study, and the easy access to food compared to natural conditions may have improved final condition. A somewhat lower maximum value, $K_{\max} = 1.25$, was therefore selected. In a starvation experiment, cod died when condition factors reached 0.44 (range 0.36-0.56; length 31-55 cm), although liver energy stores were depleted before this (Dutil and Lambert 2000). The K_{\min} in this model should, however, reflect the condition at which routine energy stores are depleted, not the level to which severe food stress can atrophy muscle mass before death occurs. A value of $K_{\min} = 0.75$ was therefore chosen through thorough testing since it reproduced appropriate weight-at-length compared to field data (e.g. Fig. 4.). Conditions factors in the model are given relative to a standard length $L_{\text{std}} = 70$ cm, which means that realised K_{\min} is in the range 0.71-0.74 for the lengths used in Dutil and Lambert (2000).

Table 1. Parameters used for Northeast Arctic cod (*Gadus morhua*) in a model for state-dependent energy allocation.

Parameter	Value and unit	Biological interpretation
ε	0.065	Value of coefficient above 3 for allometric scaling between body mass and length
K_{\min}	$0.75 \text{ g}\cdot\text{cm}^{-3}$	Minimum condition factor at standard length L_{std}
K_{\max}	$1.25 \text{ g}\cdot\text{cm}^{-3}$	Maximum condition factor at standard length L_{std}
L_{std}	70 cm	Length for which K_{\min} and K_{\max} are defined
ρ_E	$8700 \text{ J}\cdot\text{g}^{-1}$	Energy density of muscle and liver energy stores
ρ_S	$4000 \text{ J}\cdot\text{g}^{-1}$	Energy density of somatic tissue
Act_{Std}	1.25	Proportional increase in metabolic rate due to activity
κ_1	$1693 \text{ J}\cdot\text{g}^{-\beta_1}\cdot\text{month}^{-1}$	Coefficient of allometric metabolic function
β_1	0.828	Exponent of allometric metabolic function
κ_2	$276 \text{ J}\cdot\text{cm}^{-\beta_2}\cdot\text{month}^{-1}$	Coefficient of allometric feeding function (of length)
β_2	2.408	Exponent of allometric feeding function (of length)
$\bar{\chi}$	0.75	Mean food intake relative to feeding function
C_1	0.9	Auto-correlation coefficient for environmental stochasticity
C_2	0.15	Scaling of environmental stochasticity
ΔL_{\max}	$18 \text{ cm}\cdot\text{year}^{-1}$	Maximum growth rate
D_M	$7.8\cdot 10^5 \text{ m}$	Distance for spawning migration
U_S	$0.3 \text{ m}\cdot\text{s}^{-1}$	Swimming speed during spawning migration
U_C	$0.1 \text{ m}\cdot\text{s}^{-1}$	Speed of northwards current during spawning migration
κ_4	$320 \text{ cm}\cdot\text{s}^{1.5}\cdot\text{m}^{-1.5}$	Coefficient for empirical cost of swimming function
P_{lipids}	0.63	Proportion of total energy stored as lipids in liver
LCI_{\max}	9%	Maximum weight of liver relative to body weight
δ_{store}	0.4	Efficiency of storing ingested energy
δ_{growth}	0.08	Efficiency of building somatic body mass from ingested energy
κ_5	$0.256 \text{ eggs}\cdot\text{J}^{-1}$	Conversion between stored energy and spawned eggs
M	0.25 year^{-1}	Natural mortality
M_S	0.1 year^{-1}	Increased mortality during spawning and migration
F_F	0.20 year^{-1}	Feeder fisheries mortality
F_S	0.22 year^{-1}	Spawner fisheries mortality
a_{\max}	25 years	Maximum age
a_{\min}	2 years	Age at which recruits are introduced in the model

L_{\min}	25 cm	Length of recruits
------------	-------	--------------------

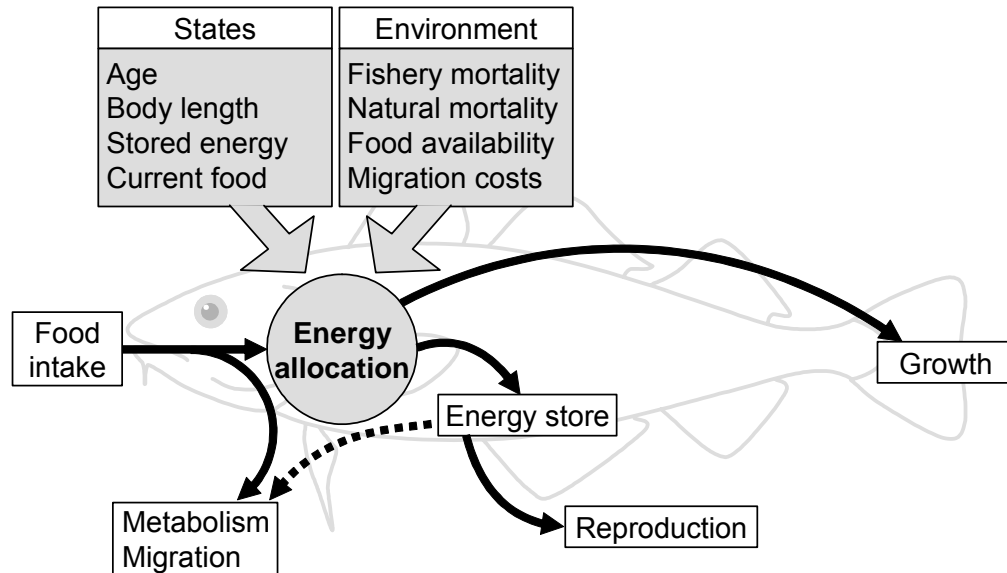


Figure 1. Schematic overview over a life-history energy allocation model for the Northeast Arctic cod (*Gadus morhua*). Energy allocation and the states influencing it are shaded in grey. Black arrows indicate energy flow. The dotted line indicates that energy stores are drained in periods when food intake cannot sustain metabolic demands.

Example Florida Snail Kite

The original model description, including all full references, is presented in:

Mooij, W. M., R. E. Bennetts, W. M. Kitchens, and D. L. DeAngelis. 2002. Exploring the effect of drought extent and interval on the Florida snail kite: interplay between spatial and temporal scales. *Ecological Modelling* 149:25-39.

Abstract: The paper aims at exploring the viability of the Florida snail kite population under various drought regimes in its wetland habitat. The population dynamics of snail kites are strongly linked with the hydrology of the system due to the dependence of this bird species on one exclusive prey species, the apple snail, which is negatively affected by a drying out of habitat. Snail kites require water depths to be above about 10 cm for apple snails (their only prey) to be accessible to foraging. The apple snail population will itself decline to effectively 0 under drought conditions and be only 50% recovered the following year (called a 'lag year'). The quality of the habitat for apple snails will deteriorate if a site remains flooded for too long a period. Based on empirical evidence, it has been hypothesised that the viability of the snail kite population critically depends not only on the time interval between droughts, but also on the spatial extent of these droughts. A system wide drought is likely to result in reduced reproduction and increased mortality, whereas the birds can respond to local droughts by moving to sites where conditions are still favourable. This paper explores the implications of this hypothesis by means of a spatially-explicit individual-based model. The specific aim of the model is to study in a factorial design the dynamics of the kite population in relation to two scale parameters, the temporal interval between droughts and the spatial correlation between droughts. In the model high drought frequencies led to reduced numbers of kites. Also, habitat degradation due to prolonged periods of inundation led to lower predicted numbers of kites. Another main result was that when the spatial correlation between droughts was low, the model showed little variability in the predicted numbers of kites. But when droughts occurred mostly on a system wide level, environmental stochasticity strongly increased the stochasticity in kite numbers and in the worst case the viability of the kite population was seriously threatened.

Modified model description written by: **Donald DeAngelis and Wolf Mooij**

Notes: Here the model description is reduced to the very skeleton of the model (structure and processes). Future developments of the protocol should go in this direction, but then a standard way of designing the skeleton is needed (cf. Example Shore Birds I). Regarding the structure, something similar to the class diagrams of UML might be an option; regarding scheduling, the way scheduling is organized in ABM software platforms like Swarm or Repast might be an option (see description of scheduling in Pitt et al. 2003).

Purpose

The purpose of the model is to assess the viability of the snail kite population of Florida under different temporal and spatial patterns of drought and other factors determining the water depths in the breeding sites of the snail kites. The closed population of snail kites is modeled under different climatic scenarios and different management plans for water regulation. The model follows the entire population of snail kites in Florida.

State variables and scales

Individual organism structure:

The number of individuals in the simulation is variable, and each individual is described by four characteristics, which are variables for each individual, changing with time.

Individual variables:

- age
- life stage
- breeding status
- spatial location (wetland sites)

Age: Weekly age increments (0 to open)

Life stage

variables: The snail kites go through a sequence of 4 stages:
Nestlings, Fledglings, Yearlings, Adults

Breeding status

variables: Individuals may be breeding or not breeding

Spatial location

variables: Individuals may move between any of 14 wetland sites on which reproduction can take place or 1 refuge site on which reproduction cannot take place, but which is available for survival purposes. They move to the refuge site when the other available sites are in drought conditions

Spatial structure:

14 spatial wetland sites on which reproduction can take place and one site that is a refuge where kites can survive but not reproduce. For each of the 14 breeding sites, the following hold.

Each site has a constant maximum carrying capacity

- parameters exist for maximum capacity of each site.

Carrying capacity is modulated multiplicatively by two factors; structural habitat quality and snail recovery, both of which depend on time since last drought, which causes some period of zero water depth at a site.

Spatial site variables:

- snail recovery status
- structural habitat status

Snail recovery variables:

- 0 (during drought)
- 0.5 (year after drought)
- 1 (≥ 2 years after drought). This represents fact that snails are unavailable during drought and take two years to recover to maximum population size.

Structural habitat quality variables:

- Ranges from 0 to 1. Starts to decline after 4 years with no drought, due to site structural degradation (lack of vegetation regeneration).1: wetland refuge site is always available for survival and does not vary in quality. Structural habitat quality as a function of years beyond 4 years without a drought is described in a table of values.

Temporal structure:

- Weekly time steps, 31-year time horizon

Process overview and scheduling

Environmental processes:

These processes can be driven either by historical data on water depths at each site on 2-week intervals, or by artificial driving functions, which may include stochasticity.

Drought

- parameters exist for various drought frequencies
- parameters exist for the spatial scale of droughts; that is, the degree to which there is spatial autocorrelation in the occurrence of drought conditions among sites

Recovery of habitat structure from drought

- parameters exist for recovery of habitat structure of sites (as indicated above under spatial structure)

Recovery of prey (apple snails) from drought

- parameters exist for time to recovery of apple snails (as indicated above under spatial structure)

Habitat degradation

- parameters for degradation of habitat in absence of drought (as indicated above under spatial structure)

Population processes:

Aging occurs in two week time steps

- Transitions between the four stages occur at fixed ages. A newly fledged bird has age zero

Movement between spatial sites

At each time step there is some probability of movement by a kite from one site to another. In the current version of this model, the highest probability is to move to the nearest non-dry site. A basic probability of movement per time step is set, which is modulated multiplicatively by four factors:

- probability as function of stage
- probability as function of time of year
- probability as function of drought condition
- probability as function of nest status

Breeding

Breeding consists of four possible processes; nest initiation, egg laying, nest failure, and nest desertion. A basic probability at each time step for each process is set, which may be modulated by one or more factors.

nest initiation

- probability modified as function of stage
- probability modified as function of time of year
- probability modified as function of drought condition
- probability modified as function of current breeding status

egg laying

- parameter for maximum possible fecundity
- probability modified as function of drought condition
- probable number modified as function of ratio of individuals to carrying capacity of a site

nest failure

- probability modified as function of drought condition

nest desertion

- consequence of nest failure

Mortality

Survival is set at a maximum possible survival value, which is modulated multiplicatively by three factors:

- parameter exists for maximum possible survival
- probability modified as function of stage (four stages)
- probability modified as function of time of year (12 months)
- probability modified as function of drought condition

Scheduling

The model iterates over each kite in each week in a fixed, age based order. This is possible because kites in the model only interact with their environment, not with each other directly (in which case the order of

evaluation would become an issue). Autonomous environmental processes are simulated at the start of each week.

Design concepts

Emergence:

- Growth rate of the total population
- Spatial distribution of the total population
- Age and stage distribution

Adaptation:

- Fitness seeking is modelled as probability of moving to a new site if conditions are detrimental to breeding or survival in the currently occupied site

Interaction:

- Pair formation for mating. It is assumed that pairs automatically form if nesting occurs
- Indirectly through carrying capacities of sites

Sensing:

- Individuals can sense environmental conditions
- Individuals know locations of other sites

Stochasticity:

- Model is usually run in stochastic mode, with all processes being probabilistic.

Initialization

Environment is started with arbitrary environmental conditions (drought or number of years following a drought) for each site.

Each of the fourteen habitats is started with 8 birds; 1 yearling male, 3 adult males, 1 yearling female, and 3 adult females

Input

If data are available on yearly site-specific drought conditions, these can be read in.

Submodels

[Not included here; please refer to the original publication.]

Example Vertical Migration of Cod

The original model description, including all full references, is presented in:

Strand, E., 2003. Adaptive models of vertical migration in fish. Dr. scient. Thesis, University of Bergen, Bergen, 150 pp. Paper IV.

Abstract: We investigate the trade-offs associated with vertical migration and swimming speed in a top predator like adult Atlantic cod using an adaptive individual-based model. Simulations with varying distribution and occurrence of prey, with and without swimbladder constraints, currents and visual predation were performed. Most simulations resulted in cod migrations between the bottom and pelagic zones. In simulations with high probability of encountering pelagic prey, the cod spent the daytime in the pelagic, moving to the bottom to feed only when no pelagic prey was encountered. At night the cod stayed in the pelagic to attain neutral buoyancy. In simulations with low occurrence of pelagic prey or high visual predation pressure, the cod remained at the bottom feeding on the consistently present benthic prey. If the pelagic prey occurred close to the surface or there was no benthic prey, the cod abandoned all bottom contact. The study thus predicts that the probability of encountering energy rich pelagic prey is the key factor in driving vertical migration in large predators such as cod. Buoyancy regulation is further shown to be an important constraint on vertical migration.

Modified model description written by: **Espen Strand**

Purpose

The presented model was developed in order to investigate how different internal and external forces impact on the vertical migration behaviour of a top predator fish such as adult cod. In this study, vertical migration behaviour includes both vertical positioning (depth) and swimming speed. Special emphasise was put on investigating the influence on vertical migration strategies caused by the variables; prey type, prey abundance, prey distribution, foraging tactics, stomach fullness, swimbladder dynamics, currents, and predation risk.

State variables and scales

The model environment is constructed to resemble a one-dimensional water column, divided into discrete depth intervals of 1 meter. Each depth interval is characterised by hydrostatic pressure, temperature, current speed, prey abundance, and the amount of light. The first two variables are independent of time while the latter three may vary with time. Each individual within the model is uniquely described by the state variables depth position and swimming speed (also referred to as behavioural variables) together with body mass, stomach fullness, swimbladder volume.

Process overview and Scheduling

At each time step, variables are updated by a series of processes. See Fig. 1 for a schematic overview of how behavioural variables are linked to state- and environmental variables through the implemented physiological and mechanical processes.

The model has a nested loop structure containing a generation loop, a day loop, and a time-step loop inside each other, respectively. At the beginning of each step of the day loop, prey densities and locations are updated. The vertical position of the cod and thus experienced current speed and light regime is updated at the beginning of each time-step loop before calculations of all the individuals foraging success and metabolic expenditure are performed. After these calculations, but still within the time-step loop, the cod decides its depth for the next time-step. Reproduction is scheduled to occur just before a new step in the generation loop begins.

Design concepts

The model is based on the ING (Individual based, Neural network, Genetic algorithm) modelling approach (Huse and Giske, 1998; Huse et al., 1999; Strand et al., 2002) where behaviour is evolved using a genetic algorithm that simulates evolution in a population of artificial individuals through numerous generations. Each individual carries a unique genetic string or strategy vector (Huse, 2001; Huse et al., 2002), consisting of a finite number of characters, each assigned a character value. The character values on the genetic string are used as weights in an artificial neural network (ANN, Rosenblatt, 1958; Rummelhart et al., 1986), a simplified model of a brain, for transforming input variables to behaviour (see figure 2). Behavioural decisions are hence based solely on locally obtained information about internal state and the environment.

The character values are refined by a genetic algorithm (Holland, 1975) by simulating hundreds of generations in order to find a set of character values that enables individuals to behave (response to input variables) in manner that maximise a chosen fitness criterion. The genetic algorithm thus mimics the process of natural selection by differentiating between the reproductive success of individuals (based on acquired fitness) and introducing new genetic variability due to recombination and mutations on the genetic string in the formation of offspring. To select between different behaviours, we have chosen maximisation of growth as a fitness criterion, since we believe this to be of great importance for adult non-spawning cod. This criterion hence entails both maximisation of feeding rate and minimisation of energy expenditure. If an individual dies, its body mass is set to zero, which will correspond to zero fitness.

The two behavioural variables, depth positioning and preferred swimming speed, will hence emerge during a simulation as a mean to maximise the fitness criterion, growth. Each generation is modelled for 20 consecutive days with a time resolution of 10 minutes. Such a temporal scale allows the model to distinguish between the behavioural success of different individuals, and at the same time, enables studying of relatively short-term behaviour. A period of 500 generations was found sufficient to train the ANN.

Initialization

At the beginning of a simulation, each individual in the population is assigned a random depth position (1 , 300), and a genetic string consisting of random values in the range (-5 , 5). Initial stomach fullness is set to 2% of the initial body mass of 4 kg. The body length (l) of such a cod is set to 0.76m. The initial swimbladder volume was set as to give each individual neutral buoyancy at its randomly initiated starting depth. Each model simulation was run for 500 generations, with 5 replicate runs. Several simulations were carried out to determine the effect

of different factors believed to affect cod vertical migration. The different simulations are summarised in Table 1.

Input

The model environment is parameterised to resemble conditions found on the continental shelf off Northern Norway during winter. This includes the temperature (surface = 3.5°C, bottom = 5.5°C, with a marked thermocline at 150m), current profile (Loeng et al., 1997; Aglen et al., 1999), and the amount of surface light (Skartveit and Olseth, 1988). Current speed reaches the maximum strength every 6h and 15min and varies from 0.0 m·s⁻¹ at the bottom and increases parabolically until reaching 0.3 m·s⁻¹ at the surface. 18m above the bottom the current reaches a maximum value of 0.2 m·s⁻¹. Visual range (*r*) depends on the light condition at the current depth (Aksnes and Giske, 1993; Aksnes and Utne, 1997) and is calculated from beam attenuation, background irradiance, prey contrast, prey radius, a sensitivity threshold of eye detection of changes in irradiance, and maximal irradiance processed by the eye. The two latter parameters have never been experimentally determined for cod. These values are thus established by adjusting values from other species. The exact visual range at any depth may consequently be inaccurate, but the slope of the curve each time-step, as a function of depth, will be unaffected by the irradiance parameters (Fig. 3). Also, the density of prey is adjusted to allow reasonable foraging during the simulation period.

Two different prey sources are included in the model, a pelagic and a benthic, based on capelin and shrimp respectively, which are common prey of cod (Bogstad et al., 2000). To include the dynamics of a prey item resembling pelagically schooling fish, we choose to make its presence stochastic. Either the pelagic prey is present in high density or not at all. The likelihood of pelagic prey being present is given by a frequency variable (*Fp*), whose value is varied between simulations. The presence or absence of pelagic prey was decided on a daily basis using random numbers and Monte Carlo simulations (Judson, 1994). The depth at which the pelagic prey appears is also modelled as being stochastic within given limits. The width of the school is set to 9 meters (+/- 4 meters from centre). As opposed to the stochastic occurrence of the schooling pelagic prey, the benthic prey was always present, with a maximum density at the bottom that decreases exponentially up to 270m to resemble the vertical distribution of prawns.

Submodels

ING modelling approach

Every time a behavioural decision is to be taken, the values of the genetic string are embodied into the artificial neural network. In this way, the inherited genetic string is used to weight the connections between the experienced stimuli and states (input), and the decided behavioural responses (output). The calculations that take place in the ANN are described in detail by Huse and Ottersen (2003). Both depth position and swimming speed responses are adapted. At the end of a generation, the individuals are sorted according to the chosen fitness criterion (maximisation of body mass) and the 20% best individuals produce 5 offspring each. For each of these spawners, a partner is picked randomly from the 50% best individuals. The genetic string of the offspring may be a recombination of the two parents (probability=0.6) or a clone of the spawner. In addition to recombination, mutations may occur. Mutations in the ANN occurs node wise (van Rooij et al., 1996) at a probability of 0.1. In case of a mutation, the weights associated a node are changed randomly by up to 100% of the weight value. In this way, the behavioural response to different inputs is adapted through an evolutionary process. By simulating numerous generations in this manner, the behavioural response to changing

external stimuli and internal states will become better and better according to the fitness criterion.

Swimbladder regulation

The swimbladder dynamics are calculated using the model of Strand et al. (2005). The model is based on calculations of the swimbladder volume, the maximum rates of gas secretion and absorption (Harden Jones and Scholes, 1985), and the rate of leakage through the swimbladder wall (Lapennas and Schmidt-Nielsen, 1977). If the cod moves vertically faster than the swimbladder can accommodate by secretion or absorption, the cod will experience a buoyant force (Archimedes' principle), working either up (floating) or down (sinking). To compensate this force the cod will have to swim through the water with a tilt angle while extending its pectoral fins (Alexander, 1972) to generate a positive or negative lift. The energetic cost associated with cod swimming has been estimated (Schurmann and Steffensen, 1997; Webber et al., 1998; Reidy et al., 2000), and these equations are used to calculate the energetic cost of compensatory swimming needed to counteract non-neutral buoyancy. See Strand et al. (2005) for more details.

It was assumed that the cod modified its swimming speed to provide the necessary lift given the present swimbladder volume. This is referred to as compensatory swimming. At the same time it was assumed that the cod modified its swimming speed to avoid being transported with the current. An adapted cruising speed was calculated using the ANN. The highest of these three swimming speeds at any time step was used to calculate the cod's velocity through the water and its activity metabolism.

Growth

A basic balanced energy budget is the foundation of the bioenergetics in this model (Hewett and Johnson, 1992). This is a way to account for energy flow in an organism:

$$(1) \quad \Delta B = C - R - S - F - U$$

where C is consumption, R is respiration, S is specific dynamic action, F is egestion, and U is excretion. Net energy gain (ΔB) is used for structural growth. The equations are fitted with parameters for cod (Hansson et al., 1996) (Table 2). The prey encounter probability (PE) was calculated by:

$$(2) \quad PE = \pi(r \sin \theta)^2 \cdot N \cdot v$$

where r is the visual range, θ is the reactive half angle (Luecke and O'Brien, 1981; Dunbrack and Dill, 1984), N is the prey density, and v is swimming speed (see Aksnes and Giske (1993) for details). If PE was greater than a random number picked by Monte Carlo simulation, one prey item was consumed. The same equation was applied both for benthic and pelagic food. It is assumed that swimming to overcome currents do not influence foraging rate, but only metabolic rate. This would be the case if the mobile pelagic prey also matched the current speed by swimming in the opposite direction. In some simulations, cod was given an extra 0.01m visual range to account for, in a very simple way, tactile foraging when searching for prey at the bottom (300m).

Stomach evacuation is based on a temperature depended gastric evacuation model for cod (dos Santos and Jobling, 1992) with prey specific values for capelin and prawn. The basic evacuation model must keep track of the time each food particle has been in the stomach, which means that all prey items must be kept track of separately. This yields very time consuming calculations. Further, if the temperature would change while evacuating, the basic

model would predict a steep increase in evacuation if the temperature is raised or decrease in evacuation rate if temperature is lowered (see gastric evacuation equation in Table 2). It was therefore necessary to construct some time independent equations that could account for the stomach evacuation at different temperatures (3.5 and 5.5 °C), of different prey types (P_1 or P_2) and with varying stomach fullness SC . Assuming a cod at $t = 0$ ate 0.40 kg (i.e. full stomach, 10% of body mass) of capelin (P_1) at an ambient temperature (T) of 3.5°C one can calculate the amount of stomach contents $SC_t(P_1, T, SC_0, t)$ as a function of temperature, initial meal size and time from the original equation. When fitting a 2nd order polynomial function to these data one would get:

$$(3) \quad SC_t(P_1, 3.5, 0.4, t) = 2 \cdot 10^{-5} \cdot t^2 - 0.0045 \cdot t + 0.3935 \quad (R^2=0.999)$$

Similar equations were constructed for initial meal size of 0.3, 0.2, 0.15, 0.10, 0.05kg prey at 3.5 and 5.5 C°. The derived of this equation, $SC'_t(P_1, 3.5, 0.4, t) = 4 \cdot 10^{-5} \cdot t - 0.0045$, will return the rate of evacuation at time t . To make a time independent equation, we needed to find the time until $SC'_t(P_1, 3.5, 0.4, t)$ equals $SC'_t(P_1, 3.5, 0.3, 0)$ down to $SC'_t(P_1, 3.5, 0.05, 0)$. Then, by plotting this relationship and fitting a 2nd order polynomial function to these data one obtains:

$$(4) \quad t = 247.8 \cdot SC^2 - 307.8 \cdot SC + 84.0 \quad (R^2 = 0.999)$$

Finally, by inserting this equation into the derived equation of the 0.4 kg evacuation and setting $t = 0$, one get the instantaneously evacuation rate $ER(P_1, 3.5, SC)$ given any stomach fullness SC :

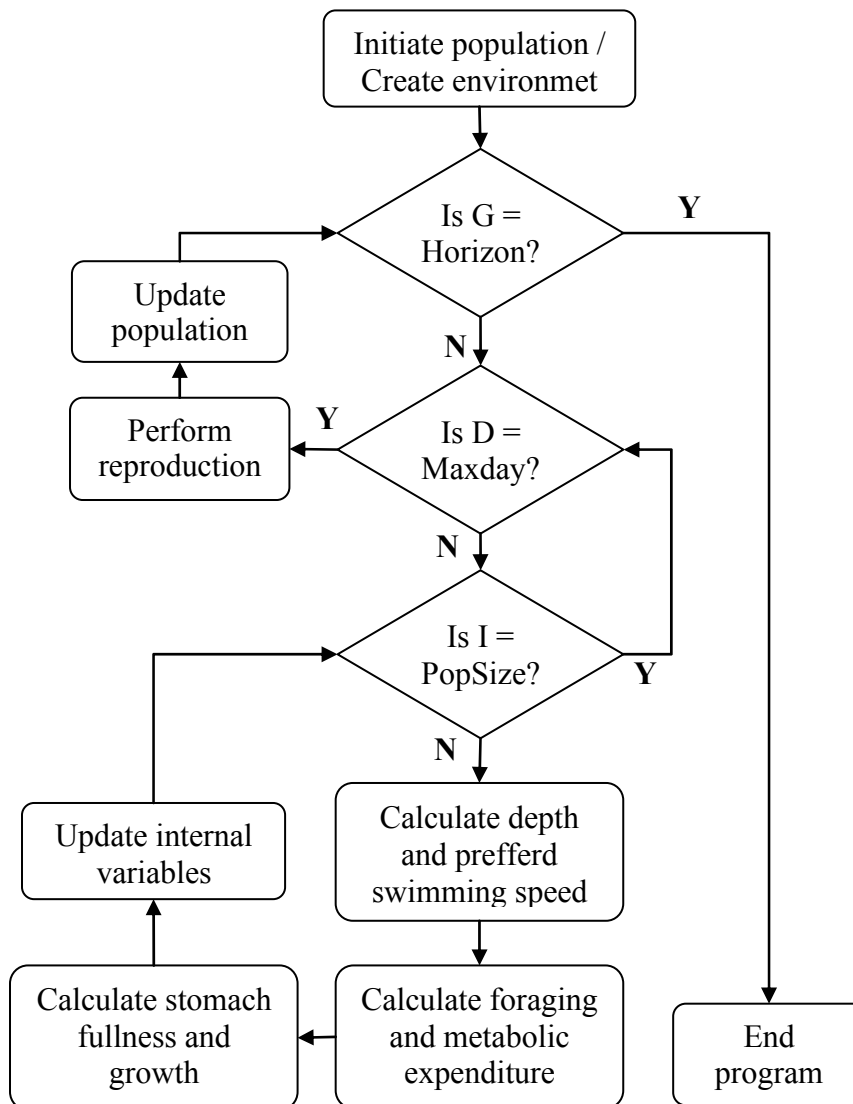
$$(5) \quad ER(P_1, 3.5, SC) = 4 \cdot 10^{-5} \cdot (247.8 \cdot SC^2 - 307.8 \cdot SC + 84.0) - 0.0045$$

In this model, four such equations were made to account for both prey types at two different temperatures. Assuming the cod will completely empty the stomach, such a simplification will give slight overestimate of the evacuation at a late stage of evacuation. This is due to fact that the original equation assumes an asymptotic evacuation curve that reaches zero stomach contents at $t \rightarrow \infty$.

Table 2. Bioenergetic equations used in the model. Fish activity equation from Strand et al. (2005). All other equations are from Hewett and Johnson (1992).

Description	Equation	Parameter (value) and variable (unit)
Total metabolism	$R = R(W_s) \cdot f(T) \cdot A(v)$	
Resting metabolism	$R(W_s) = \alpha W_s^\beta$	W_s = body weight (g), $\alpha = 0.0033$ $\beta = -0.23$
Temperature dependent metabolism	$f(T) = e^{(R_q \cdot T)}$	T = temperature (°C), $R_q = 0.055$
Activity metabolism	$A(v) = \left(3.2 \cdot \left[\frac{v}{l} \right]^{1.5} \right) \cdot l^{-1} + 1$	v = swimming speed (m·s ⁻¹) l = body length (m)
Egestion	$F = F_a \cdot C$	C = consumption (g) $F_a = 0.16$
Excretion	$U = U_a(C - F)$	$U_a = 0.10$
Specific dynamic action	$SDA = S_a(C - F)$	$S_a = 0.175$

Figure 1. A flowchart of the model showing the scheduling of all major events and calculations. G refers to generation, D to day, and I to individual.



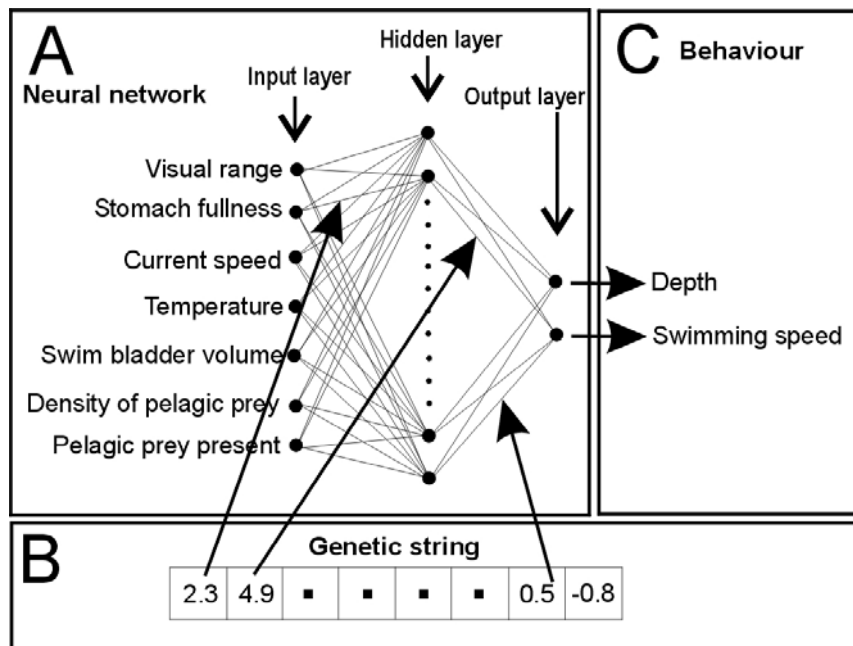


Figure 2. The neural network design. Panel A shows the neural network structure and the applied input variables. Panel B displays how the genetic string codes the neural network. Behaviour is determined in the neural network by weighting the input values with the adapted genetic string in the (Panel C).

Example Migration of Fish

The original model description, including all full references, is presented in:

Huse G, Giske J (1998) Ecology in Mare Pentium: an individual-based spatio-temporal model for fish with adapted behaviour. Fish Res 37: 163-178

Abstract: A conceptual approach to study spatial movements of fish using an individual-based neural network genetic algorithm model is presented. Artificial neural networks, where the weights are adapted using a genetic algorithm, are applied to evolve individual movement behaviour in a spatially heterogeneous and seasonal environment. A 2D physical model (for the Barents Sea) creates monthly temperature fields, which again are used to calculate zooplankton production and predation pressure. Daily fish movement is controlled by reactive or predictive mechanisms. Reactive movement governs search for local optimal habitats, whereas predictive control enables adaptation to seasonal changes. Levels of growth and predation pressure at the time of decision are used to assess whether to apply reactive or predictive movement control. To make the model realistic on a large scale, each of the individuals are scaled up to represent a clone of one million siblings acting and growing synchronously. The fish lives for up to two years, and may reproduce in its second year. In order to spawn it has to be at the designated spawning area in the south-western part of the lattice in January. During spawning it produces a number of offspring in proportion to its body size. The "genetic constitution" of offspring (the weights of the synapses in the neural networks) is a mix of their "mother's" and a randomly picked member of the population. The model is able to solve the problem of navigating in a heterogeneous and seasonal environment. The movement of the artificial fish follows a seasonal pattern, typical for migrating pelagic fish stocks. During summer and autumn the distribution is widespread whereas during spring it is more concentrated. When trophic feedback is removed (i.e. zooplankton survival is independent of fish predation) the distribution of the fish is less dispersed which shows that the model allows for density dependent behaviour. Large-scale migration is an interplay between reactive and predictive movement control and when only one of these is allowed, the individuals are unable to adapt properly. Throughout most of its life the fish relies heavily on reactive movement, but during the spawning migration predictive movement control is applied almost exclusively

Modified model description written by: **Geir Huse**

Purpose

The model was developed to investigate hypotheses regarding migration control in fish and the effect of density dependent foraging on fish distribution. Thus simulations with and without density dependent feeding are performed. The study is based on simulating a population of artificial fish inhabiting a 2D lattice, by using an individual based model where movement is determined by artificial neural networks (ANN) whose weights are evolved using a genetic algorithm (GA).

State variables and scales

The model comprises the individual states and their zooplankton prey resource. The model area is a lattice describing the Barents Sea divided into 60 by 60 squares with 20 km resolution. However, in order to make the landscape easier to move about in, land areas were converted to sea by linear interpolation (and extrapolation) of temperature fields. The individual based model operates on daily time steps. For each individual, age (in days), position on the lattice, growth and weight is kept track of. Each individual also has a “genetic” code (see below) that is used in generating movement behaviour. Individuals can live for up to two years after which they are terminated in order to maintain a short generation time and have an efficient population structure. To make the model more realistic on a large-scale each individual represents a clone of one million siblings, and mortality operates collectively so that the entire clone, or super-individual (Schaffer et al. 1995), dies concurrently. Consequently the zooplankton ingested by one super-individual is scaled up by one million to represent the feeding of all the siblings.

Process overview and scheduling

Zooplankton dynamics are modelled as a function of temperature and predation from the fish. The flow chart in Fig. 1 outlines the activities that the fish goes through. For each day the fish sequentially feeds, grows, and may die or reproduce. At the end of the day it decides whether it should stay at its present location or move to one of the eight surrounding squares. Growth was modelled by using a modified version of the Hewett and Johnson (1992) bioenergetic model.

Predation risk on the fish is assumed temperature dependent (Fiksen et al. 1995), as if predators were more active, efficient, and/or abundant in warmer waters.

Reproduction can only take place for two-year olds and is confined to the area in the south-west corner of the lattice during January. Particular to this model, reproduction involves both the transfer of energy as well as “genetic information” to offspring.

Movement is determined in a rather intricate manner. First the fish has to “decide” whether to use reactive (RMC) or predictive (PMC) movement control. If a uniformly distributed random number is below an inherited threshold value, or if current growth is below a threshold value, or current predation risk is above a threshold value then PMC is applied (Fig. 1). Else RMC is applied. Habitat choice is then calculated by using the reactive or predictive ANN, implemented as two separate networks with different kinds of input.

The individuals are numbered and feed each day according to this number, starting with the lowest number. Essentially this means that the oldest fish consistently feed first, as if there was a hierarchical feeding order.

Design concepts

Emergence. – Population dynamics, movement and resource dynamics emerge as a result of the adaptive modelling process.

Adaptation. – Movement is the sole adaptive trait in the model.

Fitness. – Reproduction is performed by ranking the survivors at the end of age two by size and let them reproduce in proportion to their size, given that they prevail in the right area during spawning time. The fitness measure used here is consequently not an explicit criterion, but rather an emergent property in itself that incorporates aspects of both survival and growth. Individuals die after spawning.

Interaction. – There is no direct interaction between individuals, but indirect interaction through density dependent foraging.

Sensing. – As illustrated in Fig. 1, movement of the fish relies on various kinds of environmental information such as temperature and mortality risk, and individual attributes such as age, weight, position in the grid and growth.

Stochasticity. – Mortality is imposed by calculating mortality risk and use random numbers to decide whether individuals live or die. The input data are deterministic.

Observation. – The key output monitored from the model are population dynamics, spatial dynamics, and the individual state variables.

Initialization

Initially individuals are placed randomly in a cell of the lattice, and their “genetic” strings of 0’s and 1’s are initiated randomly. At the start of each simulation, 4000 individuals were initiated randomly in the south-west part ($North < 41$, $East < 31$) of the lattice as one year olds with a weight of 8 g. The same initiation was made for new offspring in July of each generation. Population size was limited upwards to 15000 individuals.

Input

The only external input are monthly temperature fields taken from simulations using a physical model of the Barents Sea (Slagstad, 1981, 1987; Slagstad et al., 1989; Støle-Hansen and Slagstad, 1991). These data were previously used by Fiksen et al. (1995) for studying capelin migrations. Four of the monthly temperature fields are shown in Fig. 2.

Submodels

Zooplankton

A daily temperature dependent production of zooplankton is added at the start of each day and zooplankton is continuously removed by fish feeding:

$$(1) \quad Z_{jkt} = Z_{jkt-1} + R(T_{jkt}) - \sum_{i=1}^{pop} P_{ijkt}$$

where Z_{jkt} is the zooplankton abundance in cell jk at the end of day t , $R(T_{jkt})$ is the temperature dependent production of new zooplankton, P_{ijkt} is the number of zooplankton eaten by the siblings of individual number i in cell jk during day t , and pop is the population size. The zooplankton here consists of one size group only (weighing 0.7 mg). Quarterly distributions of zooplankton are shown in Fig. 3.

Growth

Some modifications have been made to allow for trophic level interactions. Hence food consumption is estimated from the concentration of food in the area searched rather than by a temperature dependent function, as commonly used in bioenergetics models. The volume searched is calculated as a product of distance covered during a day and search radius. In order to implement seasonal variation in light conditions the search radius is varied over the year by a normally distributed curve with a peak at the end of June (Table 1). We do not take vertical gradients in light and zooplankton concentration into account.

After each individual feeding the zooplankton abundance is updated (Eq. 1). Food intake was assumed to be effectively a linear function of with food density, and was limited by stomach capacity. If more food is encountered during a day than there is room for in the stomach, this

extra food is not consumed. Daily stomach capacity is assumed to be 10% of the body weight, and at the start of each day the stomach is assumed to be empty. The model was parameterised for herring, which is a boreal species and hence adapted to the temperature regime of the physical model. The basic function of bioenergetic models is:

$$(2) \quad G = C - (R + S + F + U)$$

where G is growth, C is energy consumed, R is energy spent on respiration, S is energy spent on specific dynamic action, F is energy lost in egestion, and U is energy lost in excretion (Wootton, 1990). For further introduction to implementation of bioenergetic models to optimisation tools, readers are referred to Rosland and Giske (1994, 1997) and Fiksen et al. (1995). Parameter values and equations can be found in Hewett and Johnson (1992).

Mortality

Daily predation risk on the fish (M_p) is assumed temperature dependent (Fiksen et al. 1995), as if predators were more active, efficient, and/or abundant in warmer waters (Fig. 4):

$$(3) \quad M_p = \frac{T_{jkt}^2}{C_1}$$

where T_{jkt} is the temperature in cell jk at day t , and C_1 is a constant (Table 1). The daily predation risk varies between 0 and 0.128 over the temperature range. Mortality is also a decreasing function of individual body weight (M_s):

$$(4) \quad M_s = e^{-\ln W_i \cdot C_2}$$

where W_i is the weight of individual i , and C_2 is a constant (Table 1). Whether an individual (and all siblings) dies during a day is determined by Monte-Carlo simulations in the following manner: IF random number $< M_p$ OR random number $< M_s$ THEN the clone is dead.

Reproduction

Reproduction can only take place for two-year olds and is confined to the area in the south-west corner ($North < 11$, $East < 11$) of the lattice during January. Mature individuals are ranked by size and spawn in descending order. Spawning is terminated when the carrying capacity (15000) is reached, and the smallest of the mature individuals may not be allowed to reproduce. During reproduction an individual (Mum, Fig. 6) produces a number of offspring in proportion to its body weight. A partner (Mate) is selected randomly from the population (both age groups included), and the string of the offspring is a recombination of the strings of Mum and Mate (Fig. 6). The “crossing over” point can only occur between characters (van Rooij et al., 1996). Further string variability may be added through changes in bit value from 1 to 0 or 0 to 1 mimicking biological mutations. This is done probabilistically by using Monte-Carlo simulations (Table 1). The individuals who manage to reproduce the most will by definition be those that are more fit for life in “Mare Pentium”. The selection scheme is hence very similar to the way in which natural selection acts (Darwin 1859). By repeating this procedure over and over the population will consist of increasingly fit members. We assume that eggs and larvae drift passively north-eastwards as they grow and develop. This life history phase is not modelled explicitly here. Rather, offspring are released into the southwest part of the lattice as half-year olds in July.

A disadvantage of using the individual based approach the way it is applied here is that one is dependent on having a non-extinct and reproducing population for the model not to terminate. This causes some obstacles in the initial phases of a model run when individuals are poorly

adapted, which often results in population crashes. To overcome this problem we decomposed the training of the ANN by starting with low mortality rates and then increased the mortality in a stepwise manner to the desired level when the population had become sufficiently adapted to cope with it. Training decomposition was also used to gradually restrict the geographic area for successful spawning. The model was always run for at least 200 years with its final configuration.

Movement

Movement was implemented using the combination of the GA and ANN, collectively termed the ING concept here (Individual based Neural network Genetic algorithm). The GA is a heuristic technique that uses the principle of evolution by recombinations, mutations, and natural selection to search for optimal solutions to a problem (Holland, 1992). ANNs use the neurobiological principles of brain-activity to perform complicated decisions. In the same way that brain cells are connected by synapses, an ANN is made up of clusters of nodes. These clusters learn by adjusting the weights between them so that input can be processed and proper output can be performed (firing or not firing of output nodes). The ANN consists of an input layer an output layer and from zero to several hidden layers (Anderson, 1996). The weights of the ANN are presently evolved using the GA (Montana and Davis, 1989, van Rooij et al. 1996).

In order to avoid confusion between biological genetics and GA “genetics” we adopt the GA terminology suggested by Goldberg (1989), hence a ‘chromosome’ will be termed string, a ‘gene’ will be termed character, and ‘allele’ will be termed character value. An important aspect of the GA is the representation of solutions as vectors of binary digits. Each individual has a string of binary digits with a length of 516 bits, each of which has the value 0 or 1. This string is divided into characters of 5 bits each. Character values are calculated relative to the potential maximum value using the binary digit system. For example the value of the character 01010 is calculated as $0^0 + 2^1 + 0^2 + 2^3 + 0^4 = 10$, which is then divided by the maximum value (all 1’s) of 31 to give a character value of 0.322. The character values were used as weights in the ANN and as threshold values for switching between RMC and PMC (as described below).

The input layer is connected to the hidden layer by a matrix of weights that gives their connection strength (Fig. 5). The hidden layer is further connected to the output layer by a second set of weights. Altogether 100 weights are applied in the two networks. The values coming into a node are added together (n_o):

$$(5) \quad n_o = \sum_{h=1}^5 W_{ho} L_h$$

where L_h is the standardised value (see Eq. 6) coming out of nodes in the hidden layer, and W_{ho} is the weight matrix between the hidden- and output layers (Fig. 5). Before being passed on to the output nodes the values are converted using the standard sigmoid function (e.g. Anderson, 1996):

$$(6) \quad L_o = \frac{1}{(1 + e^{-n_o})}$$

This procedure is performed for the hidden layer as well, and is similar for both the reactive and predictive networks. There are four nodes in the output layer, each of which may be excited or not during a time step. An output node is excited if the standardised sum of weights and input values in the output layer (L_o , Eq. 6) is above the level of excitation ($\theta=0.91$, Fig.

5). If an output node is excited it takes a value of 1 or else the value is 0. Each of the nodes has specific features upon firing, and node one and two work in the north-south direction whereas node three and four work along the east-west axis (Fig. 5). Change in habitat value along the north-south axis is denoted by the ΔN value and by the ΔE value along the east-west axis. If node one is excited the ΔN value is increased by one and if node two is excited the ΔN value is decreased by one. The relative change in habitat is thus calculated simply by subtracting the value of node one from the value of node two:

$$(7) \quad \Delta N = \eta_1 - \eta_2$$

where η_1 and η_2 refer to output nodes number 1 and 2. Similarly the relative change in the east-west extension is calculated by:

$$(8) \quad \Delta E = \eta_3 - \eta_4$$

It follows that if neither of the output nodes or both are excited, ΔE and/or ΔN will be zero. The individual will then move (or stay) relatively to its present location according to the ΔN and ΔE values in the next time step.

Swimming velocity is 0.1 ms^{-1} when the fish stays within the same cell as the previous day, assuming that the fish moved about within the cell in a random walk. If the fish moves the swimming speed is equal to the distance travelled divided by the time it has used (24 hours). The distance is calculated as minimum distance between the centre of the cells in the lattice:

$$(9) \quad d = D\sqrt{\Delta N^2 + \Delta E^2}$$

where d is distance travelled, D is the length of a cell (20 km), and ΔN and ΔE is net movement in the north-south and east-west directions respectively. Eq. 10 underestimates the actual swimming costs, as fish normally do not swim in straight lines over long distances. Individuals are restricted from moving beyond the outer boundaries of the lattice.

Table 1. Parameters used in the model. DL is dimensionless.

Parameter	Description	Value	Unit
C_1	-	500	DL
C_2	-	2.5	DL
-	Offspring per parent body weight	1	individuals g^{-1}
-	Maximum search radius	0.5	m
-	Standard swimming velocity	0.1	$m\ s^{-1}$
-	Mutation probability (per bit)	0.001	DL

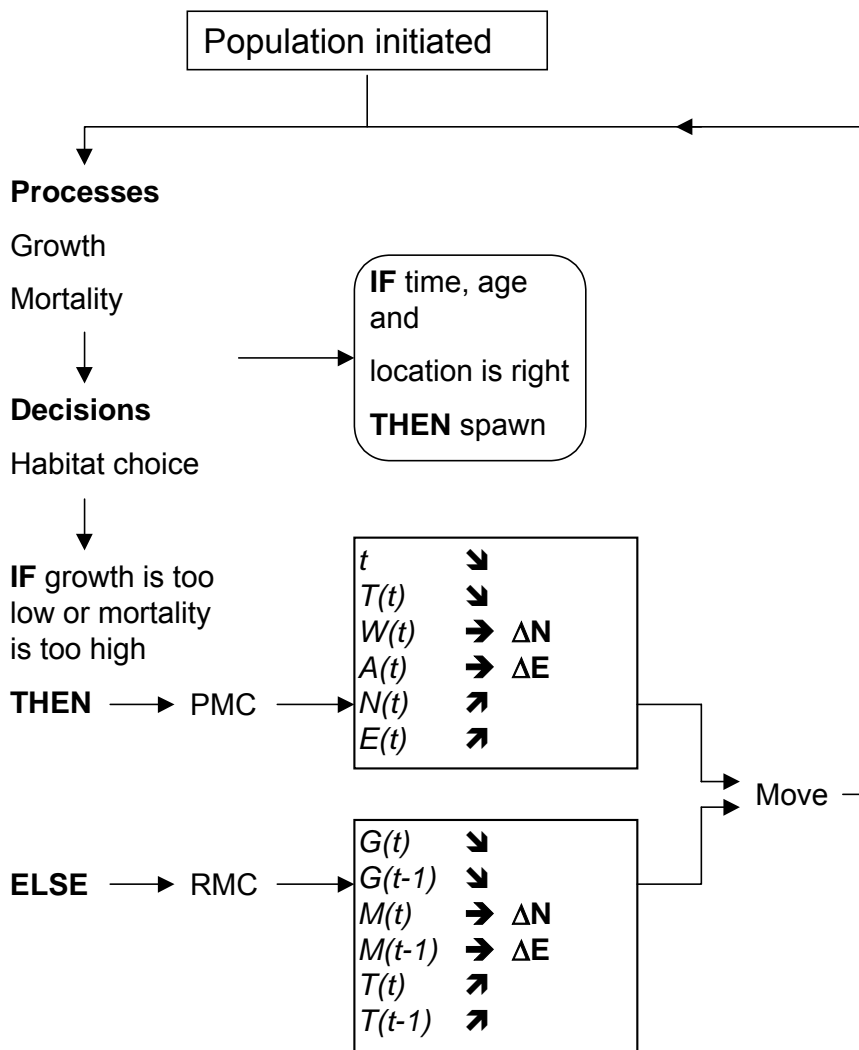


Figure 1. Flow chart of the daily activities of the fish where t is Julian day, $T(t)$ is temperature, and $W(t)$, $A(t)$, $N(t)$, $E(t)$, $G(t)$, and $M(t)$ are weight, age, northerly position, easterly position, daily growth, and daily mortality risk at day t respectively.

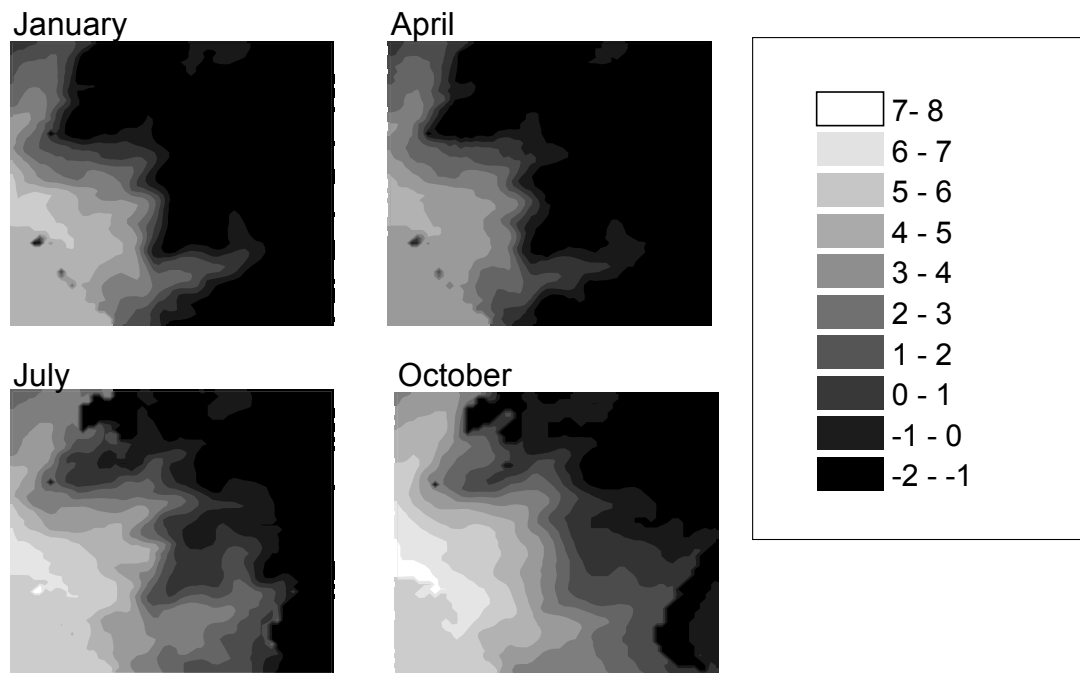


Figure 2. Temperature (°C) distribution at the beginning of quarterly intervals throughout the year. The top of the figure is north, and east is to the right.

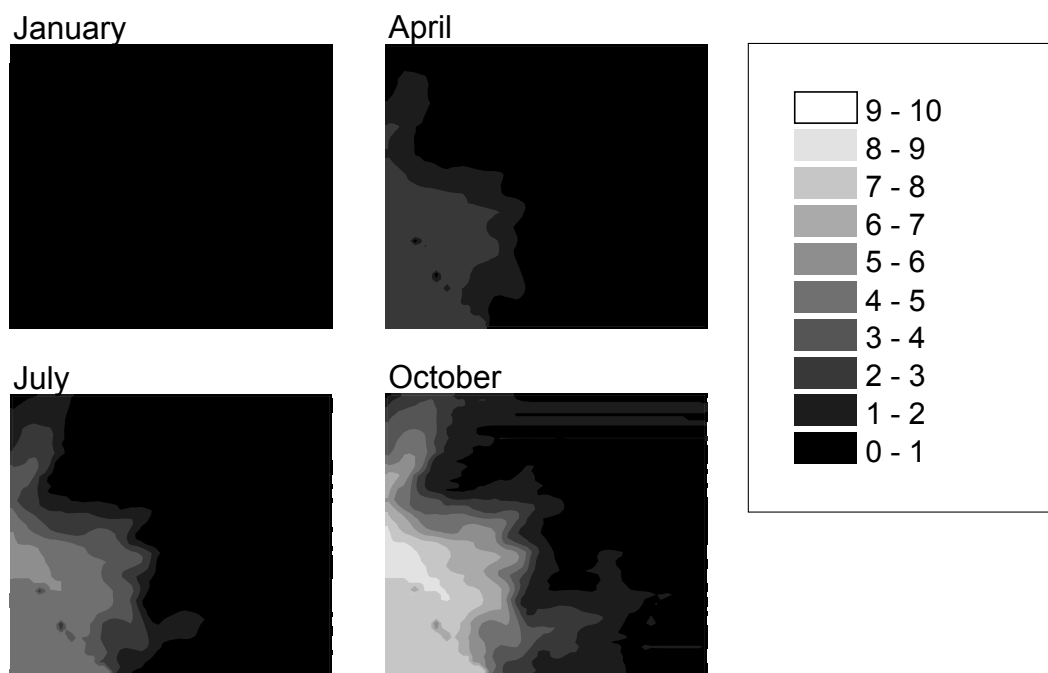


Figure 3. Zooplankton distribution ($\times 10^{13} \text{ cell}^{-1}$) at the beginning of quarterly intervals throughout the year.

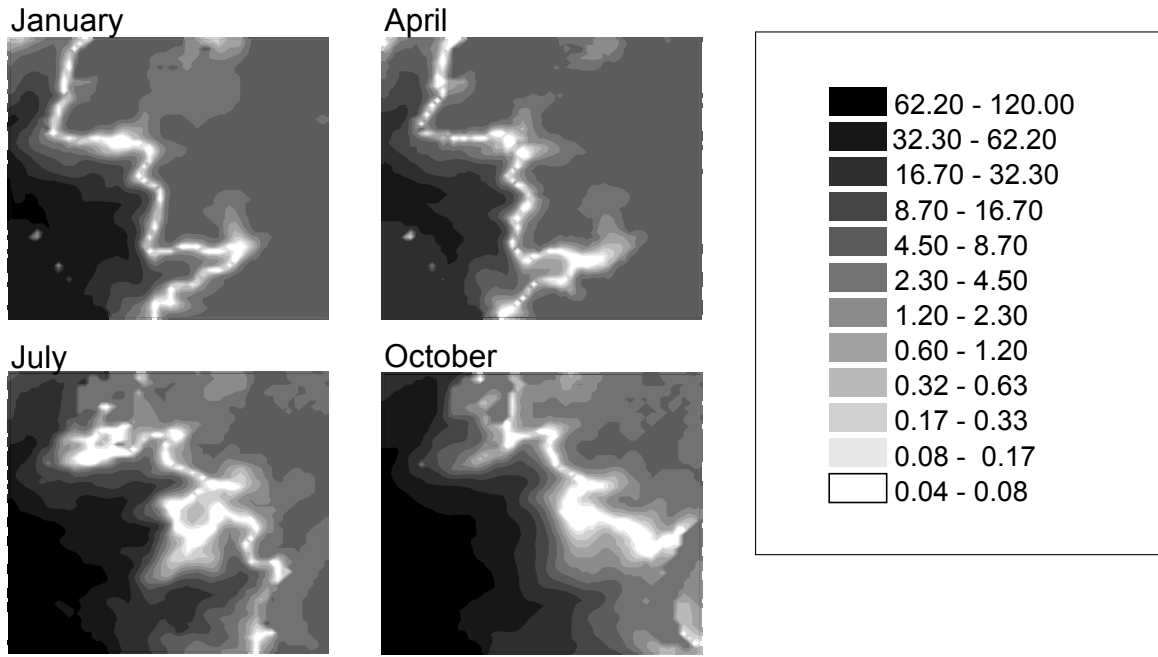


Figure 4. Distribution of daily predation risk (log scale, $\times 1.0^{-3}$) at the beginning of each quarterly interval throughout the year.

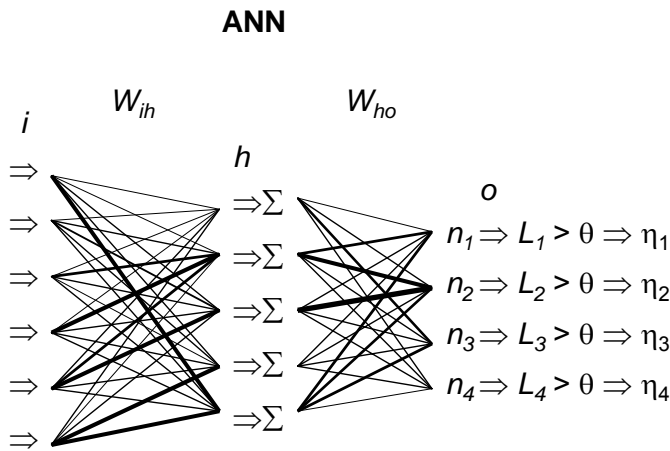


Figure 5. Description of the ANN (RMC or PMC) applied in the present model. The i , h , and o refer to input-, hidden-, and output layers respectively. The input layer consists of internal or environmental input that is different for RMC and PMC. The output nodes fire if the L_o value is above the threshold value ($\theta=0.91$). The lines indicate the relationship between the different layers. Each of the nodes in the i -layer are connected to all the nodes in the h -layer and each of the nodes in the h -layer are connected to all the nodes in the o -layer. W_{ih} and W_{ho} are the weight matrices of connection strengths between the nodes of the layers. Potential weight differences are indicated by the variation in line thickness of the connections.

Mum	Mate	Offspring	
1	1	1	
1	0	1	
0	1	0	←Character
1	0	1	
0	0	0	
<hr/>		1	←Break point
0	1	0	
0	0	0	
1	1	1	←Character
1	0	0	
1	0	0	

Figure 6. Example of how recombination and hence creation of new individuals is carried out. Mum is the individual who reproduces and Mate is a randomly drawn individual from the population. The string of offspring is a mix of “Mum” and “Mate”, and bits above and below the “crossing over” point are copied from “Mum” and “Mate” respectively.

Example Shore Birds I

The original model description, including all full references, is presented in the following two papers:

Stillman, R.A., Goss-Custard, J.D., West, A.D., Durell, S.E.A. le V., Caldow, R.W.G., McGrorty, S. & Clarke, R.T. (2000). Predicting to novel environments: tests and sensitivity of a behaviour-based population model. *Journal of Applied Ecology*, 37, 564-588.

Abstract: 1. In order to assess the future impact of a proposed development or evaluate the cost effectiveness of proposed mitigating measures, ecologists must be able to provide accurate predictions under new environmental conditions. The difficulty with predicting to new circumstances is often that there is no way of knowing whether the empirical relationships upon which models are based will hold under the new conditions, and so predictions are of uncertain accuracy.

2. We present a model, based on the optimality approach of behavioural ecology, which is designed to overcome this problem. The model's central assumption is that each individual within a population always behaves in order to maximize its fitness. The model follows the optimal decisions of each individual within a population and predicts population mortality rate from the survival consequences of these decisions. Such *behaviour-based* models should provide a reliable means of predicting to new circumstances because, even if conditions change greatly, the basis of predictions – fitness maximization – will not.

3. The model was parameterized and tested for a shorebird, the oystercatcher *Haematopus ostralegus* L.. Development aimed to minimize the difference between predicted and observed overwinter starvation rates of juveniles, immatures and adults during the model calibration years of 1976-80. The model was tested by comparing its predicted starvation rates with the observed rates for another sample of years during 1980-91, when the oystercatcher population was larger than in the model calibration years. It predicted the observed density-dependent increase in mortality rate in these years, outside the conditions for which it was parameterized.

4. The predicted overwinter mortality rate was based on generally realistic behaviour of oystercatchers within the model population. The two submodels that predicted the interference-free intake rates and the numbers and densities of birds on the different mussel *Mytilus edulis* L. beds at low water did so with good precision. The model also predicted reasonably well (i) the stage of the winter at which the birds starved, (ii) the relative mass of birds using different feeding methods, (iii) the number of minutes birds spent feeding on mussels at low water during both the night and day and (iv) the dates at which birds supplemented their low tide intake of mussels by also feeding on supplementary prey in fields while mussel beds were unavailable over the high water period.

5. A sensitivity analysis showed that the model's predictive ability depended on virtually all of its parameters. However, the importance of different parameters varied considerably. In particular, variation in gross energetic parameters had a greater influence on predictions than did variations in behavioural parameters. In accord with this, much of the model's predictive power was retained when a detailed foraging submodel was replaced with a simple functional response relating intake rate to mussel biomass.

6. Although we applied the model to oystercatchers, the general principle on which it is based applies widely. We list the key parameters which need to be measured in order to apply the model to other systems, estimate the time scales involved and describe the types of environmental changes that can be modelled. For example, in the case of estuaries, the model can be used to predict the impact of habitat loss, changes in the intensity or method of shellfishing, or changes in the frequency of human disturbance.

7. We conclude that behaviour-based models provide a good basis for predicting how demographic parameters, and thus population size, would be affected by novel environments. The key reason for this is that, by being based on optimal decision rules, animals in these models are likely to respond to environmental changes in the same way as real ones would.

Goss-Custard, J.D., Stillman, R.A., West, A.D., Caldow, R.W.G., Triplet, P., Durell, S.E.A. le V. dit & McGrorty, S. (2004). When enough is not enough: shorebirds and shellfish. *Proceedings Royal Society B*, 271, 233-237.

Abstract: In a number of extensive coastal areas in NW Europe, large numbers of long-lived migrant birds eat shellfish that are also commercially harvested. Competition between birds and people for this resource often leads to conflicts between commercial and conservation interests. One policy to prevent shellfishing from harming birds is to ensure that enough food remains after harvesting to meet most or all of their energy demands. Using simulations with behaviour-based models of five areas, we show here that even leaving enough shellfish to meet 100% of the birds' demands may fail to ensure that birds survive in good condition. It needs up to eight times this amount to protect them from being harmed by the shellfishery, even when the birds can consume other kinds of non-harvested prey.

Modified model description written by: **John Goss-Custard**

Notes: Similar to the Snail Kite model, the structure of the model (state variables and scales) is described by using a list. This is very clear and useful, but a comparison to the Snail Kite model description shows that there are different ways to organize such a list. A standard, for example following UML, will be needed in the future.

Purpose

To predict the mortality rate and body condition of the birds during the non-breeding season (September to March), and the parameters (slope and intercept) that describe the density-dependent mortality and body condition functions in (a) existing environmental conditions and in (b) the novel conditions brought about by a change in their feeding environment arising, for example, from habitat loss and/or deterioration, disturbance, shellfishing, sea-level rise and climate change, and (c) by the provision of measures aimed to mitigate the effects of such changes in the feeding environment.

State variables and scales

ENTITIES

Individual birds

Food patches

STATE VARIABLES

Individual birds:

1. Daily energy requirements
2. Body reserves
3. Foraging efficiency
4. Dominance
5. Feeding method
6. Age

Food patches:

1. *Either* The density, size and ash-free dry mass of the prey
Or interference-free intake rate of the average bird
2. Exposure time on Neap and Spring tides
3. Fraction of patch exposed at low water and at high water on Neap and Spring tides

Environmental variables:

1. Daily air temperature
2. Number of people disturbing a patch, and when they are present (Neap or Spring tides; state of tide (low or high or receding *etc*); day of week; night or day; time of year)
3. Amount of shellfishing done on a patch, and when it is done (Neap or Spring tides; state of tide (low or high or receding *etc*); day of week; night or day; time of year)

Temporal scales:

1. 1-2 hour tidal stages (low; advancing; *etc*)
2. 12.44 hour tidal cycle
3. 24 hour diurnal cycle
4. 14 day Neap-Spring tide cycle
5. 6-7 month non-breeding season

Spatial scales

1. Hectares (food patches)

Process overview and scheduling

(This description has partly been taken from: Goss-Custard, J.D., Stillman, R.A., West, A.D., Caldow, R.W.G., Triplet, P., Durell, S.E.A. le V. dit & McGrorty, S. (2004). When enough is not enough: shorebirds and shellfish. *Proceedings Royal Society B*, **271**, 233-237.)

The models represent individual birds that use optimisation decision rules to decide how to obtain most rapidly their daily energy requirements that, in the model as in reality, depend on the ambient temperature. Individuals vary in competitive ability and each bird takes into account the decisions made by competitors in deciding when (*e.g.* night or day), where (*e.g.* which shellfish bed) and on what (*e.g.* cockles or mussels or alternative prey species) it should feed. Because shellfish are more profitable for oystercatchers in winter, the birds attempt first to obtain their requirements from shellfish alone but, should they fail, they eat other intertidal invertebrates over low water or terrestrial prey, such as earthworms, over high water in some estuaries. Once an individual has obtained its current daily energy requirements, it stores subsequent consumption as body reserves up to a daily limit. A bird uses its reserves should it ever fail to obtain its daily requirement from current foraging. It starves to death if its body reserves are ever used up.

The model uses three discrete time steps - tidal stages (*e.g.* high tide, tide receding), tidal cycles and daily cycles. The following processes and events are grouped into actions that are executed together over the 24 hour daily cycle: (a) In the birds - food consumption and assimilation, meeting energy demands, laying down surplus energy as body reserves, using reserves if this is needed and calculating the state of the reserves; (b) in the prey - the reduction in prey density due to depletion by the birds and other sources of mortality, the change in the size distribution of the prey due to these mortalities and the change in the ash-free dry mass of each prey.

All actions are executed in specified order: for example, a bird's daily assimilated consumption is compared with that day's temperature-related demand for energy to determine if there is a surplus that can be used to build up the body reserves or whether, instead, existing reserves should be metabolised to meet a current energy shortfall.

Design concepts

The sub-headings and numbers in brackets follow the sequence in section 5.12.1 *Conceptual design checklist* in Grimm V, Railsback SF. 2005. Individual-based modeling and ecology. Princeton University Press, Princeton, N.J.

In each of the sections (1) – (25), the questions asked in that checklist are shown first in italics.

Emergence

(1) *Which processes in the IBM are modeled as emerging from a mechanistic representation of adaptive traits of individuals? Do the system-level phenomena the IBM is designed to explain emerge from individual traits, or are they imposed by rules that force the model to produce a certain result?*

1. Mortality through starvation over the non-breeding season in relation to population size, bird age, feeding method *etc.*
2. Body reserves at any stage of the non-breeding season (but usually at the end just before the start of spring migration) in relation to population size, bird age, feeding method *etc.*

3. Aggregated behaviour of all individuals; distribution across food patches, time spent feeding per 24 hours, usage of terrestrial feeding areas over low and high water, occurrence of feeding at night

These system-level phenomena emerge from the individual traits and environmental conditions and are not imposed by rules.

Adaptation

(2) *What adaptive traits do the model individuals have to improve their potential fitness, in response to changes in themselves or their environment?*

Survival over the non-breeding season: birds starve to death when body reserves fall to zero, for example, during prolonged periods of severe weather with high energy demands but low prey availability.

Departure in spring with enough body reserves to migrate successfully to the breeding areas and to start breeding

(3) *Which adaptive traits are modeled as direct fitness-seeking, with individuals making decisions explicitly to improve their expected success at passing genes on to future generations?*

None.

(4) *Which adaptive traits are modeled as indirect fitness-seeking, in which individuals make decisions to meet a specific objective that indirectly contributes to future success at passing genes on?*

Survival and body mass in spring enable birds to breed in summer elsewhere

Fitness

(5) *For traits modeled as direct fitness-seeking, how complete is the fitness measure used to evaluate decision alternatives? The fitness measure is the individual's internal model of how its expected fitness depends on which alternative it chooses. Which elements of potential fitness – survival to reproduction, attainment of reproductive size or life stage, gonad production, etc. – are represented in the fitness measure? Is the completeness of the fitness measure consistent with the IBM's objectives?*

1. Survival to reproduction

2. Attainment of body condition for spring migration

The fitness measures are entirely consistent with the IBM's objectives.

(6) *How direct is the fitness measure? What variables and mechanisms are used to represent how an individual's decision affects its future fitness? Is the choice of variables and mechanisms consistent with the IBM's objectives and the biology of the system being modeled? Does the fitness measure have a clear biological meaning? Does the fitness measure allow the individual to make appropriate decisions even when none of the alternatives are good?*

Indirect fitness measure, which has clear biological meaning. The mechanism is for each individual to make the decisions that minimise the time it takes to attain its target body reserves (*i.e.* it maximises its intake rate while foraging) and thus maximise its chances of reaching that target. The fitness measure does allow an individual to make the best of a bad job through its rate-maximising decision rules.

(7) *How is the individual's current state considered in modeling fitness consequences of decisions?*

An individual continues foraging whenever and wherever it can in order to reach its body reserve target each day as quickly as it can.

(8) *Should the fitness measure change with life stage, season, or other conditions?*

No: the fitness measures always apply

Prediction

(9) *In estimating future fitness consequences of their decisions, how do individuals predict the future conditions (internal as well as environmental) they will experience? Do the simulated prediction methods produce realistic behavior while being biologically realistic? Are prediction methods appropriate for the time scales used to model fitness-seeking? Do the individual's predictions make use of memory? Of learning? Environmental cues?*

'Prediction' of the future conditions is done using the pre-set target body reserves which vary seasonally according to the expected difficulty the birds will have in acquiring their energy requirements; for example, target body reserves are high in mid-winter when the feeding conditions can be difficult because of severe weather. This prediction method does produce realistic behaviour: for example, it predicts when birds will start supplementing their consumption over low tide on the estuary by using fields over high tide when their estuary food sources are unavailable. The time scales are appropriate. There is no memory or learning or environmental cues.

(10) *What tacit predictions are included in the IBM? What assumptions are implicitly embedded in the tacit predictions?*

The main tacit assumptions are (a) that individuals aim to balance their energy demands over each 24 hour period, (b) that an individual's foraging efficiency and dominance remain constant throughout the non-breeding season and do not change if it approaches starvation, and (c) that the animals are not subjected to attack by parasites and predators.

Interaction

(11) *What kinds of interaction among individuals are assumed? Do individuals interact directly with other individuals? (With all others or only with neighbors?) Or are interactions mediated, e.g., through competition for a shared resource? Or do individuals interact with a "field" of effects produced by neighbors?*

Individuals interact with non-identified neighbours as they feed and this causes interference competition. Competition also occurs through depletion of the shared food resource. Both interference and depletion competition are 'field' effects produced by non-specified competitor individuals.

(12) *What real interaction mechanisms, at what spatial and temporal scales, were the IBM's interaction design based on?*

Interference competition arises because dominant individuals attack sub-dominant individuals for their prey or feeding spot on the mussel bed. Sub-dominants can avoid these attacks when bird densities are low but cannot do so when bird density is high. The intake rate of sub-dominants therefore decreases as the density of birds increases on the feeding patch, the effect being most marked in the least dominant individuals.

Sensing

(13) *What variables (describing both their environment and themselves) are individuals assumed to sense or "know" and consider in their adaptive decisions?*

The birds know their current intake rate in the food patch where they are located and their potential intake rate in all the other patches where they could feed.

(14) *What sensing mechanisms are explicitly simulated? Does the IBM represent the actual sensing process?*

No sensing mechanisms are explicitly represented.

(15) *If sensing is not simulated explicitly, what assumptions are made about how individuals “know” each sensed variable? With what certainty or accuracy are individuals assumed able to sense each variable? Over what distances?*

At the beginning of every tidal stage, each individual ‘visits’ each potential feeding patch and moves to the patch that at that time gives it the highest intake rate, given the food supply and the intensity of interference competition present on the patch. The birds can only detect differences between patches if their intake rates on the patches differ by $>3\%$. Birds visit all potential patches within the estuary; in the larger estuaries, this is an unrealistic assumption.

Stochasticity

(16) *Are stochastic processes used to simulate variability in input or driving variables? Is stochasticity preferable to using observed values? Is it clearly desirable for these inputs or drivers to be variable?*

The only source of stochasticity is that the values for foraging efficiency and dominance given to each individual is drawn at random from empirically-determined distributions of each characteristic. As a result, the combinations of foraging efficiency and dominance amongst the birds vary a little from simulation to simulation. Foraging efficiency and dominance are vital characteristics of the model birds because this individual variation enables the model to predict mortality rates that lie between the extremes of 0% and 100%. Without it, of course, either all the birds would survive or all would starve.

(17) *What traits use stochastic processes to reproduce behavior observed in real organisms? Is this approach clearly recognized and used as an empirical model?*

The intake rate of an individual is affected by its foraging efficiency and dominance which therefore affect the chances that it will achieve the current target mass. This is clearly recognised.

(18) *What variable low-level processes are represented empirically as stochastic processes? Is the variability important to include in the IBM?*

Foraging efficiency and dominance. This variability is vital as between them they describe the variation in competitive ability between individuals.

Collectives

(19) *Are collectives represented in the IBM? Collectives are aggregations of individuals (flocks, social groups, stands of plants) included in an IBM because the state and behavior of an individual depends strongly on (a) whether the individual is in a collective, and if so, (b) the state of the collective.*

Aggregations are included in the model.

(20) *How are collectives represented? Do collectives occur only as phenomena emerging from individual behavior, or are individuals given traits that impose the formation of collectives? Or are collectives represented as explicit entities with their own state variables and traits?*

Aggregations are represented as the density of birds on each food patch. Bird density on each patch emerges solely as a consequence of model individuals responding separately to their common feeding environment (the food supply and competitive pressure on each patch). The density that results from this process is then increased by the empirically-determined factor of

3-10 times because, in nature, birds aggregate in the best parts of a patch, and this affects the level of interference competition that each bird experiences as it forages. Collectives are not represented as explicit entities (e.g. flocks, family parties) with their own state variables and traits.

Observation

(24) *What kinds of model results must be observed to test the IBM and meet its objectives?*

The following are used to test model predictions:

- Proportion birds starving over the non-breeding season
- The stage of the season when most starvation occurs
- Body reserves
- Amount of time spent feeding per tidal cycle
- The amount of feeding done on supplementary foods, over high tide, for example
- Intake rates of particular classes of birds on particular prey species
- Distribution of birds across food patches

(25) *From what perspectives are observations of results taken: omniscient, model individual, or virtual ecologist?*

Both ‘omniscient’ and ‘virtual ecologist’

Initialization

BIRDS All birds within each age-class and feeding method group are given the same initial mass but their individual competitive abilities (foraging efficiency and dominance) are chosen at random from empirically-determined distributions of foraging efficiency and dominance.

PREY PATCHES The initial areas of each patch, along with the densities, size distribution and ash-free dry masses of each size class of prey on each patch, are taken from field surveys conducted in September for the year in question. The subsequent mortality and loss of flesh-content (if any) of the prey between September and March are taken from field surveys.

Input

TIDAL STAGES The start time (hours after high tide) and duration of each tidal stage on each patch, along with the proportion of the patch exposed at low tide and high tide on Neap and Spring tides, as determined by field observation.

WEATHER The daily mean the minimum and maximum air temperature as measured in a weather station near to the estuary.

DISTURBANCE The number of disturbers on each patch, their length of stay on the patch, whether two or more disturbers are in a group or spread out over the patch and the radius of the circle around a

disturber into which birds will not venture. The time and energy costs of being disturbed are also specified along with the amount of time it takes birds at different stages of the non-breeding season to resume feeding after being disturbed.

SHELLFISHING

The number of fishers along with their daily catch quota, fishing method and the duration of their presence on the patch during a tidal cycle.

Submodels

[Not included here; please refer to the original publication.]

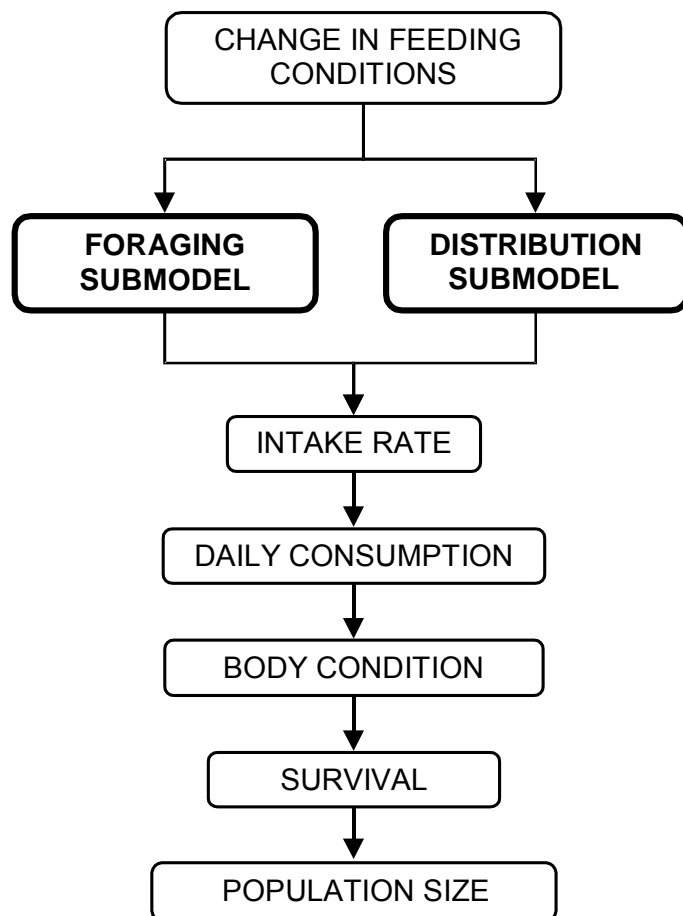


Figure 1. Flowchart showing how the model predicts the effect of the winter mussel food supply on the body condition of individual oystercatchers and on the starvation rates of the population. The two behaviour submodels are outlined with heavy lines.

Example Shore Birds II

The following model description has not been published elsewhere, but represents work in progress.

The model description was written by: **Richard Stillman**

Purpose

The overall purpose of the model is to predict how environmental change (e.g. habitat loss, changes in human disturbance, climate change, mitigation measures in compensation for developments and changes in population size itself) affects the survival rate and body condition in animal populations. The model does not itself predict reproductive rate but its survival and body condition predictions can be input into other models that do make this prediction.

The model has been designed to be very flexible (hence the name MORPH), so that it can produce both general predictions (when parameterised in a very simple way), and predictions for specific systems (when parameterised using detailed system-specific data). The model itself contains only very general aspects of behaviour and ecology, applicable to a wide range of systems. Site-specific versions of the model are being parameterised for ten shorebird species in three European estuaries, and multi-site versions for two shorebirds in the UK, one goose species in western Europe, and one duck species in the Irish Sea.

State variables and scales

The model represents time as discrete time steps with a fixed duration. Space is represented by discrete patches with fixed location. The model defines the following five entities.

- *Global environment* - State variables which apply throughout the modelled system.
- *Patches* - Locations with local, patch variables, containing resources and foragers. Foragers may experience travel costs when moving between patches.
- *Resources* - The food consumed by foragers. Foragers can simultaneously consume one or more resources from a patch. Such collections of resources are termed *diets*.
- *Components* - Elements within resources which foragers assimilate into their bodies.
- *Foragers* - Animals which move within the system attempting to maximise their survival and body condition. One or more forager *morphs* / *species* may be present within the modelled system.

Table 1 lists the state variables used to describe each entity. The global state variables are the major driving variables in the model system. Patch variables may depend on these global variables. Patches contain one or more resources, which in turn contain one or more components. Foragers have a range of possible diets, which are simply a collection of resources. Foragers consume diets, from which they assimilate components. Components can either have positive, neutral or negative effects on foragers. Foragers are not forced to consume diets, but instead may occupy a patch and not feed.

Table 1. State variables used to describe model entities.

Entity	State variable	State variable description
<i>Global</i>	<ul style="list-style-type: none"> Global variables 	Zero or more environmental variables which apply throughout the modelled system
<i>Patches</i>	<ul style="list-style-type: none"> Location Size Patch variables 	<p>Central coordinates</p> <p>Surface area / volume of patch</p> <p>Zero or more patch-specific environmental variables</p>
<i>Resources</i>	<ul style="list-style-type: none"> Density on patch 	Density of each resource on each patch
<i>Components</i>	<ul style="list-style-type: none"> Density in resource 	Density of each component within each resource on each patch
<i>Foragers</i>	<ul style="list-style-type: none"> Morph / species Forager constants Forager variables Location Patch Diet Proportion of time moving Proportion of time feeding Diet consumption rate Component consumption rate Component assimilation rate Component metabolic rate Component reserve size 	<p>Forager morph / species to which forager belongs</p> <p>Zero or more forager-specific constants which remain constant throughout a simulation</p> <p>Zero or more forager-specific variables which can change throughout a simulation</p> <p>Coordinates of foragers location</p> <p>Patch number being occupied by forager during current time step</p> <p>Diet number being consumed by forager during current time step (zero if no diet is being consumed)</p> <p>Proportion of time moving during current time step and averaged over previous time steps</p> <p>Proportion of time feeding during current time step and averaged over previous time steps</p> <p>Rate at which diet is being consumed during current time step and averaged over previous time steps</p> <p>Rate at which a component is being consumed during current time step and averaged over previous time steps</p> <p>Rate at which a component is assimilated into the body during current time step and averaged over previous time steps</p> <p>Rate at which a component is metabolised / excreted from the body during current time step and averaged over previous time steps</p> <p>Amount of a component within the body's reserves during current time step and averaged over previous time steps</p>

<ul style="list-style-type: none"> • Perceived survival probability 	Perceived survival probability associated with current state, location and diet during current time step and averaged over previous time steps
------------------------------------------------------------------------------------	------------------------------------------------------------------------------------------------------------------------------------------------

Process overview and scheduling

The model defines the following processes.

- *Change in resource density.* Changes in the density of a resource on a patch caused by consumption by the foragers and / or other factors.
- *Change in component density.* Changes in the density of a component in a resource.
- *Forager immigration.* The movement of foragers into the system.
- *Forager decision making.* The optimal patch and diet selection of foragers and decisions to emigrate from the system.
- *Forager emigration.* The movement of foragers away from the system.
- *Forager movement between patches.* Movement of foragers between patches. Movement may have associated costs and may take more than one time step.
- *Forager diet consumption.* The transfer of resource components into foragers when diets are consumed.
- *Forager physiology.* Change in the size of a forager's component reserve due to the balance of consumption and metabolism.
- *Forager mortality.* Death of foragers.

Time is represented using discrete time steps which are of constant duration. Foragers are either processed synchronously or asynchronously. The order in which foragers are processed can either be random or based on the value of a specified forager constant. Figure 1 shows the sequence of events during each time step. Global events are processed first, followed by patch events and then forager events. Finally, results are displayed and saved.

Design concepts

Emergence

The following phenomena emerge from the interaction between individual forager traits and global and patch variables, resource and component densities, and forager constants and variables.

- *Resource depletion.* The amount of each resource consumed by foragers from each patch during each time step.
- *Forager distribution and diet selection.* The location of each forager and its diet during each time step.
- *Proportion of time foragers spend feeding.* Proportion of each time step each forager spends feeding.
- *Forager component reserve size.* The amount of each component within each forager's reserves during each time step.
- *Forager mortality and emigration.* The number of foragers remaining in the system after a given number of time steps.

Adaptation

Foragers adaptive traits are their location and diet selection. During each time step, foragers select the patch / diet combination which maximises their perceived fitness, or emigrate from the entire system if this has a higher perceived fitness than any patch / diet combination.

Fitness

Fitness is assumed to equal the probability of surviving to the end of a time step. Survival probability is influenced by a number of mortality sources (causes of death). Each mortality source has associated submodels (see below) to calculate (i) the true probability of surviving the mortality source during a time step and (ii) the perceived probability of surviving, both as functions of any combination of state variables, and patch / diet selection. The combined true and perceived survival probabilities are the product of the survival probabilities associated with each mortality source (see below). The forager selects the patch and diet combination (including no diet) which maximises its perceived survival, or emigrates from the system if this has a higher perceived survival than the possible patch and diet combinations. Once the forager has selected a patch and diet, the consequences of this decision are determined by true probability of survival.

Prediction

Foragers remember their foraging success during a given number of previous time steps. This memory is used to calculate average state variables over previous time steps (see Table 1 for a list of these variables). These average values can be used by submodels which predict that future foraging success will be some function of past foraging success. The model does not allow foragers to know the future values of any state variables, instead these must be predicted.

Interaction

Foragers interact within patches through the consumption of a shared resource (depletion competition). The number and / or density of other foragers within a patch can also effect any of a forager's state variables, and hence perceived and true survival probabilities. These effects can be either positive or negative, depending on the submodels used. Increased competitor numbers or density can either increase consumption rate (facilitation) or decrease consumption rate (interference competition), again depending on the submodels used. Foragers can only interact within patches. The actual mechanisms of interactions within patches are not incorporated explicitly.

Sensing

The amount of knowledge foragers have can be varied. This can range from perfect knowledge of the complete system during the current time step, through complete knowledge of local patches, to no knowledge at all. Similarly, the amount of knowledge a forager has of its own state, both during the current time step and previous time steps, can be varied. Foragers base their decisions on the perceived survival probability associated with different patches and diets (or no diet). The perceived survival probability may or may not be equal to the true probability. Foragers will tend to avoid patches and diets with low perceived survival probabilities. Depending on the relationship between the true and perceived probabilities, this can mean that foragers avoid safe patches and diets (i.e. high true survival probability) because these are perceived as dangerous (i.e. low perceived survival probability), or select dangerous patches or diets because these are perceived as safe. The model does not explicitly represent any sensing mechanisms.

Stochasticity

The amount of stochasticity can be varied. Any state variables, except for patch size and location, and forager morph / species can be stochastic. The probability of a forager (or the

individuals within the forager (see below)) dying during a time step is a stochastic event unless the probability is zero or one.

Collectives

Collectives are included in the model. These are represented by the number and / or density of foragers on each patch, and arise from the patch and diet selection of foragers. Collectives are not represented as social groups, instead each individual behaves independently albeit with its behaviour influenced the number and / or density of competitors on different patches. Super-individuals can be incorporated, with each forager (super-individual) representing more than one individual. The number of individuals within a forager is set at the start of a simulation, but can decrease through time as some individuals within the forager die. In contrast, all individuals within a forager simultaneously immigrate to or emigrate from the system.

Observation

The results used to test the model depend on the particular system for which it is parameterised. All state variables can be displayed and saved during each time step. Omniscient results are calculated.

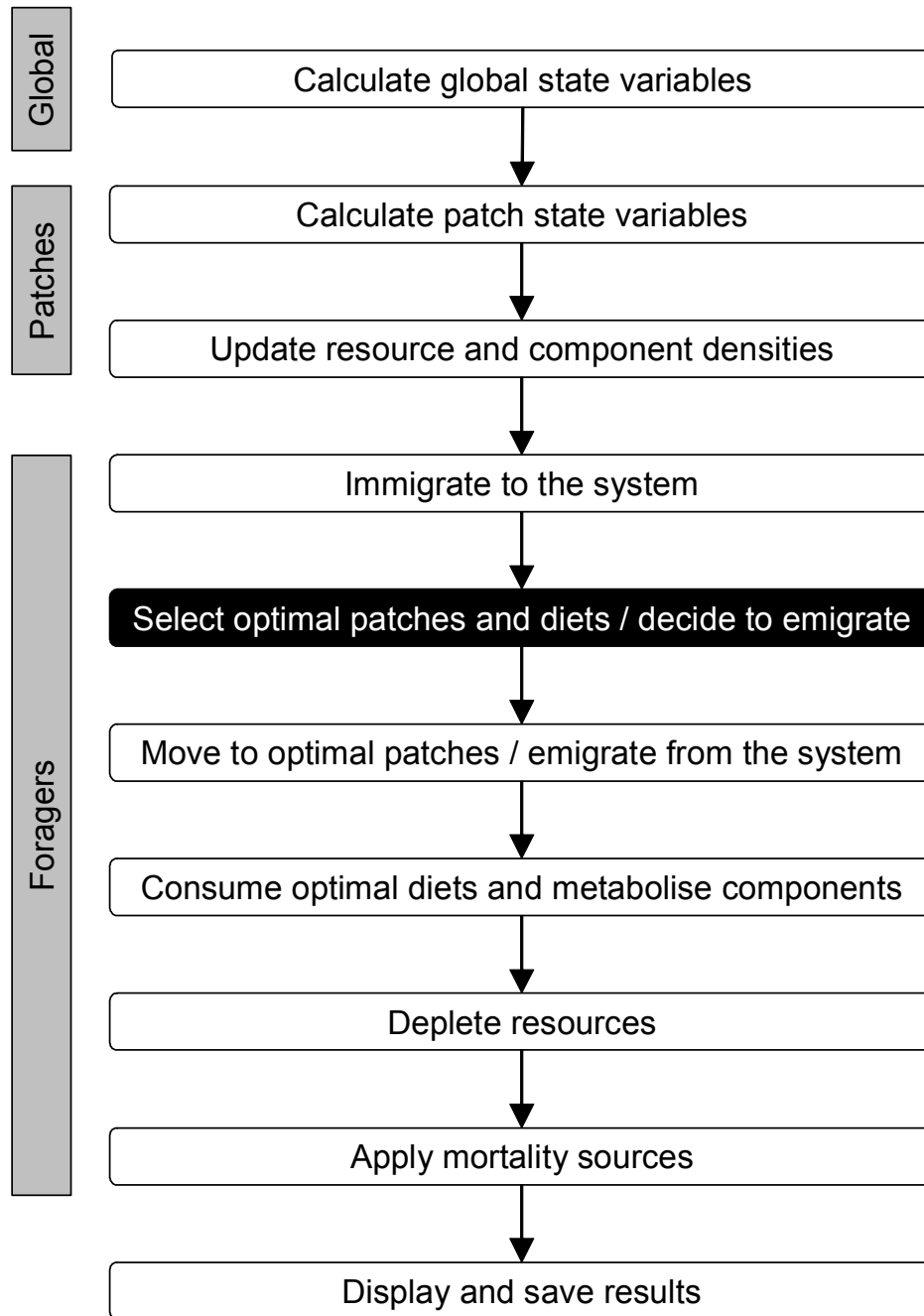


Figure 1. The sequence of events during each time step. The grey bars show the entity in which each event occurs. The black box indicates where foragers adaptive traits are executed to determine which patch and diet to feed on or whether to emigrate from the system. Forager events are either processed synchronously or asynchronously. Foragers are only processed once they immigrate to the system, and are no longer processed after they emigrate or all their individuals have died. Patch and diet selection does not occur while foragers are moving. Components are metabolised while a forager is moving, unless moving is instantaneous.

Initialization

The initial values of state variables are either read from a parameter file, created using random numbers, or calculated from state variables defined earlier in the parameter file. The sequence of random numbers is itself randomised at the start of each simulation so that replicate simulations using the same set of parameters will produce slightly different predictions. All global and patch variables are initialised at the start of the simulation. Forager state variables are initialised once the forager has immigrated into the system, and so foragers immigrating at different times may have different initial state variables.

Input

The particular data used to parameterise the model will depend on the particular system to which it is applied. However, Table 2 lists the basic set of parameters, which would be required for any system. Parameters can either be single values, values for each time step read in from a file, or an equation (submodel) to calculate values during each time step.

Table 2. Basic set of parameter values / submodels required by the model.

Entity	Parameter
<i>Global environment</i>	<ul style="list-style-type: none">• Number and names of global variables• Value / submodel for each global variable
<i>Patches</i>	<ul style="list-style-type: none">• Number and names of patches• Size of each patch• Location of each patch• Value / submodel for each patch variable on each patch
<i>Resources</i>	<ul style="list-style-type: none">• Number and names of resources• Initial density of each resource on each patch• Submodel for change in density (excluding consumption by foragers) of each resource on each patch
<i>Components</i>	<ul style="list-style-type: none">• Number and names of components• Value / submodel for density of each component in each resource on each patch
<i>Diets</i>	<ul style="list-style-type: none">• Number and names of diets• Number and names of resources in each diet
<i>Foragers</i>	<ul style="list-style-type: none">• Number and names of forager morphs / species, and morph / species of each forager• Number and names of forager constants• Value of each forager constant for each forager• Number and names of forager variables• <i>Value / submodel for each forager variable</i>• Speed of movement between patches• Number and names of diets consumed by forager morph / species• Rule to determine whether patches can be located

- Rule to determine whether fitness can be perceived on a patch
 - Value / submodel for diet consumption rate
 - Value / submodel for maximum diet consumption rate
 - Value / submodel for assimilation efficiency of each component
 - Value / submodel for rate of metabolising each component while feeding, resting or moving
 - Value / submodel for target reserve size for each component
 - Number of mortality sources
 - Value / submodel for perceived survival probability for each mortality source
 - Value / submodel for true survival probability for each mortality source
 - Value / submodel for expected survival probability on patches on which survival cannot be perceived
 - Value / submodel for expected survival probability of emigrating
-

Submodels

Many of the model's submodels will be read in as equations from the parameter files. In these cases the particular submodels will depend on the specific system to which the model is being applied. These are termed *parameter submodels* in the follow sections. However, a number of submodels are incorporated into the model itself. The following sections describe the submodels used to represent each of the models processes.

Change in resource density

Resource densities change on patches due to (i) *non-depletion change* and (ii) *depletion* when foragers consume diets on a patch.

Non-depletion change is calculated at the start of each time step, using a parameter submodel which determines how resource density is updated at the start of each time step.

$$(1) R = f(p_1, p_2 \dots p_n) R_{previous}$$

where R = new resource density at start of current time step, $R_{previous}$ = old resource density at end of previous time step, $f(p_1, p_2 \dots p_n)$ = a submodel containing n parameters. The submodel's parameters may be any number of global or patch state variables.

After the resource density has been calculated at the start of each time step, the density of each diet is updated. Diets are simply a collection of resources, and so the density of a diet is simply the sum of all of the resources it contains.

$$(2) R_{diet} = \sum_{r=1}^N R_r$$

where R_{diet} = diet resource density, r = resource number, N = number of resources in diet and R_r = density of resource r .

Depletion is incorporated by reducing the amount of a resource in a patch by the amount consumed by foragers. Foragers consume diets, rather than separate resources and so the model needs to calculate the amount of each resource consumed in the diet. The model

assumes that resources are consumed in proportion to their relative density within a diet. The amount of a resource is consumed within a diet is therefore given by.

$$(3) E = E_{diet} \frac{R}{R_{diet}}$$

where E = amount of resource consumed (eaten), E_{diet} = amount of diet consumed, R = density of resource and R_{diet} = density of diet. The density of the resource on the patch is updated by assuming that depletion occurs uniformly throughout the patch.

$$(4) R = R_{previous} - \frac{E}{A}$$

where R = new density of resource, $R_{previous}$ = previous density of resource before depletion, A = size (area / volume) of patch and E = amount of resource eaten.

Depletion either occurs at the end of a time step (if foragers are processed synchronously) or continually during a time step (if foragers are processed asynchronously). Diet densities are updated every time depletion occurs.

Change in component density

Component density within each resource on each patch is either read in as a single value which applies throughout the simulation, read in as different values during each time step, or read in as a parameter submodel to calculate values during each time step. Component density submodels can depend on global or patch state variables.

The density of a component within a diet is a weighed mean of the component density within each of the resources contained in the diet.

$$(5) C_{diet} = \frac{\sum_{r=1}^N C_r R_r}{\sum_{r=1}^N R_r}$$

where C_{diet} = density of component in diet, r = resource number, N = number of resources in diet, C_r = density of component in resource r and R_r = density of resource r .

Forager immigration

The probability of immigrating to the system for each forager morph / species is read in as a single value which applies throughout the simulation, read in as different values during each time step, or read in as a parameter submodel to calculate values during each time step.

Forager decision making

Foragers in the model make three types of decisions.

- Patch choice
- Diet choice
- Emigration from the system

The model uses the same submodel to determine how foragers make these decisions. The model's basic assumption is that foragers behave in order to maximise their fitness, which in turn is assumed to be measured as the probability of survival. Reproductive components of

fitness are not considered directly as these are outside of the scope of the model. Model foragers test the fitness consequences of moving to different patches, consuming different diets, consuming no diet or emigrating from the system. The list of possible diets depends on the diets consumed by the forager morph / species to which the forager belongs. Foragers select the combination which maximises their survival probability.

Foragers do not necessarily have perfect knowledge of their survival probability when moving to different patches or consuming different diets. This uncertainty operates at two levels.

- Ability to perceive the survival consequences
- Accuracy of perceived survival

Ability to perceive the survival consequences. Figure 2 shows how the ability to perceive the survival consequences of different decisions is incorporated. Foragers are assumed to be able to perceive the survival probability associated with consuming different diets on their current patch. Other patches fall into one of three different categories. (1) Foragers may know the location of a different patch and be able to perceive survival probability on the patch. They can assess the survival consequences of moving to this patch consuming any diet, and know the values of all of the patch's state variables. (2) Foragers may know the location of a patch, but not be able to perceive survival probability associated with different diets. They cannot assess the survival consequences of consuming different diets, and are unaware of any of the patches state variables. However, they do have an expected probability of survival on this patch ($S_{expected}$), which is used to compare this patch with others. (3) Patches may be of unknown location, and so cannot be considered as potential locations to move to. Emigration from the system also has an expected probability of survival, which is used to determine whether emigration is the decision which maximises survival ($S_{emigrate}$).

Accuracy of perceived survival. For patches on which survival consequences can be detected, the following process is used to assess perceived survival probability, which may differ from the true survival probability. Survival is assumed to be affected by a number of mortality sources. Each mortality source has an associated submodel to predict the perceived survival probability given the foragers state (including average state over previous time steps) and any combination of global or patch state variables. The combined perceived probability of surviving all mortality sources is found by assuming that mortality sources act independently.

$$(6) S_{perceived} = \prod_{m=1}^N p_m$$

where $S_{perceived}$ = perceived probability of surviving all mortality sources; m = mortality source number, N = number of mortality sources, p_m = perceived probability of surviving mortality source m . $S_{perceived}$ is calculated for all possible combinations of patches and diets, including the option to occupy a patch but not feed. The forager selects the patch and diet combination which maximises either $S_{perceived}$ or $S_{expected}$ (depending on whether survival can be perceived on the patch), or emigrates if $S_{emigrate}$ exceeds any of these values. In the event that more than one decision maximises survival, the forager takes a random option, but weighed by patch area, or remains in the system if $S_{emigrate}$ equals the probability associated with remaining in the system.

Once the forager has selected a patch and diet, it is allowed to move and consume its selected diet (see below). The consequences of this decision are then determined by true probability of survival.

$$(7) S_{true} = \prod_{m=1}^N s_m$$

where S_{true} = true probability of surviving all mortality sources; m = mortality source number, N = number of mortality sources, s_m = true probability of surviving mortality source m . The perceived survival probability may or may not be equal to the true probability. Foragers will tend to avoid patches and diets with low perceived survival probabilities. Depending on the relationship between the true and perceived probabilities, this can mean that foragers avoid safe patches and diets (i.e. high true survival probability) because these are perceived as dangerous (i.e. low perceived survival probability), or select dangerous patches or diets because these are perceived as safe.

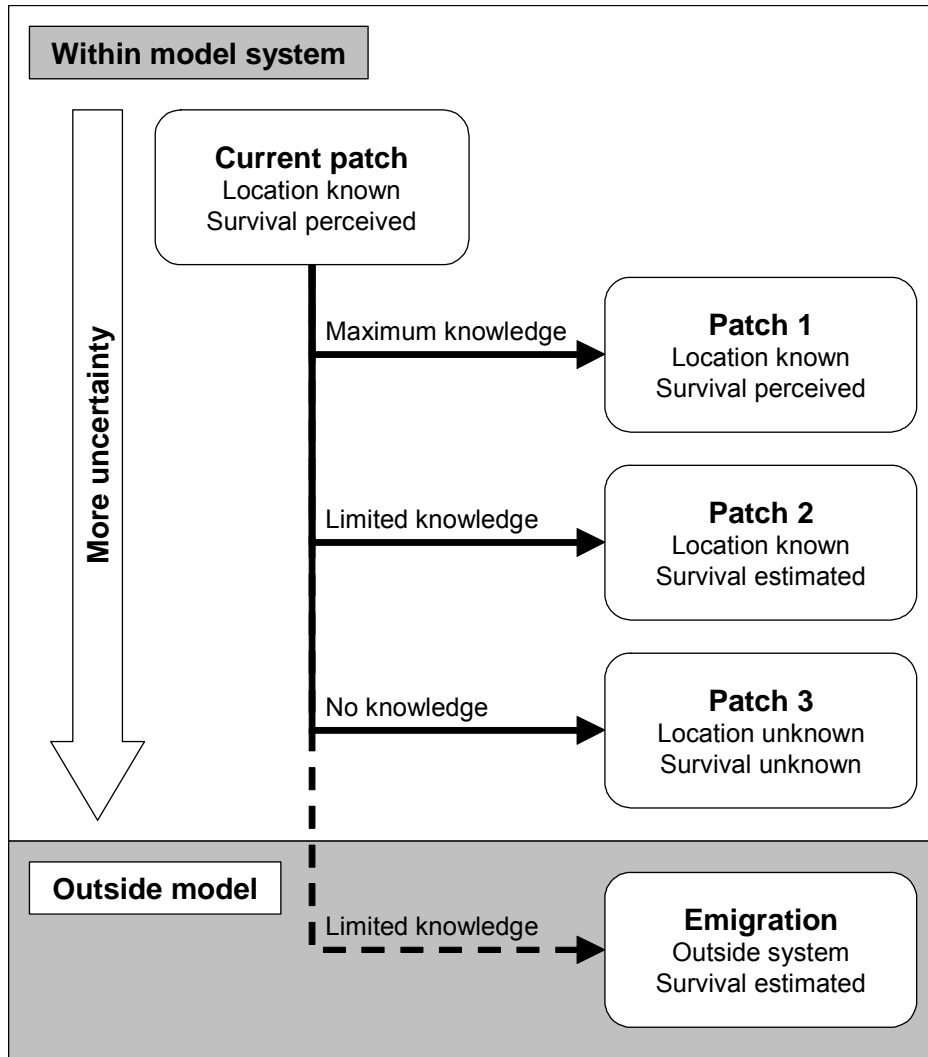


Figure 2. How uncertainty is incorporated into the model. Foragers are assumed to be able to perceive the survival probability associated with consuming different diets on their current patch. Other patches fall into one of three different categories. (1) Foragers may know the location of a different patch and be able to perceive survival probability on the patch (e.g. Patch 1). (2) Foragers may know the location of a patch, but not be able to perceive survival probability associated with different diets (e.g. Patch 2). In this case the estimated survival probability of the patch is used. (3) Patches may be of unknown location (e.g. Patch 3). Emigration from the system also has an expected probability of survival. Although, the figure shows increasing uncertainty associated with increasing distance between patches, this does not have to be the case.

Forager emigration and movement between patches

Foragers move when they emigrate from the system or change patches. Emigration is assumed to be instantaneous, with foragers leaving the system during the same time step in which they decide to emigrate. Movement between patches is also instantaneous if the patches have the same central coordinates. Otherwise, movement may take one or more time steps. If movement takes one or more time steps, foragers are assumed to reach a patch at the start of a time step. This means that they are able to respond to the local conditions on the patch (i.e. decide which diet to select or move to another patch), as these may not have been fully known when the forager initially decided to move to the patch. The time to travel between patches is calculated from the following equation.

$$(8) \quad T_{move} = \frac{D}{v}$$

where T_{move} = time to move between patches, D = distance between the central coordinates of the two patches and v = speed at which the forager moves.

For simplicity, the movement submodel assumes that movement always takes a whole number of time steps. This is achieved by initially calculating the number of whole time steps.

$$(9) \quad N_{whole} = \text{int}\left(\frac{T_{move}}{T_{timestep}}\right)$$

where N_{whole} = whole number of time steps, T_{move} = time to move between patches and $t_{timestep}$ = duration of one time step. The fractional number of time steps (N_{frac}) is then calculated.

$$(10) \quad N_{frac} = \frac{T_{move}}{T_{timestep}} - N_{whole}$$

The actual number of time steps ($N_{timestep}$) is then determined using a uniform random number between 0 and 1 (u).

$$(11) \quad N_{timestep} = N_{whole} \quad \text{if } (u < N_{frac})$$

$$N_{timestep} = N_{whole} + 1 \quad \text{if } (u \geq N_{frac})$$

While moving, forager's metabolise their component stores at a rate determined by the moving metabolic rate. The change in component reserve size while moving is.

$$(12) \quad C_{final} = C_{initial} - N_{timestep} T_{timestep} M_{moving}$$

where C_{final} = final component reserve size after moving, $C_{initial}$ = initial component reserve size and M_{moving} = rate of metabolising / excreting component while moving.

For simplicity, it is assumed that foragers cannot make any decisions or die while moving between patches.

Forager diet consumption and physiology

A submodel parameter is read in to calculate the diet consumption rate of foragers of each forager morph / species. The efficiency of assimilating each component from the resources in

the diet to the body (i.e. the proportion of the component in the diet that is transferred to the body) is also read in as a submodel parameter. Both submodels can depend on any forager constant or variable, patch state variable or global variable. The rate of assimilating a component is calculated from.

$$(13) \quad I_{assim} = aC_{diet}I_{diet}$$

where I_{assim} = rate of assimilating component, a = efficiency of assimilating the component, C_{diet} = density of component in the diet and I_{diet} = rate of consuming the diet.

The amount of the component assimilated during a time step also depends on the proportion of time spent feeding during the time step. The proportion of time spent feeding can be limited in two ways.

- Regulation of diet consumption rate
- Regulation of component reserve size

Regulation of diet consumption rate. A submodel is used to calculate the maximum diet consumption rate (I_{max}) during a time step. The maximum proportion of time that can be spent feeding (P_{max}) is calculated from.

$$(14) \quad P_{max} = \frac{I_{diet}}{I_{max}} \quad \text{if } I_{diet} > I_{max}$$

$$P_{max} = 1 \quad \text{if } I \leq I_{max}$$

Regulation of component reserve size. If the forager were to feed for P_{max} of the time step, its component reserve size at the end of the time step would be.

$$(15) \quad C_{final} = C_{initial} + T_{timestep} (P_{max} I_{assim} - P_{max} M_{feeding} - (1 - P_{max}) M_{resting})$$

where C_{final} = final component reserve size at end of time step, $C_{initial}$ = initial component reserve size at start of time step, $M_{feeding}$ = rate of metabolising / excreting component while feeding and $M_{resting}$ = rate of metabolising / excreting component while resting. The model uses a parameter submodel to calculate the target component reserve size (C_{target}) during any time step. The required proportion of time needed to exactly match this target, or approach it as closely as possible is found by setting C_{final} to C_{target} , and P_{max} to P_{target} and rearranging the previous equation.

$$(16) \quad P_{target} = \frac{C_{final} - C_{initial} + T_{timestep} M_{resting}}{T_{timestep} (I_{assim} - M_{feeding} + M_{resting})} \quad \text{if } \frac{C_{final} - C_{initial} + T_{timestep} M_{resting}}{T_{timestep} (I_{assim} - M_{feeding} + M_{resting})} \leq 1$$

$$P_{target} = 1 \quad \text{if } \frac{C_{final} - C_{initial} + T_{timestep} M_{resting}}{T_{timestep} (I_{assim} - M_{feeding} + M_{resting})} > 1$$

where P_{target} = proportion of time that forager needs to feed for to match its target or approach it as closely as possible.

The actual proportion of time spent feeding depends on the value of P_{max} and the values of P_{target} for each component in the diet. The model attempts to exceed or match the target

reserve size for each component, with the constraint the proportion of time feeding cannot exceed P_{max} . It does this by comparing the maximum value of P_{target} with P_{max} .

$$(17) \quad P_{feed} = \max(P_{target}) \quad \text{if } \max(P_{target}) \leq P_{max}$$

$$P_{feed} = P_{max} \quad \text{if } \max(P_{target}) > P_{max}$$

where P_{feed} = proportion of time feeding during time step. The component store size at the end of the time step is then found from.

$$(18) \quad C_{final} = C_{initial} + T_{timestep} (P_{feed} I_{assim} - P_{feed} M_{feeding} - (1 - P_{feed}) M_{resting})$$

Forager mortality

A submodel parameter is read to calculate the probability of dying due to each mortality source based on a forager's state, and any combination of global or patch variables. A uniform random number generator is used to determine whether each of a forager's individuals is killed by any of the mortality sources. In the event of two or more mortality sources killing an individual, one is selected at random. When all the individuals in a forager are killed, the forager is removed from the simulation.

Example Search Behaviour of Fish

The original model description, including all full references, is presented in:

Vabø, R., Huse, G., Fernø, A., Jørgensen, T., Løkkeborg, S., and Skaret, G. 2004. Simulating search behaviour of fish towards bait. -- ICES Journal of Marine Science, 61:1224-1232.

Abstract: Search by olfaction is common in many aquatic animals. This feature is exploited by the fishing industry, which has a long tradition for using long lines, pots and other kinds of baited gear. Here we discuss a range of possible search strategies that fish might apply when searching for prey, in order to improve our understanding of fish movement dynamics towards baited gear. Various search strategies were investigated using an individual-based behavioural model. The search phase was divided into search for relevant stimuli (plume search), and bait search when an olfactory stimulus has been encountered. The search strategies were evaluated based on their efficiency in providing guidance to the goal (plume or bait). The model was developed based on previous tagging studies of cod (*Gadus morhua* L.). The results for plume search show that when the landscape is considered to be continuous, strategies based on moving at an angle against the current performed better than strategies moving straight into the current, or random walk based strategies. When it is assumed that the fish is constrained to a home range, the results are reversed so that random walk based strategies perform better than the counter current strategies. For bait search the counter current strategies performed a lot better than strategies based on gradient search, which rarely resulted in contact with the bait.

Modified model description written by: **Rune Vabø**

Purpose

The model was developed in order to investigate the effectiveness of possible search strategies that fish might apply when searching for prey using olfactory stimulus. Based on tagging studies of cod, various theories about the search strategy of fish towards baited gear were formulated and implemented as behavioural rules. Simulation studies were performed in order to investigate the effectiveness of these presumed behavioural rules, adding knowledge to our understanding of natural fish behaviour exposed to odour regimes.

State variables and scales

The model space is spatially explicit, defined as a two-dimensional and continuous area, constrained by a circle with radius 750 m. The size of the system is based on the width of the fjord system (Ramfjord, in Northern Norway) where earlier tagging studies on cod were carried out. The system has been defined with both fixed and continuous boundary conditions. One odour source with a diameter of 30 cm is placed in the centre of the area. The odour source contains 50 000 odour particles which are continuously released over time. A spatial grid with cell size 1.05 m covers the whole system area. The number of odour particles within one cell then defines the odour concentration in the given location. A current vector is defined for the system. The current is used to transport particles and to guide fish

agents when searching for prey. Time is modelled in discrete time steps of 0.5 and 0.25 seconds. The progress of time has been modelled explicitly using a clock, which is set to a specific time at the start of each simulation in order to synchronise the time series of measured current vectors with the initiation of the odour source (the bait bag) into the water, and thereby matching the corresponding event in the tagging experiment. Search behaviour of fish is based solely on current direction and odour concentrations. Each fish agent has a body length of 50 cm and a constant swimming speed based on experimental values on cod.

Process overview and scheduling

Four dynamic aspects of the fjord system have been modelled.

- The current through the fjord
- The release of odour from the bait
- Transport of odour concentrations with the current
- The swimming behaviour of fish searching for prey

The general direction and strength of the current is assumed to be homogeneous through the whole area, with normal distributed variations. Both *in situ* measurements and a constant current vector has been used.

Following an asymptotic decrease in odour concentration, the bait releases odour particles, which are carried away with the current.

Fish are released into the system at some time after the bait has been initiated in order to have an odour plume present in the system when the fish starts. The search behaviour of fish is divided into two distinct phases, which have been simulated separately. *Plume search* is the initial search for relevant olfactory stimulus, while *bait search* is the search for the actual bait initiated when an odour plume has been detected. Different behavioural rules have been implemented and tested for these two phases. The role of each rule is to determine which direction to move. In plume search, each rule uses the observed current direction as input, while in bait search the observed odour concentration is also used. A rule applied in plume search is evaluated in terms of the time it takes to find the odour plume, i.e. encounter odour concentration. A rule applied in bait search is evaluated in terms of the time it takes to find the bait.

Design concepts

Emergence, Adaptation

During bait search the search patterns of the fish are constantly influenced by fluctuations in the current and in odour concentrations. Odour concentrations fluctuate as a consequence of the fluctuations in the current (causing spreading of the plume) and by the process of time as the initial concentration in the source decreases, thereby causing different variation by distance at different times. Fish experiencing the plume at different locations or at different times therefore produce different search patterns.

Sensing

Each fish agent is able to sense the current direction and strength and the odour concentration in its given location. The fish also has a vision, but it is used only in the vicinity (3 m) of the bait.

Stochasticity, Prediction

Each time a fish observe the current vector, this observation is subject to a normal distributed random fluctuation. The current vector used to determine changes in swimming direction is

however based on a conservative approach using the memory of previously observed current vectors in combination with the last observation. The last observation is much less weighted than the value residing in memory. The observation and application of odour concentration uses a memory in the same way. The decision of each fish is subject to no stochasticity.

Initialization

The bait source were initiated with 50 000 particles at 1500 hrs. The number of independent replicates, i.e. the number of independent fish using the same behavioural search rule, was always 1000. The system was initiated differently for plume search and bait search.

Plume search

A time step of 0.5 seconds, were used. Simulations were performed with both fixed and continuous boundary conditions. In each computer run the fish were put in a randomly chosen position located in between the two radiuses 200 m and 750 m away from the bait. The fish started at 1530 hrs.

Bait search

A time step of 0.25 seconds, were used. A higher resolution in response time and attention of the fish is thus assumed. Only fixed boundary conditions were used. The fish were initiated directly 280 ± 5 m downstream from the bait. Fish were released at 1630 hrs. At this time at this position the fish start up at the front of the plume entering straight into the bait search phase.

Input

We designed the simulation experiments based on a previous field study performed in September 2000 (Løkkeborg, 2000). In this field study the bait bag was put in the water at 1500 hours. In simulating plume search behaviour we use simultaneous current measurements synchronised using a simulated clock. During bait search a constant current direction (always the same downstream direction) was used. The rate of particle release (λ) from the bait source was based on previous experiments with mackerel baits (Løkkeborg, 1990). The measured swimming speed of cod was used to define a constant swimming speed of the fish agents; 1 bl s^{-1} for plume search and 2 bl s^{-1} for bait search.

Submodels

The current

The current was assumed to be homogeneous in the study area. It is defined by a superposition of a constant velocity vector ($\mathbf{U}_{\text{const}}$) and a fluctuation vector ($d\mathbf{U}_{t,p}$) varying in time and space:

$$(1) \quad \mathbf{U}_{t,p} = \mathbf{U}_{\text{const}} + d\mathbf{U}_{t,p}$$

The general current direction $\mathbf{U}_{\text{const}}$ was predefined for bait search simulations, and taken from *in situ* measurements in plume search simulations. Fluctuations are implemented as a parallel and perpendicular perturbation on $\mathbf{U}_{\text{const}}$:

$$(2) \quad d\mathbf{U}_{t,p} = \mathbf{n}_{pd} \cdot f_1 \cdot |\mathbf{U}_{\text{const}}| + \mathbf{n}_{pl} \cdot f_2 \cdot |\mathbf{U}_{\text{const}}|$$

where \mathbf{n}_{pd} and \mathbf{n}_{pl} are the unit vectors perpendicular and parallel to $\mathbf{U}_{\text{const}}$, respectively, f_1 and f_2 are Gaussian distributed random numbers ($\sigma = 2 \text{ cm s}^{-1}$).

Release and transport of odour particles

An odour source or bait bag (BB) is defined by the position $P^{BB}(x,y)$, time of entering the water T^{BB} , diameter of the bag (D^{BB}), leaching rate, $\lambda \geq 0$ and initial concentration, S_0 at time $t=T^{BB}$. The leaching rate determines how fast odour is washed out. The amount of odour left in the bait at any time t can be expressed as:

$$(3) \quad S_t = \frac{S_0}{(1+\lambda \cdot t)}$$

Real odour units released from mackerel baits or artificial baits are units of different amino acids given in μmole (Løkkeborg, 1990). In our model (3) we simply define $S_0=1$. Units of odour are represented by a number of particles (N) residing inside the bait bag (randomly placed within the diameter of the bag) when it is placed into water at $t=T^{BB}$. Using (3) the amount of odour released during a time interval dt , is equal to $S_{t-dt}-S_t$. The number of particles released during dt is then:

$$(4) \quad dN = (S_{t-dt}-S_t) \cdot N$$

Particles released from the bait bag are transported with the current according to a simple particle model. Each particle is accelerated by the current as:

$$(5) \quad dV = (U-V) \cdot a_{\max}$$

where U is given by (1), V and dV are the particle velocity and acceleration respectively, and $a_{\max} [0,1]$ is an acceleration constraining factor. When $a_{\max}=1$, V changes instantaneously to U . The dynamics of the particles are given by the standard dynamic equations:

$$(6) \quad V_t = V_{t-1} + dV \cdot dt$$

$$(7) \quad P_t = P_{t-1} + V_{t-1} \cdot dt + \frac{1}{2} dV \cdot dt^2$$

where dt is the time step, P_t position at time t .

The individual-based fish model

Each fish agent is defined by a set of properties and a set of behaviour rules. The implementation of a rule, also referred to as strategy, is defined by a set of rule parameters, which have different specific meanings for each type of rule. In addition to spatial variables like position (P), velocity (V) and acceleration (dV), a memory structure is used to hold time-averaged values of current directions (U^m) and odour concentrations (ρ^m). A parameter defines a reaction threshold (χ , Table 1).

At each time step the fish observes both odour concentration (ρ_t) and current vector (U_t), and adjusts its memories according to:

$$(8) \quad \rho_t^m = \rho_{t-1}^m \cdot w_1 + \rho_t \cdot (1-w_1)$$

$$(9) \quad U_t^m = U_{t-1}^m \cdot w_2 + U_t \cdot (1-w_2)$$

where w_1 and w_2 are parameters determining the weight of the previous memory vs. new information in updating memory of odor concentration and current direction.

In plume search the search strategy is always associated with only one of four possible behavioural rules termed “random walk”, “random turn”, “counter current” and “upstream”.

In bait search the fish uses one of three search strategies: “counter current”, “gradient search” and “upstream”. When outside the plume during bait search, the fish uses an excited plume search behaviour in trying to relocate the plume.

The role of each rule is to calculate the desired swimming directions (unit vector η) for the fish. In addition the fish has a desired swimming cruise speed (v_c), thus the fish accelerates by:

$$(10) \quad dV = V_{\text{Desired}} - V$$

in order to achieve a swimming vector:

$$(11) \quad V_{\text{Desired}} = \eta \cdot v_c$$

All of the rules are implemented in this way. If there are no constraints on the acceleration, the fish can change its swimming velocity and direction instantaneously. The spatial dynamics of each fish is calculated by Equations 6 and 7, with the velocity and acceleration being the sum of both advection and active swimming. During plume search, the fish was assumed to swim at a speed of 1 body length (bl) s^{-1} . In bait search, the swimming speed was increased to 2 bl s^{-1} , as a marked increase in swimming speed in responding fish has been observed by Løkkeborg (1998), while in excited plume search the fish was assumed to slow down and swim at 0.5 bl s^{-1} , based on unpublished observations.

The “random walk” rule (Berg, 1993; Turchin, 1998) is implemented by choosing a random η and moving in this direction for dt seconds.

In the “random turn” rule η is adjusted each time step by rotating it $\pm d\alpha$ ($^\circ s^{-1}$) during dt seconds. The sign of $d\alpha$ is chosen randomly after each time interval dt .

“Counter current” movement is implemented by choosing a direction η deviating $\pm d\alpha$ from the upstream direction U^m . The sign of $d\alpha$ is chosen randomly. The “upstream” rule is simply an implementation of this rule with $d\alpha = 0^\circ$.

“Gradient search” is implemented by going straight until the observed concentration drops below $\rho_t^m \cdot c$, where c (0,1) is a threshold parameter. Low c values require consistent drops in odour concentration in order to change course. When this happens the fish turns randomly.

When the fish is outside the plume during bait search it initially chooses a random sign of $d\alpha$ and applies an everlasting “random turn”, but continuously decreases $d\alpha$ until reaching a minimum turn angle, creating a spiral movement. Then it goes on by increasing $d\alpha$ until reaching a maximum turn angle when it decreases $d\alpha$ again and so forth.

The evaluation of search performance (or fitness) for plume search was calculated by using the time taken to find the plume $d\tau$:

$$(12) \quad F_p = \frac{dT^P - d\tau}{dT^P}$$

where dT^P is the maximum search time allowed for the fish. The fitness was calculated in a similar manner for bait search, using dT^B , but in this case $d\tau$ is the time taken to find the bait (getting within a 3m radius of the bait). If the fish does not reach the goal it is given zero fitness.

Table 1. Simulation settings and general parameters (*: Taken from field data at 01/09/2000. **: Derived from Løkkeborg (1990).

Parameter	Value	Description
dt	0.5, 0.25 s	Simulation time step in plume search, bait search
dT ^{Sim}	4.5, 2.5 hours	Total simulation time in plume search, bait search
dT ^P	4 hours	Total simulation time in plume search when fish is active
dT ^B	2 hours	Total simulation time in bait search when fish is active
T ^{BB} *	15:00	Time when the bait bag goes into water
T ^{fish}	15:30, 16:30	Starting time for all fish in plume search, bait search
R ₁ , R ₂	200 m, 750 m	Radii defining at toroidal area around the bait bag where fish initially are placed in plume search simulations
R ₃	280 m	Distance downstream from bait where the fish initially is placed in bait search simulations
N ^{Fish}	1000	Number of independent replicates
L	50 cm	Fish length
v _c	1, 2 bl s ⁻¹	Fish cruise speed plume search, bait search
χ	>1 m ⁻²	Odour reaction threshold
θ	300°	Angle of view
r	3 m	Visual range
w ₂	0.95	Memory weight for current vector
R	1.5 km	Diameter of home range
U _{const} *	1- 15 cm s ⁻¹	In situ current vector corresponding to T ^{BB} + elapsed time
D ^{BB} *	30 cm	Diameter of bait bag
P ^{BB} *	-196.5, 104.7 m	x and y positions of bait bag
λ **	0.00008 s ⁻¹	Leaching rate of bait
N	50 000	Total number of odour particles

Example Copepods

The original model description, including all full references, is presented in:

Souissi S, Ginot V, Seuront L & Uye S-I. (2004) Using multi-agent systems to develop individual based models for copepods: consequences of individual behaviour and spatial heterogeneity on the emerging properties at the population scale. In *Handbook of Scaling Methods in Aquatic Ecology: Measurement, Analysis, Simulation*. Seuront L & Strutton P (Eds.) CRC Press. pp 527-546.

and

Souissi S., Seuront L., Schmitt F.G. & Ginot V. (2005) Describing space-time patterns in aquatic ecology using IBMs and scaling and multiscaling approaches. *Nonlinear Analysis: Real World Applications*, 6:705-730.

Abstract: In this paper a new simulation platform, “*Mobidyc*”, dedicated to non-computer expert end-users, is used to illustrate the advantages of such platforms for simulating population dynamics in space and time. Using dedicated and open-source platforms probably represents a necessary step to guarantee the readability and comparison between models and/or scenarios. The “*Mobidyc*” platform is specifically dedicated to population dynamics with 2D-discrete spatial representation. We show first how to build easily stage-structured population dynamics models, on the basis of an experimental parameterization of the population dynamic of the copepod *Eurytemora affinis*, the most dominant species in estuaries of the Northern hemisphere. We subsequently focus on the role of spatial representation and the possible sources of heterogeneities in copepod populations. The sources generating patterns in our examples are strictly endogenous to the population and individual characteristics. They are generated by the random walk of individual at local scale and the demographic processes (birth, metamorphosis and mortality) at the population scale in the absence of any externally imposed pattern.

The large spatio-temporal data sets of abundances of total population are analysed statistically. Spatial and temporal patterns are investigated using models and data analysis techniques initially developed in the fields of turbulence and nonlinear physics (e.g. scaling and multi-scaling approaches for data analysis and stochastic simulation). Finally, the role of simulation tools for theoretical studies is discussed in this paper.

Modified model description written by: **Sami Souissi**

Notes: This is the only Example application of ODD describing a model that was developed by using a generic software platform for implementing IBMs: *Mobidyc*.

Purpose

The purpose is to use develop an individual based model of the complete life cycle of a copepod (crustacean small animal living in most aquatic habitats) by combining local behaviour (small scale moving) and demographic processes (egg laying, moulting, mortality, etc.) in order to study the consequences of these behavioural and demographic processes on the spatial and temporal patterns at the population level.

State variables and scales

We can use here a schematic representation of the life cycle of a copepod and the considered state variables. Figure 1 shows an example of life cycle representation used in Souissi et al. (2005). Each stage (or group of stages) represent one state variable.

From an individual point of view, each individual of a copepod population has to follow the schematic template shown in Figure 1. Most copepods exhibit a clear sexual dimorphism with only one reproductive stage (adults: C6). After copulation each mature female can produce a certain number of eggs. Between embryonic and mature stages each individual should pass successively through the six larval (naupliar) stages and the five juvenile (copepodite) stages. In order to simplify the copepod life cycle, the naupliar stages were aggregated into two groups as proposed by Souissi and Ban (2001) whereas the copepodite stages were represented in detail. Moreover, females and males are separated since the last copepodite stage (C5), because their development is different.

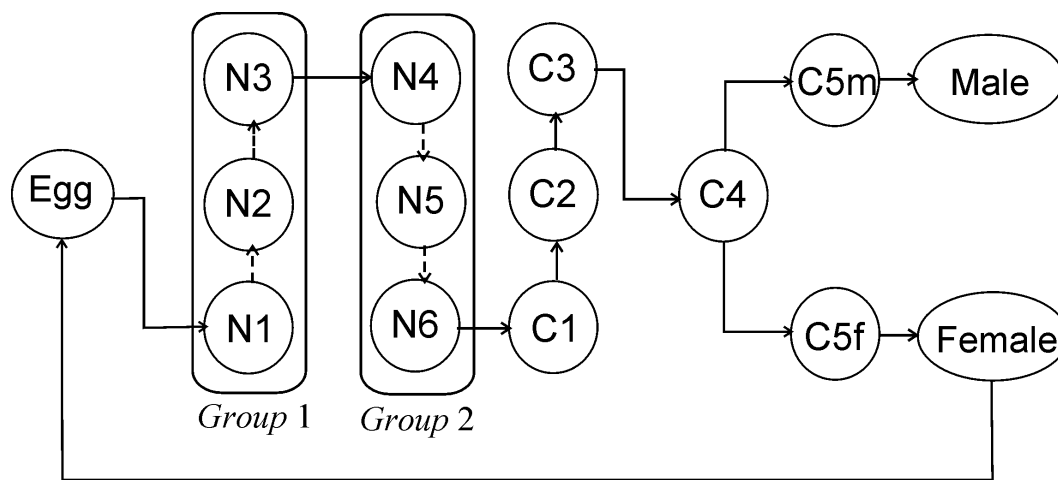


Figure 1. Schematic representation of life cycle of the copepod *Eurytemora affinis* with aggregation of the larval stages into two groups: N1-N3 and N4-N6. Sexes are separated at the last juvenile stage (C5).

The model developed here will be applied to the estuarine copepod species *Eurytemora affinis*, which is the most dominant copepod species in the temperate estuaries of the Northern Hemisphere and its spatial repartition is generally restricted to the low-salinity zone. Several experimental studies were carried out in the laboratory in order to study the development of the population of this species under several conditions of food, temperature and salinity (Souissi and Ban, 2001; Devreker et al., 2004). This species offers a good example for estimating the parameter values and then get realistic representation of the development of a population dynamics model. However, for the sake of simplicity, the simulation will be done under constant and optimal conditions of development corresponding to the temperature of 15 °C.

The complete list of attributes used in the model are defined in Table 1.

Table 1. List of attributes used to define the life cycle of the copepod *Eurytemora affinis*.

Attribute	Owner	Definition
age	all stages	age (days)
location	all stages	position in the grid of cells
number	all stages	number of individuals per agent
rand	all stages	Intermediate, used to assign a random real between 0 and 1
state	all stages	Intermediate, used to define the state of survival
pSurv	all stages	Probability of survival in the stage
meanDuration	all stages	Mean stage duration for stages Egg to C5, and life span in stage adult (C6)
alpha	all stages	Parameter for the variability around mean stage duration
minDuration	all stages	Intermediate, used to compute the minimum stage duration
maxDuration	all stages	Intermediate, used to compute the maximum stage duration
duration	all stages	Stage duration
stateSex	C4	Intermediate, used to define the type of sex in the stage C5
pFemale	C4	Sex-ratio of the population (proportion of females)
fecund	Female	Fecundity

Process overview and scheduling

The model proceeds in 6-hour time steps. During each time step, all agents executed the first 4 tasks shown in figure 4: compute the age of the agent, determine the state of the agent for survival, conditional mortality and computation of the duration in each stage. Then the transfer from one stage to another (excepting for adults) is considered. In order to complete the parameterization of the model a 1:1 sex-ratio is adopted (“*pFemale*” = 0.5). The same procedure used for survival is applied to determine randomly whether the individual in stage C4 will moult into C5f or C5m. Finally a constant fecundity rate is considered for females (5 eggs per female every time step) and reproduction starts after an observed delay of 2 days.

Table 2 : List of the tasks used to develop the life cycle of the copepod *Eurytemora affinis*.

Agent task	Owner
Grow older	all stages
StateSurvive	all stages
CondMortality	all stages
TempDuration	all stages
Hatching Moulting	/ all stages

DefineSex	Stage C4
MoultingM MoultingF	Stage C4
Reproduction	Female

Design concepts

Emergence. – Population dynamics emerges from the behaviour of individuals, but the individual's life cycle and behaviour are entirely described by simple empirical and stochastic rules. The development from one stage to another and the survival were represented stochastically. In order to understand the combined effects of demographic processes (at the population level) and the local behaviour (random walk) on the emerging patterns the parameterization of the model was kept as simple as possible. Although these simplistic assumptions were used in the model, the generated (emerging) patterns showed significant scaling and multi-scaling properties (Souissi et al., 2005).

Fitness. - This initial model made no attempt to quantify the fitness consequences of individual behaviors, nor did it assume that those behaviors would optimize individual fitness.

Sensing. - Individuals are assumed to know their stage (sex) and apply their specific tasks.

Interaction. – The interaction between individuals was introduced in the model developed in Souissi et al. (2004), where late developmental stages are assumed to be omnivorous and can feed on their early developmental stages. An example of building a predation task using Mobidyc's primitives is shown in Figure 2.

As this task was build with the primitives developed under Mobidyc platform, again the connection between the platform architecture and the modelled process (here predation) was obvious.

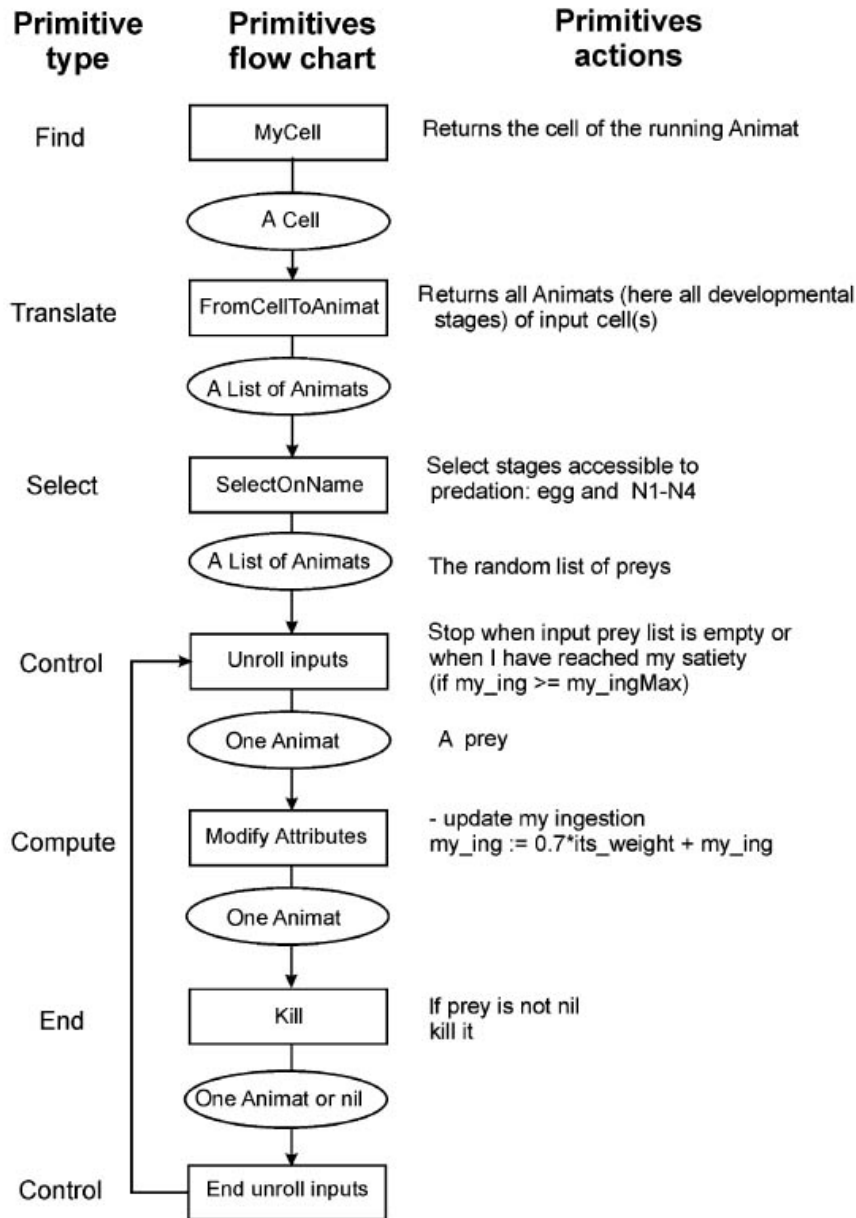


Figure 2. An example of building a task with primitives, here a task of predation of omnivorous stages (C6m and C6f) on early developmental stages (eggs, N1–N4). Seven primitives (represented with boxes) corresponding to six types are strung out to build this task. The output arguments of each primitive (represented with ellipses) represent the input argument of the next primitive. Example modified from Souissi et al. (2004).

Stochasticity. – The main demographic parameters (i.e. survival) are interpreted as probabilities. For example, if an individual has 95% probability of survival, then it dies only if the random number is more than 0.95. Moreover, stage duration and fecundity are taken randomly in a distribution of values centred on the mean values obtained experimentally.

Observation. – When the model is used without spatial representation the number of individuals in each developmental stage were counted for each time step. This procedure allowed to draw the cohort development (see Figure 3 in Souissi et al. 2005). When a grid of cells was used (2D spatial representation), in order to obtain spatio-temporal patterns of total density of the population a computation of the value of this descriptor in each cell and for each time step is necessary.

Initialization

Again here, we will only consider the general presentation of the initialization independently of the platform (Mobidyc) specificities.

An open grid of square cells where each cell has 8 neighbours represents space. After each time step, individuals move to a cell randomly (or according some rules) selected from its neighbourhood (parameterised by a radius depending on the capacities of each stage).

The numerical experiments performed here allowed to test:

- i) The effects of the initial conditions (composition of the population and the positions of the individuals at t_0).
- ii) The effects of the size of the spatial grid.
- iii) The sensitivity of the model to some demographic parameters (probability of survival, egg production, etc.).

All simulations were repeated n times in order to consider the variability between outputs for the same set of parameters and the same initial conditions.

Input

In recent version of *Eurytemora affinis* model (not yet published) we added some forcing parameters and some scenarios. The most obvious scenario (input) is temperature. Instead of using constant temperature, stage duration and egg production depend on temperature.

For stage duration we consider a cumulative variable of °C.Days and a threshold value to be reached before moulting. However the effect of temperature on egg production is parameterised by a dome-shaped function showing an optimum of temperature around 15°C. We are carrying several experiments in the laboratory to verify and define these functions.

Submodels

We can use a combination of ‘macro-language (i.e. Mobidyc settings of mathematical expressions)’ and a short verbal description of the different processes (tasks) and behaviours of individuals. We present also a schedule of the execution of these processes. A simplified example is shown in Table 3.

Table 3. Definition of the tasks used to develop the life cycle of the copepod *Eurytemora affinis*.

Agent task	Definition	Setting
Grow older	Compute the age of the agent	$my_age := my_age + simulator_timeStep$
StateSurvive	Determine the state of the agent for computing its survival	$my_rand := Random_real(0,1)$ $my_state := my_pSurv - my_rand$
CondMortality	Conditional mortality	if $my_state < 0$ then I am dead
Move	Moving from one cell to another	
TempDuration	Computation of the duration in each stage. A simple dispersion	$my_MinDuration := ((1 - y_alpha) * my_MeanDuration)$ $my_MaxDuration := (1 + my_alpha) * my_MeanDuration$

	according a fixed parameter (alpha) was considered here.	my_duration := Random real (my_MinDuration,my_MaxDuration(
Hatching / Moulting	Transfer from one stage to the next one depending on the stage duration	If my_age > my_duration
DefineSex	Define the sex of agent after moulting in the stage C4	my_rand := Random_real (0,1(my_stateSex := my_pFemale – my_rand
MoultingM / MoultingF	Transfer from C4 to C5m (male) / from C4 to C5f (female)	If ((my_stateSex<0) AND (my_age > my_duration)) / ((my_stateSex>=0) AND (my_age > my_duration))
Reproduction	Reproduction of Females into Eggs depending on a constant (fecund) for each individual	Number of offsprings per individual equal to my_fecund

Example Colorado pikeminnow

The original model description, including all full references, is presented in:

Grand, T.C., Railsback, S.F., Hayse, J. And LaGory, K.E. Juvenile Colorado pikeminnow nursery habitat model formulation. Unpublished report written for the Electric Power Research Institute.

Abstract: An individual based model for age-0 Colorado pikeminnow has been developed to evaluate potential cumulative impacts of various stressors (including competition with and predation by red shiner) on growth and survival of age-0 Colorado pikeminnow in nursery habitats. Components of the model describe the effects of changes in flow on habitat conditions in nursery areas and anticipated effects on growth and survival of the fish. Because pikeminnow can be prey, competitors or predators of red shiner, we model shiners as individuals too. The model consists of linked physical and biological sub-models. The physical sub-model operates at an hourly time step and predicts volume, depth and temperature for a single backwater habitat in the Ouray reach of the Green River based upon information from the Jensen, Utah stream flow gage. The biological sub-model operates on a daily time step and predicts the response (i.e., growth and survival) of age-0 Colorado (and red shiner) to those conditions. The primary management concern to be addressed by the model is the current recommendation that within-day flow fluctuations be limited to less than 0.1 m (i.e., less than 0.1 m greater than or less to the mean daily backwater depth). This recommendation is based upon the observation that the average depth of backwaters where juvenile pikeminnow are found is 0.3 m. The model will be used to identify the relative effects of flow variation and to evaluate the effects of hydrologic and operational scenarios for Flaming Gorge Dam on pikeminnow growth and survival. Simulation experiments may also be useful for gauging the importance of competition and predation with non-natives on the pikeminnow population. In addition, the model will serve to guide future research and management decisions for Colorado pikeminnow.

Modified model description written by: **Tamara Grand and Steve Railsback**

Notes: The above reference can be requested from the authors.

Purpose

The endangered Colorado pikeminnow (CPM; *Ptychocheilus lucius*) is endemic to the Colorado River Basin. The decline of the CPM has been attributed to water development, nonnative fish introductions, fish harvesting, and water pollution (Miller 1961; Minckley and Deacon 1968; Seethaler 1978; Behnke and Bensen 1983; Miller et al. 1982; Holden 1991; Quartarone 1995). Large storage and hydroelectric dams on the Green and Colorado rivers are frequently cited as having the greatest impact on the CPM (Behnke and Benson 1983; Tyus 1991). However, nonnative fish introductions may pose an equally great threat through predation, competition, or disease (Behnke and Benson 1983; Haines and Tyus 1990; Minckley 1991; Muth and Snyder 1995). One of the most common of these introduced species is the red shiner (RS; *Cyprinella lutrensis*). Recent evidence suggests that in addition

to competing with native fishes for food, RS may also consume significant numbers of CPM larvae and small juveniles (e.g., Ruppert et al. 1993).

The greatest potential for impact on the CPM population likely occurs during the first year of life, when age-0 fish use small channel-margin backwater areas as nursery habitats. In these habitats, CPM are exposed to variable water conditions (e.g., daily changes in temperature and food availability), large concentrations of nonnative fishes, and variation in backwater water levels attributable to hydropower operations and precipitation events. Designing effective conservation measures requires an understanding of the relative importance of these stressors to the fish.

We developed an individual-based model to address one specific problem related to how hydroelectric dam operation affects CPM: how do within-day fluctuations in flow affect survival and growth of juvenile CPM inhabiting backwaters in the presence of aquatic competitors and predators? One of the major advantages of large hydropower projects is that they can safely and inexpensively increase generation to follow the within-day cycles in electric power demand. However, following the daily demand cycle requires large changes in flow during each day, and the extent to which these flow changes affect downstream aquatic life is often a controversial management issue. Our study sites are on the Green River in Ouray National Wildlife Refuge, Utah, approximately 240 km downstream of Flaming Gorge Dam. During the period studied, daily flow typically consisted of a single cycle of gradually rising then falling flow. This cycle flushes mainstem water into and out of backwaters, which has been hypothesized to affect CPM by altering backwater temperatures and by reducing the availability of benthic and planktonic food. The model's specific objective is therefore to understand and predict how different levels of river flow and within-day variation in flow affect backwater temperature and food availability and, therefore, growth and survival of juvenile CPM.

While the model's objective is to understand how hydropower-caused changes in flow affect CPM, the study acknowledged from the start that these effects could be strongly mediated by exotic fish. Given that RS both compete for food with and prey upon CPM, it is not at all clear that managing flows to improve general conditions in backwaters would benefit CPM; instead, it could promote growth of RS and consequently, increase aquatic predation on CPM. Consequently, another key part of the model's objective is to consider how exotic fish mediate the relationship between flow and CPM growth and survival.

State variables and scales

The model consists of linked physical and biological sub-models which operate at different spatial and temporal scales (see Figure 1). The physical sub-model operates at an hourly time step and predicts volume, depth, temperature and benthic invertebrate production for a single backwater habitat in the Ouray reach of the Green River. Hourly values of habitat variables are averaged into mean daily values, which are used by the biological sub-model. The biological sub-model operates on a daily time step and predicts the growth and survival of individual age-0 CPM and RS. CPM and RS are both represented as individuals, and both species have the same variables (but have different parameter values). We follow the actions of individual fish from the onset of the base flow period (which can vary from year to year and is defined by the period of relatively stable flow that occurs following peak spring flows) until December 31st.

Here, we focus only on the biological sub-model. For further details about the physical habitat model, see Grand et al. (submitted). A complete list of all variables relevant to the fish model appears below (Table 1). Note that this list includes a number of habitat variables that directly influence fish growth and survival (e.g., invertebrate prey density, number of daylight hours).

While the use of separate time steps for habitat and animal simulations is unusual, it was necessary for this model. The habitat model must run at a short time step to capture the effects of within-day flow fluctuations, the model's objective. Hourly flow data are available and adequately capture the within-day flow changes, so the habitat model's time step was chosen to match the flow data. However, modeling fish growth and survival is much simpler at a daily time step; modeling fish at an hourly step would require modeling where they are within a backwater and what they are doing (feeding or hiding), because hourly growth and risk depend on location and activity. Using a daily time step makes it reasonable to ignore such short-term processes. Also, many of the equations and parameters typically used to model growth and mortality are based on empirical observations taken over longer time scales and are not reliable at an hourly scale.

The habitat model uses two spatial scales. Water depth (a function of hourly river flow) is modeled using 1-m square cells. Then, variables describing the entire backwater (mean and minimum depth, volume, area; Table 1) are calculated from all wet cells. Biological processes are simulated non-spatially: the model does not track where fish are within a

backwater. The model has been applied to six different backwaters, which range in area (at typical summer flows) from 220 to 1744 m².

Table 1. Habitat state variables describe the single habitat object, a river backwater. Fish state variables describe each individual fish, whether CPM or RS.

Variable name (units)	Description
Habitat variables	
I_{dens} (#·m ⁻²)	Density of invertebrate prey in the backwater
e_{tot} (number)	Total number of invertebrate prey encountered by all CPM and RS
I_{Δ} (number·m ⁻²)	The difference between the total number of invertebrates encountered by all fish and the number available for consumption in the backwater
D (h)	Number of hours of daylight per day
A_{min} (m ²)	Minimum daily backwater wetted area
\bar{V} (m ³)	Mean daily backwater volume
d_{max} (m)	Maximum daily backwater depth
\bar{T} (°C)	Mean daily backwater temperature
T_{min} (°C)	Minimum daily backwater temperature
Fish variables	
L (mm)	Total length
W (g)	Weight
K (unitless)	Condition (weight relative to length)

Process overview and scheduling

Habitat processes are described in detail by (Grand et al., submitted.). In brief, daily mean backwater attributes (e.g., depth, area, volume) are calculated from hourly values, which are a function of river flow. Hourly water temperature is modeled as a function of backwater size and hourly weather data then used to calculate daily mean backwater temperature. Daily food production is a function of backwater temperature (increasing with temperature up to 23 °C, then decreasing at higher temperatures), but is reduced by flow changes that flush water out of the backwater.

We model three fish actions; (1) foraging (which includes encountering and consuming prey, as well as being consumed by piscivores), (2) growth, and (3) survival (of mortality sources other than piscivory). Fish actions occur once per day after daily backwater attributes and invertebrate production have been calculated. See Figure 1 for a visual depiction of the model's processes and schedules.

We model time using discrete time steps. The habitat is updated hourly and daily habitat variables calculated at the end of the day. Habitat actions are conducted sequentially, in the order specified in Figure 1. Fish actions (foraging, growth and survival) occur after daily habitat variables have been calculated. Each action is performed in turn on all fish, in randomized order; that is, foraging actions are first performed on all live fish, followed by growth actions and survival actions. Such scheduling is required in order to determine the effects of competition for prey on fish growth and survival. See Figure 1 for a detailed depiction of the model's schedules.

The food intake of a fish is modeled as a function of (a) the total food available in the backwater, (b) the fish's encounter rate with prey, and (c) the number of other fish (both CPM and RS) foraging on the same prey type. Because the diets of juvenile CPM change from invertebrates to fish as they grow, we assume that different size fish forage on different types of prey. RS are assumed to undergo the shift to piscivory at the same size as CPM. Prey encounter rates are modeled as a function of (a) the fish's swimming speed, (b) prey availability, and (c) the number of hours available in the day for foraging.

Growth is modeled by subtracting the day's energetic expenditures from the energy acquired during feeding. Metabolic losses include those associated with standard respiration and active respiration. Standard respiration takes place 24 hours per day and assumes no activity; activity respiration is the energy needed to swim while foraging.

We simulate daily survival for the following three mortality sources: high temperature, poor condition, and terrestrial predation. Terrestrial predation is due to birds and mammals that search for prey from above the water and is generally assumed to be higher for bigger fish, in shallow water and in the absence of ice. We assume that RS are subject to the same sources of mortality as CPM and use identical survival parameter values for the two species.

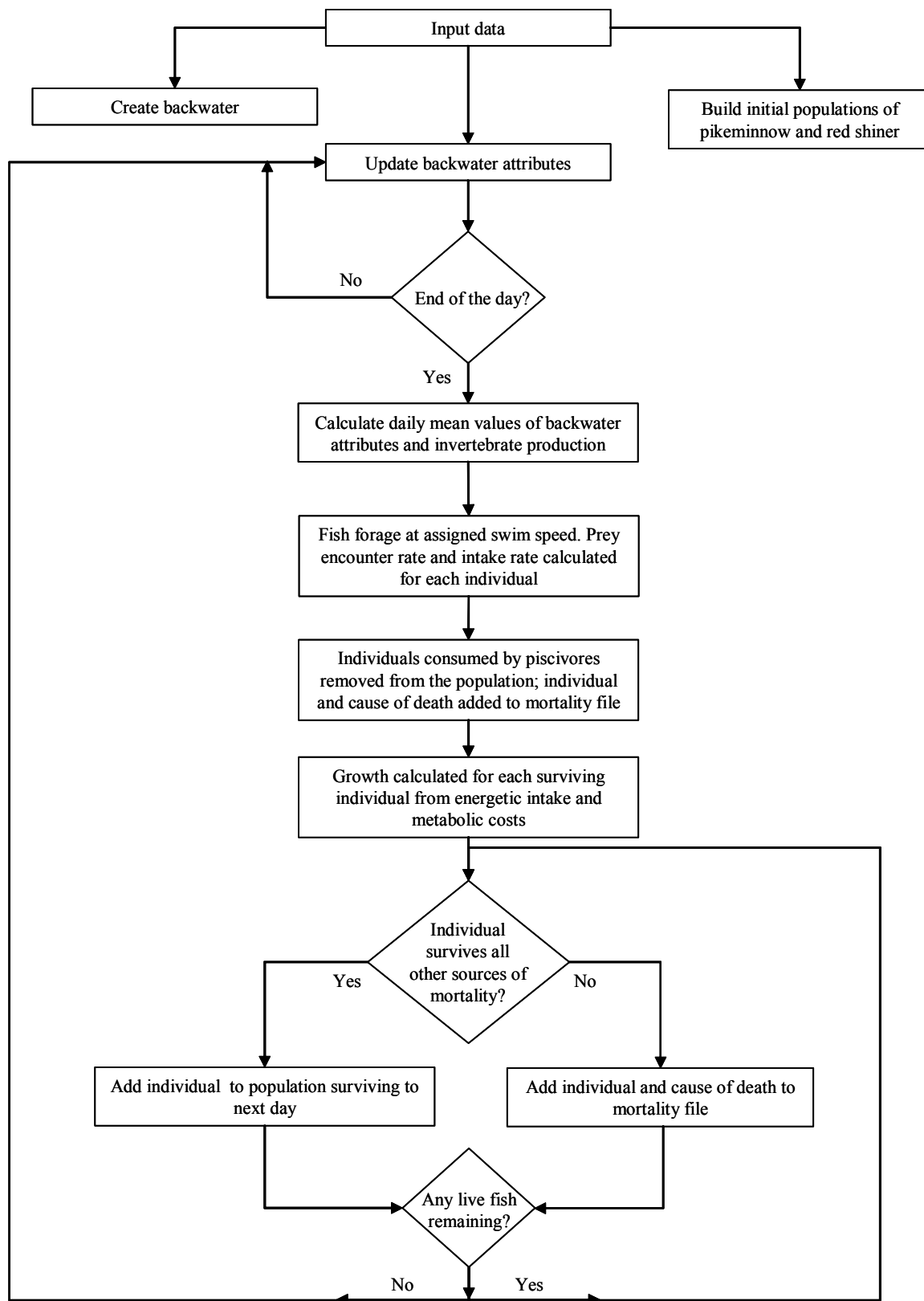


Figure 1. Flow diagram of model processes.

Design concepts

Emergence

We explicitly model the foraging behaviour of each fish, calculating swimming speed, prey encounter rate, respiration costs and growth, each of which is in some way dependent upon total fish length. Emergent system dynamics include (1) the size structure of the two fish populations (including the number of pikeminnow that survive and grow large enough to survive the following winter, the outcome of primary management interest), (2) the frequency of piscivory, and (3) the relative importance of the various mortality sources.

Adaptation

The fish have one adaptive behaviour: selecting their swimming speed for foraging each day. Energy intake from food varies with swimming speed, prey density, fish size, and day length. Energetic costs vary with swimming speed, fish size, day length, and temperature. Many of these relationships are nonlinear and we found that simple foraging rules (e.g., swim at one body length per second) produced clearly non-adaptive behaviour under some conditions. Instead, individuals adapt daily to their current size, prey density, temperature, etc. by evaluating a wide range of swimming speeds and selecting the speed that optimizes their net energy intake.

Fitness

The adaptive swim speed optimization maximizes the daily net energy intake. Growth is proportional to net energy intake, so immediate growth rate is the fitness measure that model fish attempt to maximize. Predation risk is not considered because risk is assumed not to be affected by fish behaviour.

Prediction

The only prediction fish use is in evaluating the net energy intake they would obtain for various swimming speeds. The fish calculate (predict) the energy intake they would get in the current day if they swam at a variety of speeds between zero and their maximum sustainable speed, before selecting the optimal speed.

Interaction

Fish interact with one another both directly, via piscivory, and indirectly, via competition for resources. Piscivory events are modeled explicitly: when one fish's foraging simulation includes consuming another fish, a prey fish is selected from the population and removed. Interactions are global, as we consider only a single backwater and assume that all fish within the backwater are potential competitors, prey and/or predators of one another. For the relatively small backwaters used as input to the model, this assumption is probably reasonable, given that our backwaters typically have very little hiding cover and fish have all day to encounter one another.

Sensing

Fish are simply assumed to know, without error, the internal variable (their size) and environmental variables (prey density, temperature, day length) they use to optimize swim speed.

Stochasticity

The habitat model is completely deterministic (i.e., the same input data will always produce the same habitat responses). The fish model, however, includes several stochastic processes related to the calculation of daily survival. For each potential prey fish encountered by a piscivore, the model draws a random number between 0 and 1. If this number is greater than

the probability of successful capture (a parameter set by the user), the prey is consumed by the piscivore and removed from the fish population. This probabilistic approach is frequently used when modeling predator-prey interactions (see Bestgen et al. 1997).

Collectives

Our model does not consider the formation of aggregations of individuals such as schools or flocks.

Observation

To test and analyze our model, we output data at the end of each hour (for habitat variables) and at the end of the day (for fish variables and daily habitat variables). These output files can easily be imported to a spreadsheet for analysis and visualization. In addition, we use ‘probes’ which can be used during run time to examine current values of habitat variables under a wide range of conditions. Output data, including the relative sizes of the CPM and RS populations and their relative size structures, can be compared to field observations made at different levels of flow variation to test the model’s predictions about the effects of flow fluctuation on CPM growth and survival.

The pikeminnow model’s software includes a graphical display of the backwater habitat and how backwater size, depth, and temperature varies hourly with river flow. This display is useful for demonstrating the model’s physical components; it is not useful for observing or understanding fish behavior, however, because the fish component is nonspatial.

Initialization

A model run starts by reading in the habitat characteristics that do not change during the simulation. These characteristics are the location and dimensions of square backwater cells (obtained by standard survey techniques), the values of habitat variables that do not change with time (e.g., the length of a time step, twilight length) and the input files containing weather, mainstem temperature, air temperature and flow (see Section 6). For further details about habitat initialization, see Grand et al. (in prep).

Two separate initialization dates are used: one for habitat and one for fish. The date upon which fish are initialized is selected so that CPM are typically large enough to have begun endogenous feeding (Tyus et al. 2000). This date varies among years because spawning and hatching dates of CPM can vary annually (between early June and mid to late July), as can the onset of the base flow period. Habitat simulations start several days before fish are initialized because the backwater temperature prediction module must run several days before effects of initial conditions are lost.

We build the initial populations of CPM and RS from input data specifying (1) their density in the backwater, (2) the mean and standard deviation in length of individuals arriving in nursery habitats at the onset of the base flow period, and (3) weight-length relations. The initial number of fish is calculated by the model as their initial density times the backwater’s minimum wetted area on the day of fish creation. Lengths for each fish are drawn randomly from normal distributions with the specified means and standard deviations. In order to avoid drawing lengths that are unrealistically small, we limit initial fish lengths to no less than half the mean: if a length is drawn that is less than half the mean, we do not use it and instead draw another random length. Weights are then calculated from length according to empirically derived weight-length relationships.

Initialization dates and the values of variables requiring initialization are indicated below.

Table 2. Initial values of variables and initialization dates.

Variable	Value ^a	Reference ^a
Initial fish density (fish per m ²)	0.5 – 1; 1 – 5	Haines and Tyus (1990); Bestgen et al. (1997)
Initial mean fish length (mm)	12; 45	Bestgen et al. (1997)
Standard deviation about initial mean fish length	2; 4	Derived from Bestgen et al. (1997)
Date of fish creation	07/07/1994	-
Simulation start date	07/03/1994	Various sources

^a Where more than two values or references appear, the first refers to CPM, the second to RS.

Input

To predict backwater size and temperature, the habitat model requires input data on mainstem flow, mainstem temperature, air temperature, relative humidity, cloud cover and wind speed. Mainstem flow and temperature data should be obtained from a site as close to the backwater as possible. Due to the subjectivity of weather data (e.g., percent cloud cover), information from the closest weather station should suffice.

In our simulations, we use mainstem temperature and flow data measured hourly at the Jensen Gage and weather data (air temperature, wind speed, relative humidity and cloud cover) collected daily at Grand Junction, Colorado. The Jensen gage is located approximately 90 km upstream of our study site. Grand Junction is approximately 150 km southeast of our study site. Input data files are available from the authors upon request.

Submodels

Foraging

During the day, fish are assumed to be actively swimming about the backwater searching for prey. Daily food intake depends on (1) swimming speed (s , mm·s⁻¹), (2) fish length (L , mm; which influences whether the fish includes prey fish in its diet), (3) food availability and (4) the number of other fish foraging on the same prey type. We assume that both CPM and RS become piscivorous once they reach a length of 50 mm.

Swimming speed (s , mm·s⁻¹) is assumed to be the fraction (f_{swim}) of the fish's maximum swim speed (s_{max} , mm·s⁻¹) that optimizes net energy intake;

$$s = f_{swim} \cdot s_{max}$$

where s_{max} , at mean daily temperatures (\bar{T} , °C) less than or equal to 25 °C is equal to;

$$s_{max} = 0.9 \cdot (22 + 2.4 L + 5.8 \bar{T} - 0.030 L \bar{T})$$

When $\bar{T} > 25$ °C, for the purposes of calculating s_{max} , we assume $\bar{T} = 25$ °C.

Our feeding formulation uses the (1) density of invertebrate prey (I_{dens} , number of prey individuals·m⁻²) and (2) the concentration of fish prey (F_{conc} , number of prey individuals·m⁻³) available in the backwater daily to determine daily food availability. For simplicity, we assume that food is distributed evenly within the habitat. I_{dens} depends upon the rates at which food is

produced and removed from the backwater by flushing, and as such, is determined by the habitat model. F_{conc} is an emergent property of the size of individuals and will vary from fish to fish because piscivores can prey on both CPM and RS and potential prey size is positively correlated with predator size:

$$F_{conc} = \frac{F_{avail}}{\bar{V}}$$

where \bar{V} is the backwater's daily mean volume (m^3) and F_{avail} is the total number of prey fish available for consumption by an individual. The value of the variable F_{avail} is calculated for each piscivore by summing the number of fish (both CPM and RS) that are currently less than or equal to the piscivore's maximum prey size (F_{max} , mm) where:

$$F_{max} = 0.25 \cdot L$$

In cases where there are no fish less than the piscivore's maximum prey size and when prey fish consumption results in the piscivore consuming less than the fish's maximum daily ration (C_{max} , g), we assume that it reverts to eating invertebrates and forages according to the methods described for invertebrate eaters.

We assume that the search rate of fish who feed on invertebrates (S_I , $mm^2 \cdot s^{-1}$) is equivalent to the area of a rectangle with length equal to the fish's swimming speed (s , $mm \cdot s^{-1}$) and width equal to the fish's reactive distance (the distance over which it can see and respond to prey (RD , mm)):

$$S_I = RD \cdot s$$

We assume that search rate of fish feeding on other fish (S_F , $mm^3 \cdot s^{-1}$), is equivalent to the volume of a cylinder with height equal to the fish's swimming speed (s , $mm \cdot s^{-1}$) and radius equal to the fish's reactive distance (RD , mm):

$$S_F = \pi \cdot RD^2 \cdot s$$

Regardless of prey type, we assume that reactive distance increases with fish length and declines as swimming speed increases relative to the fish's maximum swimming speed:

$$RD = 3.3 \cdot L \cdot \left(\frac{S_{max} - s}{S_{max}} \right)$$

Finally, we assume that a fish's rate of encountering prey varies linearly with the rate at which food becomes available in the water column. Thus, for a fish foraging on invertebrates, the total number of prey encountered (e_I) during the day will be:

$$e_I = 0.0036 \cdot I_{dens} \cdot S_I \cdot D$$

where D equals the number of daylight hours. Similarly, for an individual foraging on fish, the total number of prey encountered (e_F) during the day will be:

$$e_F = 0.0000036 \cdot F_{conc} \cdot S_F \cdot D$$

Frequently, the density of CPM and RS in a backwater will result in the total number of prey encountered being greater than that available. Such competition will result in individuals

consuming fewer prey than they encounter. Due to differences in the methods we use to calculate invertebrate and fish prey availability, we model competition for invertebrates and fish separately. We model piscivory first, because piscivores may consume both other fish and invertebrate prey.

We calculate each piscivore's fish prey intake based upon its encounter rate with smaller, live fish and the probability of capture for each encounter. Capture probabilities are assumed to be independent of prey size. We perform these methods on one piscivore at a time, in random order, identifying captured prey as “dead” on the list of fish maintained by the computer code. Thus, competition arises as a direct consequence of the prior consumption of prey by other piscivores, and may result in some piscivores consuming no prey on a given day (even though $F_{conc} > 0$ for them).

After calculating the number of prey fish the piscivore is likely to encounter (e_F), we calculate the number of fish it consumes (c_F) by drawing e_F random numbers between 0 and 1 and evaluating how many are less than 0.25, the probability of capturing each encountered prey. We then draw c_F random integers between 0 and ($e_F - 1$) and repeat the above calculations for all remaining piscivores. Note that these steps will often result in a single prey fish being potential prey to more than one piscivore.

Then, for each piscivore, we label the fish that correspond to each of the c_F random numbers as ‘dead’ on the list of all fish maintained by the computer code (sorted in order of increasing size), thereby rendering them unavailable for consumption by another piscivore. The weight (W) of the eaten fish is added to the piscivore’s daily energy intake from fish prey (I_F , g), which is then compared to its daily maximum ration (C_{max} , g). If $I_F < C_{max}$, the piscivore continues foraging on invertebrates (and is subject to competition for invertebrate prey as outlined below) and the piscivore’s daily energy intake from invertebrates (I_I , g) is calculated (see below).

We model the effects of competition for invertebrate prey by first, calculating the total quantity encountered ($e_{I_{tot}}$, number) by all live, invertebrate-eating fish, both CPM and RS ($i = 1$ to N):

$$e_{I_{tot}} = \sum_{i=1}^N e_i$$

When the total quantity of invertebrates encountered is less than or equal to the total available in the habitat:

$$e_{I_{tot}} \leq I_{dens} \cdot A_{min}$$

where A_{min} (m^2) is the backwater’s daily minimum wetted area, then,

$$c_I = e_I$$

When the total quantity of invertebrates encountered by all fish exceeds their total availability in the backwater, we calculate the difference between the two (I_{Δ} , $num \cdot m^{-2}$),

$$I_{\Delta} = \frac{e_{I_{tot}}}{A_{min}} - I_{dens}$$

Whenever the total encounter rate with invertebrates exceeds their availability in the backwater, we assume that each individual's consumption (c_I , number of prey) is reduced proportional to its relative encounter rate with prey. Thus, for fish feeding on invertebrates:

$$c_I = e_I (I_{\Delta} \cdot A_{min}) \cdot \left(\frac{e_I}{e_{I_{tot}}} \right)$$

In order to calculate net energy intake, c_I must be converted from number of prey to grams, such that the fish's daily energy intake from invertebrates (I_I , g) is equal to:

$$I_I = c_I \cdot W_I$$

where W_I (g·prey⁻¹) is the weight of each individual prey item.

During the calculation of net energy intake, we verify that calculated intake does not exceed the physiological maximum daily intake (C_{max} , g) where C_{max} is equal to:

$$C_{max} = (0.0005904 \bar{T}^2) - (0.0001735 \bar{T}^3) + (0.0000181 \bar{T}^4) - (0.0000007 \bar{T}^5) + (9.9 \cdot 10^{-9} \bar{T}^6)$$

Currently, we use C_{max} both to determine whether piscivorous fish should include invertebrates in their diet and to limit the daily energy intake of all fish in the model.

For fish eating only invertebrates, it is straightforward to calculate the effect of maximum consumption on daily total intake. When $C_I > C_{max}$, then $C_I = C_{max}$. Similarly, for piscivores consuming only fish prey, when $C_F > C_{max}$, then $C_F = C_{max}$. However, for piscivores consuming both fish and invertebrate prey, one needs to consider whether the addition of invertebrates to the diet results in the fish's total prey intake exceeding C_{max} and if so, reducing prey intake accordingly. For simplicity, we assume that whenever total prey intake exceeds C_{max} , fish reduce only their energy intake from invertebrates. Thus, when $C_I + C_F > C_{max}$, then $C_I = C_I - (C_I + C_F - C_{max})$.

Prey energy density is used to convert grams of prey eaten into joules of energy. We adopt the values of VanWinkle et al. (1998) of 1500 j·g⁻¹ for the energy density of invertebrates and 5900 j·g⁻¹ for the energy density of fish prey. Thus, each individual's total energy intake, E_T (j) is equal to:

$$E_T = (1500 \cdot I_I) + (5900 \cdot I_F)$$

Growth

We model daily growth as the difference between total energy intake and energetic expenditure due to respiration. We assume that respiration depends on activity and can be broken down into two components: standard respiration (R_S , g O₂·g⁻¹ fish·d⁻¹) and active respiration (R_A , g O₂·g⁻¹ fish·d⁻¹). Standard respiration takes place 24 hours per day and assumes no activity; activity respiration is the energy needed to swim while foraging. Total respiration (R_T , g O₂) is the sum of these two. Respiration costs are in mass equivalents of oxygen per day:

$$R_S = 0.0004 \cdot W^{-0.087} \cdot e^{0.085 \cdot \bar{T}}$$

and

$$R_A = \frac{D}{24} \cdot (e^{(0.012 \cdot sT)} - 1) \cdot R_S$$

Thus,

$$R_T = W \cdot (R_S + R_A)$$

We use an 'oxycalorific' conversion factor of 13 560 j·g⁻¹ O₂ to convert R_T into joules of energy. Hence, the total daily energy expended while foraging (X_T , j) is equal to:

$$X_T = 13\,560 \cdot R_T$$

The daily change in fish weight (G , g) is equal to the fish's net energy intake divided by the energy density of a fish:

$$G = \frac{E_T - X_T}{5900}$$

From daily growth, the model calculates changes in length and condition factor (K). We limit the daily length increase to some proportion of the fish's length (F_L) on the previous day, thereby allowing individuals who obtained a large amount of food to increase their condition factor to greater than 1.0. Weight, length and condition factor are calculated as follows;

- The fish's weight (W) is changed by the value of G . Note that G can be negative, in which case, length is unchanged.
- The length of a "healthy" fish, given the fish's new weight (L_W) is calculated from the following weight-length relationships:

$$W = 0.000029 \cdot L_W^{2.56} \quad \text{if the fish is a CPM}$$

and

$$W = 0.0000031 \cdot L_W^{3.28i} \quad \text{if the fish is a RS.}$$

- The fish's proposed length increase (L_P) and maximum length (L_{max}) increases are calculated:

$$L_P = L_W - L$$

$$L_{max} = P_L \cdot L$$

- If $L_P < L_{max}$ and $L < L_W$ (indicating that the fish is not underweight), then $L = L_W$.
- If $L_P < L_{max}$ and $L < L_W$, then $L = L + L_{max}$
- If $L > L_W$ (indicating that the fish is underweight for its length), L is not changed, regardless of the relationship between L_P and L_{max} .
- The new condition factor is equal to the fish's new weight divided by the "normal" weight for a fish of its new length:

$$K = \frac{W}{0.000029 \cdot L^{2.56}} \quad \text{if the fish is a CPM}$$

and

$$K = \frac{W}{0.0000031 \cdot L^{3.28}} \quad \text{if the fish is a RS.}$$

Mortality

We model four sources of mortality; (1) high temperature (S_T), (2) poor condition (S_K), (3) terrestrial predation (S_{TP}) and (4) aquatic predation. Aquatic predation (predation by piscivorous CPM and RS) occurs during the foraging methods (see above).

Mortality sources 1 -3 are modelled using survival probabilities. Survival probabilities are the daily probability of not being killed by one or more mortality sources. We use survival probabilities (S) instead of mortality risks ($1 - S$) so that survival of multiple mortality sources can be calculated simply by multiplying together the survival for each individual source. Thus, total daily survival (S_{tot}) is equal to:

$$S_{tot} = S_T \cdot S_K \cdot S_{TP}$$

We treat each mortality source as independent of the others. On each day, for each fish, we evaluate each mortality source by (1) obtaining the survival probability from the fish's mortality methods (see below), (2) drawing a new random number from a uniform distribution between zero and one, (3) considering the fish dead as a result of the mortality source if the random number is greater than the fish's survival probability, (4) recording the time of death and mortality source responsible, and (5) identifying the fish as “dead” on the fish list maintained by the computer code.

High temperature mortality is due to physiological breakdown at peak temperatures and is modeled as a decreasing logistic function of the mean daily temperature in the backwater (\bar{T}):

$$S_T = \frac{e^{43.94 - (1.1 \cdot \bar{T})}}{1 + e^{43.94 - (1.1 \cdot \bar{T})}}$$

Mortality due to poor condition (i.e., when the fish has low weight for its length) occurs in response to starvation, disease and increased risk of predation. We use an increasing logistic function to represent mortality as a function of condition:

$$S_K = \frac{e^{-6.45 + (13.73 \cdot K)}}{1 + e^{-6.45 + (13.73 \cdot K)}}$$

Terrestrial predation is due to birds and mammals that do not hunt while submerged and is generally assumed to be higher for bigger fish, in shallow water. Following Railsback et al. (1999), our formulation for terrestrial predation assumes a minimum survival probability (S_{min}) that applies when fish are most vulnerable to terrestrial predators, and a number of factors that can increase the probability of survival. We model three survival increase factors; maximum backwater depth (S_D), fish length (S_L), and ice cover (S_I). We assume that survival increase factors act independently of one another. Hence, we obtain survival of fish from terrestrial predation by increasing the minimum survival (decreasing the difference between minimum survival and 1.0) by the maximum of the independent survival increase factors.

$$S_{TP} = S_{min} + ((1 - S_{min}) \cdot \max(S_D, S_L, S_I))$$

Fish are assumed to be more vulnerable to terrestrial predators when there is no deep water available as a refuge. We model the survival increase function associated with water depth (S_D) as an increasing logistic function of the backwater's daily maximum depth (d_{max} , m):

$$S_D = \frac{e^{-3.53 + (4.39 \cdot dmax)}}{1 + e^{-3.52 + (4.39 \cdot dmax)}}$$

Small fish are less vulnerable to terrestrial predation, presumably because they are less visible. We model the survival increase function associated with fish length (S_L) as a decreasing logistic function of the fish's current length (L):

$$S_L = \frac{e^{7.69 - (0.22 \cdot L)}}{1 + e^{7.69 - (0.22 \cdot L)}}$$

Backwaters are prone to the development of ice cover during winter months. Such cover may provide fish with protection from terrestrial predation. Rather than explicitly modeling the process of ice formation, we simply assume that whenever water temperature falls to 0 °C (i.e., $T_{min} \leq 0$), the backwater is covered with ice. We model the survival increase function associated with the presence of ice cover (S_I) as a Boolean variable; when ice is present, $S_I = 1$, otherwise, $S_I = 0$.

Table 3. Parameter values and descriptions.

Parameter	Description	Value used
W_I (g)	Weight of each invertebrate prey	0.00008
f_{swim}	Fraction of maximum swimming speed	0.05
S_{min}	Minimum daily survival from terrestrial predation	0.95
f_L	Fraction of previous day's length	0.005

Table 4. Internal model variables and descriptions.

Variable name (units)	Description
s_{max} (mm·s ⁻¹)	Maximum swimming speed
s (mm·s ⁻¹)	Swimming speed
RD (mm)	Distance over which fish can see and respond to prey
S_I (mm ² ·s ⁻¹)	Search rate when foraging on invertebrates
S_F (mm ³ ·s ⁻¹)	Search rate when foraging on prey fish
F_{max} (mm)	Maximum size of prey fish
F_{avail} (# of fish)	Number of prey fish less than or equal to maximum size of prey fish
F_{conc} (# of fish · m ⁻³)	Concentration of prey fish
e_I (# of invertebrate prey)	Number of invertebrate prey encountered per day
c_I (#)	Number of invertebrate prey eaten

Variable name (units)	Description
e_F (#)	Number of prey fish encountered
c_F (#)	Number of prey fish eaten
I_F (g)	Energy intake from prey fish
I_I (g)	Energy intake from invertebrate prey
C_{max} (g)	Maximum consumption
R_S (g O ₂ ·g ⁻¹ fish·d ⁻¹)	Standard respiration
R_A (g O ₂ ·g ⁻¹ fish·d ⁻¹)	Activity respiration
R_T (g O ₂)	Total daily respiration
X_T (j)	Total daily energy expended
E_T (j)	Net energy intake
G (g)	Daily growth
L_W (mm)	Desired new length given new weight
L_P (mm)	Proposed length increase given daily growth
S_T (prob)	Daily probability of surviving high temperature mortality
S_K (prob)	Daily probability of surviving poor condition mortality
S_{TP} (prob)	Daily probability of surviving terrestrial predation
S_{tot} (prob)	Total daily probability of survival
S_D (prob)	Increase in survival from terrestrial predation due to backwater depth
S_L (prob)	Increase in survival from terrestrial predation due to fish length
S_I (prob)	Increase in survival from terrestrial predation due to the presence/absence of ice

Example Mangroves

The original model description, including all full references, is presented in:

Berger, U., and H. Hildenbrandt. 2000. A new approach to spatially explicit modelling of forest dynamics: spacing, ageing and neighbourhood competition of mangrove trees. *Ecological Modelling* 132:287-302.

Abstract: The spatially-explicit mangrove model KiWi describes individual trees by the so called Field-Of-Neighbourhood (FON) approach. FON enables the influence of neighbourhood effects on the dynamics of forests and plant communities to be analysed. The feature of FON is that modelling of local competition between neighbouring trees is based on the notion of a circular scalar field of neighbourhood intensity exerted by each tree within the size dependent ZOI around its stem position. The FON intensity exerted by the neighbouring trees within the overlapping area is taken as competition index which reduces the growth rate of the focal tree. Beside that proxy, pore water salinity and nutrient availability may modify the otherwise size dependent, sigmoid growth function of a single tree. In KiWi, mortality is modelled in terms of a 'memory function', i.e. the yearly stem increment of each tree is stored in its 'memory' over a certain time period and determines — as a sign of vitality — tree mortality. The results of KiWi demonstrate that this description is sufficient to keep the maximum age of the trees within a reasonable limit. The model thus manages without a description of individual tree age. This is an important feature considering the fact that a direct relationship between tree age and mortality is questioned and there is no established method as yet for determining the age of mangrove trees. Realistic self-thinning behaviour and succession characteristics of modelled neotropical mangrove stands confirm the suitability of the FON approach for the description of intra- and inter-specific competition and the KiWi model for forests consisting in *Avicennia germinans*, *Rhizophora mangle*, and *Laguncularia racemosa*.

Modified model description written by: **Uta Berger and Cyril Piou**

Purpose

The KiWi model was developed for analysing neotropical mangrove forest dynamics affected by environmental settings (pore water salinity and nutrient availability), inter- and intra-specific competition, natural disturbances (lightning and hurricane destruction), and tree cutting. The forests consist in *Avicennia germinans*, *Rhizophora mangle*, and *Laguncularia racemosa* trees.

State variables and scales

The KiWi model has two hierarchical levels: individual trees and simulated area. At individual level, tree establishment, growth, mortality, and competition are considered. The simulated area defines abiotic conditions by mean of maps of local pore water salinity, nutrient availability or any other variable thought to interact with individual trees.

An individual tree is described by its stem position (x and y), its age (Age) its stem diameter (dbh), and its annual stem increment (Δdbh).

The size of the simulation area can be arbitrarily attributed (x_{\max}, y_{\max}). A typical size is 1-5 ha. The maps are set to cover the entire simulation area but their resolutions depend on their pixel sizes.

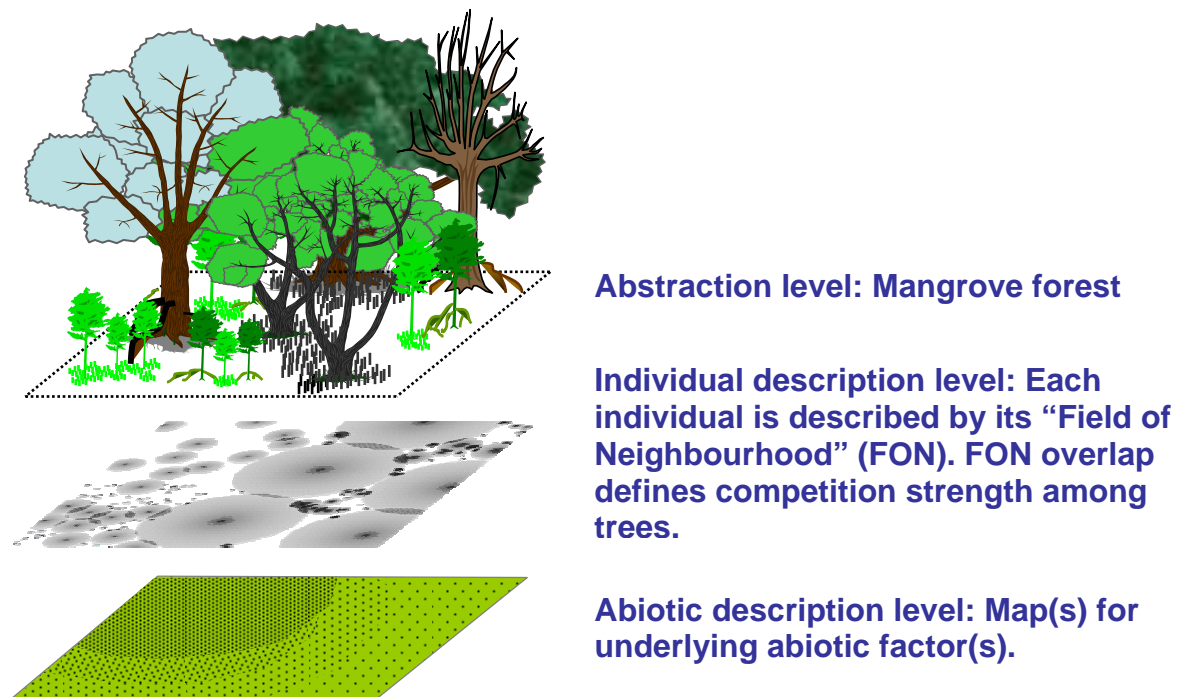
Process overview and scheduling

The trees life cycle is described by three biological sub-models operating at yearly time step. The first sub-model predicts the stem increment of the trees depending on their current stem diameter, neighbourhood competition, pore water salinity, and nutrient availability. The second simulates tree mortality depending on the growth realized within a certain time span by the focal tree. The third sub-model incorporates the establishment of new trees depending on the available space (described by the neighbourhood competition exerted by the existing trees at a certain location), and the abiotic conditions. The biological sub-models are linked to the simulated area through the maps describing the abiotic conditions (see Figure 1). Each time step, a sequence of processes is operated following the three biological sub-models (see sub-models part for details):

- 1) establishment of new trees,
- 2) growth of trees,
- 3) mortality of trees

The concrete realization of growth, tolerance to pore water salinity, effectiveness of nutrient use, thresholds for tree establishment, and mortality are species-specific.

Figure 1. Scheme of the KiWi model.



Design concepts

Emergence

We explicitly model the growth of each tree depending on neighbourhood competition and abiotic conditions, and the resulting mortality. Emergent system dynamics include (1) the size structure of the forest, (2) species composition, (3) self thinning behaviour, (4) the distribution of mortality size classes, (4) species zonation, and (5) vertical canopy zonation.

Interaction

Trees compete with one another for spatially distributed resources. This competition is phenomenologically described using the so-called Field of Neighbourhood (FON) approach. According to this approach, each tree has a circular, size-dependent FON around its stem position where the tree influences its neighbours and is influenced by them. The FON is derived from the philosophy of the Zone of Influence (ZOI) models. However, a scalar field exponentially decreasing from the stem to the boundary defines the strength of competition the tree exerts at each location. Trees with overlapping FONs are neighbours. The sum of the neighbouring FONs on the FON area of a focused tree mark the neighbourhood competition the later “receives”. We considered also for the establishment of new trees that the sum of all FONs at a certain position (x,y) marks the competition strength at this position and determine if a new tree can settle there.

Sensing

Individual trees are “informed” about the abiotic conditions at their stem position and the local neighbourhood situation via FON overlapping.

Stochasticity

The KiWi model includes several stochastic processes related to the establishment of trees and the occurrence of additional mortality. However, the tree growth and density dependent mortality are both completely deterministic.

Observation

KiWi allows to register continuously the state variables such as stem positions, and stem diameter but also derived variables such as neighbourhood competition for each tree. The output files can easily be imported to a spreadsheet for analysis and visualization. In addition, we use the run time visualization of the forest for visual debugging. Using empirical regressions among stem diameter, tree biomass, or tree height provide further analysis in terms of self thinning and stand development.

Initialization

1. An established tree has an initial height $H = 137$ cm and a stem diameter $dbh = 1$ cm. Whereby KiWi does not take into account seedlings or saplings growth.
2. Maps of pore water salinity and nutrient availability are given as initial abiotic conditions.
3. The initial number of trees is variable. A typical value is 2000 individuals per hectare.
4. The annual rate of establishment are given as input variable and might be species specific. Typical values are *L. racemosa* : *A. germinans* : *R. mangle* = 20 : 20 : 40 individuals per hectare.

Input

The salinity and nutrient maps do not vary within the time step of one year, but can be changed during the simulation. For specific cases of perturbation effect analyses, sequences of disturbance events can be defined (or randomly chosen).

Submodels

Additionally to the three sub-models related to trees' life cycle (tree growth, tree mortality, and tree establishment), the KiWi model incorporates a competition sub-model defined by the FON approach which describes interactions among individuals:

Tree – to – tree competition

Each tree applies a Field of Neighbourhood (FON) over a circular area (A_{FON}) around its stem position. The radius R_{FON} of this area is defined by :

$$(1) R_{FON} = a \times (dbh/2)^b,$$

where a and b are species specific scaling factors (Table 1). The FON intensity is defined at each location inside A_{FON} through the distance (r) from the stem position by the following formula:

$$(2) FON(r) = \begin{cases} for(0 \leq r < (dbh/2)) \Rightarrow F_{max} \\ for((dbh/2) \leq r \leq R_{FON}) \Rightarrow e^{c(r-(dbh/2))} \\ for(r > R_{FON}) \Rightarrow 0 \end{cases},$$

where F_{max} , is an input constants (Table 1) and c is an integration constant derived from F_{min} (Table 1). This description assumes that the FON within the stem is maximal (F_{max}) and decreases exponentially down to F_{min} at FON's edge. At each position (x,y) within the simulated area, the competition strength can be computed considering the N trees of the forest with the formula:

$$(3) F(x,y) = \sum_{n=1}^N FON_n(dist(x,y)),$$

where the $dist(x,y)$ function would give the distance of the considered point to the tree n . Since trees with overlapping FONs are considered neighbours, interaction among individuals is then defined for a focal tree (k) as the average (F_A) of the FON effects of the neighbours trees (N') over the focal tree FON area (A_{FON}):

$$(4) F_A = \frac{1}{A_{FON}} \times \sum_{\substack{n=1 \\ n \neq k}}^{N'} \int_{A'} FON_n(dist(x,y)) d a',$$

where A' is the overlapping area. In KiWi, the calculation of this F_A is done sequentially: for each tree in the plot the neighbours are selected and the intensity of their FONs on the FON area of the focal tree is added up. This sum is finally divided by the FON area of the focal tree for weighing the influence of smaller and larger trees on each other. All plant to plant interactions are defined according to this FON sub-model and will then determine the possibility of settlement at any (x,y) position through Eq. 3 and the influence of competition on tree growth using Eq. 4.

Tree growth

The growth of each tree is described by the stem diameter increase over time. This increase is firstly described by a sigmoid function which considers the current size of a tree. This stem increment is taken as growth under optimal growth conditions. It is then reduced by three different correction factors considering pore water salinity and nutrient availability at the stem

position, as well as the competition a focal tree “receives” from its neighbourhood. It is described by the following formula (Shugart 1984):

$$(5) \quad \frac{\Delta dbh}{\Delta t} = \frac{G \cdot dbh \cdot (1 - dbh \cdot H / (dbh_{\max} \cdot H_{\max}))}{274 + 3 \cdot b_2 \cdot dbh - 4b_3 \cdot dbh^2} \cdot cF(sal) \cdot cF(nut) \cdot cF(comp) ,$$

where H is the tree height (in cm, define as (Eq. 6) $H = 137 + b_2 dbh - b_3 dbh^2$), dbh_{\max} and H_{\max} are species-specific maximum values of diameters and heights (Table 1), and G , b_2 and b_3 are species-specific growth parameters (Table 1). To compute the two first correction factors, Chen & Twilley (1998) introduce the following equations:

$$(7) \quad cF(nut) = c_1 + c_2 \cdot RNA + c_3 \cdot RNA^2$$

where RNA is the relative nutrient availability at the stem position (x,y), c_1 , c_2 and c_3 are species-specific constants (Table 1); and

$$(8) \quad cF(sal) = \frac{1}{1 + \exp[d(sal_i - sal)]}$$

where sal_i is a species-specific parameter (Table 1). The KiWi growth function incorporate the competition effect through the $cF(comp)$ correction factor, defined as :

$$(9) \quad cF(comp) = (1 - F_A / shadTol)$$

where F_A is the received neighborhood competition (Eq. 4) and $shadTol$ is a species-specific parameter to simulate shade tolerance (Table 1).

Tree mortality

To describe the mortality of each tree, the yearly stem increment is stored in its “memory” for a defined number of years (typically 5 years). If the mean increment averaged in the memory is less than the mean stem increment that a tree can achieve under optimal conditions ($M_ \Delta dbh_{opt}$, Table 1), the tree dies. This handling keeps the maximum tree age in a reasonable limit and provides that trees under stress can recover when environmental conditions and/or neighbourhood situation becomes better. The sub-model can provide furthermore the consideration of additional mortality events caused by random effects, anthropogenic disturbances such as logging, lightning, or hurricanes.

Tree establishment

For the establishment of new trees, the potential x,y stem position is chosen either randomly or according to the position of a con-specific adult. It is then checked whether an establishment at the location is possible considering competition at x,y exerted by already existing trees. If the $F(x,y)$ (Eq. 3) is inferior to a species-specific input constant ($F_{\max_establish}$) then the new tree is set to establish, otherwise not. Thus, this sub-model describes the competition tolerance of saplings, and particularly the shading effect, that are known to be different for different mangrove tree species.

Table 1. Species-specific parameters used in the KiWi model.

Parameter	Description	<i>A.</i>	<i>L.</i>	<i>R.</i>	Comments/ Reference
-----------	-------------	-----------	-----------	-----------	---------------------

		<i>germinans</i>	<i>racemosa</i>	<i>mangle</i>	
A	scaling factor FON – Radius (Eq. 1)	11.0	11.0	7.113	typical values but stand dependent
B	scaling factor FON – Radius (Eq. 1)	0.654	0.654	0.654	typical values but stand dependent
F _{max}	FON intensity within the stem (Eq. 2)	1.0	1.0	1.0	Berger & Hildenbrandt 2000
F _{min}	FON intensity at FON's boundary (Eq. 2)	0.1	0.1	0.1	Berger & Hildenbrandt 2000
G	Growth constant (Eq. 5)	162	243	267	Chen & Twilley 1998
dbh _{max}	maximum stem diameter (Eq. 5)	140	80	100	Chen & Twilley 1998
H _{max}	maximum tree height (Eq. 5)	3500	3000	3000	Chen & Twilley 1998
b ₂	constant in height to dbh relationship (Eq. 5 & 6)	48.04	71.58	77.26	Chen & Twilley 1998
b ₃	constant in height to dbh relationship (Eq. 5 & 6)	0.172	0.447	0.396	Chen & Twilley 1998
c ₁	constant for nutrient effect on growth (Eq. 7)	-0.5	-1.0	0.0	Chen & Twilley 1998
c ₂	constant for nutrient effect on growth (Eq. 7)	2.88	4.42	1.33	Chen & Twilley 1998
c ₃	constant for nutrient effect on growth (Eq. 7)	-1.66	-2.50	-0.72	Chen & Twilley 1998
D	constant for salt effect on growth (Eq. 8)	-0.18	-0.20	-0.25	Chen & Twilley 1998
Sal _i	salt effect on growth (g kg ⁻¹) (Eq. 8)	72.0	65.0	58.0	Chen & Twilley 1998
shadTol	Shading tolerance factor on growth (Eq. 9)	0.15	0.10	0.50	typical values, but simulation exercise dependent
M_Δdbh _{opt}	mortality threshold	0.5 x 0.466	0.5 x 0.466	0.5 x 0.4	Berger & Hildenbrandt 2000
F _{max_establish}	establishment threshold	0.03	0.001	0.5	typical values, but simulation exercise dependent

Example Mangrove Crab Movement

The original model description, including all full references, is presented in:

Piou, P., Berger, U., Hildenbrandt, H., Grimm, V., Diele, K., D’Lima, C. Simulating mangrove crab movements to understand local scale recovery phenomenon after fishery. (in preparation).

Abstract: [not available]

Model description written by: **Cyril Piou**

Purpose

The IBU model was designed to simulate *Ucides cordatus* individual movement from burrow to burrow. It aimed to analyze the plausible type of such movement, which are cryptic and not known for this species. From these understanding it was also designed to have the capacity to assess diverse population management questions at local scale (<ha).

States variables and scales

The model had only two hierarchical levels: individuals and simulated area. The simulated area was described as a homogeneous continuous mangrove mud flat where were positioned individual *U. cordatus* and burrows. The size of the area was believed to not go over a maximum of few tens of meters. The temporal unit was set as a day and simulations were thought to spend less than a year.

State variables of individual crabs were defined as: identity number (id_c), position (x_{ic} and y_{ic}), carapace width (CW), occupied burrow id (id_{ba}), probability to leave the occupied burrow (P_l), probability to stop after a step of movement (P_s), angle of direction for movement (α_d) and eventually some sub-models other variables (see below). The burrows states variables were: identity number (id_b), position (x_{ib} and y_{ib}), hosted crab id (if any, id_{ca}), open/close status (Op) and time without a crab (if not occupied, t_{empty}).

Process overview and scheduling

The model proceeded in day steps, applying the following sequence of functions: calculating eventually some sub-models necessary parameters depending on the used general assumptions of crab interaction (see below), checking the status of all burrows with removing the too long empty ones, and checking the status of all crabs in a random order. During this last function, individual crabs could accomplish one of the following actions: do nothing, change the open/close status of its burrow or move away from its burrow and take over or create a new one. When a crab took over an occupied burrow the crab inside was forced to move when its turn of being checked came. However, the burrow of a crab that already moved once during the time step could not be colonized. The movement of a crab was defined in different sub-processes: reason of moving, direction of movement and reason of stopping, which determined three modules described in the sub-models section.

Design concepts

Emergence. – The IBU model produced two main emergent properties of *Ucides cordatus* population characteristics at local scale re-colonization capacity of an emptied area with burrows and re-colonization of an emptied area without burrow. In contrast, mean frequency of movement, mean distance of movement, proportion of occupied burrows or proportion of closed burrows, which were also used as pattern for sub-model validation, were resulting of combination of forcing parameters depending on the sub-models.

Interaction. – Because very few information exist on crab interaction during non-reproductive time and if they would influence the change of burrow of *U. cordatus* individuals, three assumptions of interactions were tested at different levels: -no apparent interactions (Null assumption), direct competition with neighboring individuals in a determined area (adapted from the Fixed Radius Neighborhood models, e.g. Pacala and Silander 1990, FRN assumption), indirect competition with neighboring individuals through the use of shared resources (adapted from the Field Of Neighborhood approach, Berger and Hildenbrandt 2000, FON assumption). The FRN approach adapted in IBU assumed that crabs would interact with neighbors in a fixed circular area around their burrow position. This interaction represented by the number of neighbors would then determine the probability of moving away from an occupied burrow. The FON adaptation assumed an intensity field around each crab position representing the harvest area. Any considered crab would feel the neighboring individuals and be felt by them through the overlaps of these fields. Distance and size of the neighbors were determining the intensity of their FON effect on a given crab. The sum of the FON effects of the neighbors for a given crab was assumed then to influence the probability of moving away from its burrow.

Stochasticity. – Individual crab behavior (such as closing/opening its burrow, taking over an occupied burrow, and reason, direction or stop of movement for some sub-models) and burrow disappearance were assumed to follow some determined probabilities estimated from field work information (see Table 1). Stochasticity was used for each of these probabilities to evaluate if the individual had to do the respective action at each action step.

Observation. – Crabs and burrows “populations” information could be observed at each time step and were analyzed for model testing and analysis.

Initialization

IBU simulations were initialized by first creating the number of crabs given by the input density (D_c , Table 1 and 2) together with their burrows in random position on the area; and secondly by adding the proportion ($Prop_{Unoc}$, Table 1) of unoccupied burrows at random positions as well. The open/close status of all the burrows were determined randomly following a probability corresponding to expected proportion ($Prop_{closed}$, Table 1). These last two proportions were given as input from field observation. Carapace size of individual crabs was randomly attributed according to a normal distribution around a given mean size (CW_{pop} , Table 1) with a corresponding standart deviation ($SD_{CW_{pop}}$, Table 1) for the simulated population. The size of the burrows were also following this normal distribution but the associated ones were set randomly a little bit bigger or smaller (Dif_{Bsize} , Table 1) than the inside crabs to simulate natural variance. Sub-models necessary parameters, simulation time (t_{max} , Table 1), size of the area (X_{max} and Y_{max} , Table 1), output scheduling, and experiment scheduling and parameters (cf simulation experiments part) were also given as input information at the beginning of each simulation.

Input

No input.

Submodels

In IBU model, the type of crab movement behavior was combining three modules having each of them different sub-models: Reason of movement, walking behavior and reason of stopping movement. The reason of movement and stopping modules had sub-models following the three general assumptions (Null, FRN and FON). Additionally, IBU had a simple burrow related sub-model simulating the disappearing of burrow phenomenon.

Reason of movement module

Random reason sub-model (RM_r). – This sub-model, following the first assumption (Null assumption), assumed that the crabs had a constant probability of leaving their burrow. It used an input probability (P_w , Table 2) set by the experimenter to determine randomly if the individual walk at a given step or not (for each crab at each steps, $P_l = P_w$)

Direct intraspecific competition sub-model (RM_{FRN}). – This sub-model supposed that crabs interacted in a defined area around themselves disregarding either the size nor the distance of the neighbors. The radius of interaction (R_{int}) was calculated for each crab at the starting of the simulation with the following formula:

$$(1) R_{int} = \min\{a \times (CW/2) + b, R_{max}\},$$

where a and b were constants (Table 1), and R_{max} a maximum radius assumed to be 100cm. It estimated to simulate the radius of daily action (not burrow change) of respective crab size observed on the field (Nordhaus 2004, C. Piou personal observation). The number of neighbors was counted at each starting of time steps ($NEIG_n$) and used in the following formula to influence the probability of leaving a burrow (P_l):

$$(2) P_l = P_w \times \frac{NEIG_n}{NEIG_{max}},$$

where $NEIG_{max}$ was a constant (Table 3). This sub-model supposed therefore that a crab always had a probability to leave, but also that this probability would be proportional to the number of neighbors related to a normal supported number.

Indirect intraspecific competition sub-model (RM_{FON}). – This sub-model adapted the Field Of Neighborhood approach developed by Berger and Hildenbrandt (2000) for tree and sessile organisms. The radius of action of the FON (R_{int}) was calculated for each crab with the same formula (Eq. 1) as in the RM_{FRN} sub-model. The intensity of the FON or competitive action at any point distant of r from a considered crab was considered as (Berger and Hildenbrandt 2000):

$$(3) FON(r) = \begin{cases} 1 \rightarrow \text{for}(0 \leq r < (CW/2)) \\ e^{c(r-(CW/2))} \rightarrow \text{for}((CW/2) \leq r \leq R_{int}) \\ 0 \rightarrow \text{for}(r > R) \end{cases},$$

where c was a constant. The sum of the FON intensity of the neighbors over the FON area of a considered crab was then divided by its own FON area. This competition intensity (F_A) was calculated at the beginning of each time step for each crab. When the crabs were individually checked, F_A was used to determine the probability of leaving (P_l) a burrow with the following formula

$$(4) P_l = P_w \times \frac{F_A}{F_{A-MAX}},$$

where F_{A-MAX} was a constant given as input (Table 3).

Walking behavior module

Random walk sub-model (WBr). – The walking behavior was defined as the type and order of actions a crab would execute when it left its burrow and looked for another one or created a new one. This behavior was set as a repetition of three main actions defining a movement-step: moving a short distance, checking the surrounding area and deciding if continue or not (described in the next module). For this sub-model, the direction of movement was assumed to change between each movement-step, and therefore attributed randomly at the beginning of each move. The distance of this movement step was also attributed randomly between 10 and 50cm (estimation). Arrived at its new position the crab checked for all the burrows in a radius (R_{move}) defined as:

$$(5) R_{move} = c_{Rmove} \times CW,$$

where c_{Rmove} was a constant (Table 2). If no burrow were found on this area, the crab decided directly if it should do another movement-step or not (cf next module). If a burrow was found, the crab tried to take it over with different probability of success depending on the status of the burrow (P_{c1} to P_{c4} , Table 1). The crab kept in memory the burrows that it had visited since the beginning of the walk. If an occupied burrow had been previously checked, the probability of success of taking over was set to zero. If the crab step led it outside of the simulation area, it was set to come back on the other side of the area, to keep a constant crab density and simulate new comers.

Oriented walk sub-model (WBo). – This sub-model was describing a walking behavior identical to the previous one with the exception that the angle of direction of movement was changing within a determined range between each steps. A first random angle (α_o) was attributed to the crab at the beginning of its movement and the next ones (α_n) calculated as:

$$(6) \left\{ \begin{array}{l} \alpha_1 = \alpha_o + Rnd(\alpha_{dev}) \\ \alpha_n = \alpha_{n-1} + Rnd(\alpha_{dev}) \end{array} \right\},$$

where $Rnd(\alpha_{dev})$ was a random angle between $-\alpha_{dev}^\circ$ and α_{dev}° (Table 2).

Reason of stopping movement module

Random reason sub-model (RS_r). – At the end of each movement-step the crab evaluated if it should continue moving or not. A first reason of stopping was obviously if it managed to take over another burrow. The crab position was then set to this burrow position and as described earlier, if a crab was previously inside, it was set to move when its turn of being checked came. If no burrows were taken over at this step, the crab evaluated then if it should continue according to its probability P_s . In this sub-model according to the null assumption of crab interaction, the P_s was set to follow an input value P_{end} (Table 2) (at each movement step, $P_s = P_{end}$).

Feeling of direct competition strength sub-model (RS_{FRN}). – This sub-model assumed that the crabs, besides willing to take over an already created burrow, could also feel the presence of neighbors at any new position. The sub-model add another reason of stopping to the previous sub-model by influencing the P_s with the following formula:

$$(7) P_s = P_{\text{end}} \times \frac{P_l}{P_{l-\text{local}}},$$

where $P_{l-\text{local}}$ was the probability of leaving the actual position according to the FRN assumption. This sub-model presupposed that the crab had higher probability to settle in a better area than the one it left.

Feeling of indirect competition strength sub-model (RS_{FON}). – Identically, this sub-model assumed that the crabs would feel the strength of competition and rather not install in a worse area than the one they left. It used the same formula (Eq. 7) as the RS_{FRN} sub-model, but calculating the $P_{l-\text{local}}$ according to the respective reason of movement sub-model (RM_{FON}).

Burrow related sub-model

A small mathematical sub-model for burrow status was used to simulate the probability of disappearance (P_{disap}) of the unoccupied ones, following the formula:

$$(8) P_{\text{disap}} = c_{\text{disap}} \times t_{\text{empty}},$$

where c_{disap} was a constant (Table 2). This sub-model estimated that the longer a burrow was without a crab, the higher was the probability of disappearing.

Table 1. Constants entering in the core parameterization of the IBU model.

Constant name	Description	Value	Assumptions	Source
D_c	Crab starting density (in /m ²)	3.16	Homogeneous constant area not considering habitat heterogeneity	This study
$\text{Prop}_{\text{Unoc}}$	Proportion of unoccupied burrows at start	22%	Simulate a neap tide situation	Burrow dynamic experiment, (Diele and Piou unpublished data)
$\text{Prop}_{\text{closed}}$	Proportion of closed burrows at start	60%	Simulate a neap tide situation	Burrow dynamic experiment, (Diele and Piou unpublished data)
CW_{pop}	Mean crab size of the simulated population (in cm)	6	Lower number of fishing-size crabs than other	This study
SD_{CWpop}	Standard deviation of the mean crab size of the simulated population (in cm)	1	-	This study
$\text{Dif}_{\text{Bsize}}$	Natural deviation of burrow entrance size to the inside crab carapace size (in cm)	1	Low variability, clear burrow entrance visibility assuming a neap tide situation	Estimation
t_{max}	Maximum time of simulation (days)	100	3 months of observation	-
X_{max} and Y_{max}	Size of the simulated area (in cm)	1500 and 1500		-
a and b	Constants for the interaction radius calculation (Eq. 1)	19 and 15	For a crab of $\text{CW}=1\text{cm}$ $R_{\text{int}}=24.5\text{cm}$, and above $\text{CW}=9\text{cm}$ all crabs $R_{\text{int}}=100\text{cm}$	C. Piou, Personal observation and Nordhaus 2004

P_{c1}	Probability of taking over an open burrow with larger crab	0.25%	Only possible when the crab is collecting food	Estimation from Nordhaus 2004
P_{c2}	Probability of taking over an open burrow with smaller crab	0.5%	Twice P_{c1} : the bigger crabs might also fight	Estimation from Nordhaus 2004
P_{c3}	Probability of taking over a close burrow	0%	Impossible to see closed burrows	Estimation
P_{c4}	Probability of taking over an open empty burrow	100%	Would always prefer to stop if find an open empty burrow	Estimation
$P_{closing}$	Probability that a crab close its burrow at each time step	14%	Close its burrow ~once a week	C. Piou and C. D'lima personal observation
$P_{opening}$	Once closed, probability of opening its burrow at each time step	33%	Closing period of ~3days	C. Piou and C. D'lima personal observation

Table 2. Input parameters for IBU simulations to test the Null sub-models

Parameter name	Description	Values tested
P_w	Probability of movement at each time step	1, 10, 20, 30
P_{end}	Probability of stopping movement at each movement step	0.1, 0.2, 0.4, 0.8
c_{Rmove}	Constant for the radius of visibility of burrows at end of movement-steps (Eq. 5)	1, 2, 3, 4
α_{dev}	Maximum deviation angle between each movement step (Eq. 6)	Pi, Pi/2, Pi/4, Pi/20
c_{disap}	Disappearing factor of burrows (Eq. 8)	15, 7, 2, 0.5

Table 3. Input parameters for IBU simulations to test the FRN and FON sub-models

Parameter name	Description	Values tested	Interval of increment
P_w	Probability of movement at each time step	10, 20, 30	-
P_{end}	Probability of stopping movement at each movement step	0.2, 0.4, 0.8	-
c_{Rmove}	Constant for the radius of visibility of burrows at end of movement-steps (Eq. 5)	1	constant
α_{dev}	Maximum deviation angle between each movement step (Eq. 6)	Pi/4	constant
c_{disap}	Disappearing factor of burrows (Eq. 8)	2	constant
$NEIG_{max}$	Maximum number of neighbors a crab could have without increasing its probability to leave its burrow	1 to 19	2

F_{A-MAX}	Maximum FON neighbors effect a crab could feel without increasing its probability to leave its burrow	0.1 to 1.9	0.2
-------------	-------------------------------------------------------------------------------------------------------	------------	-----

Example Mosquitofish

This model is still under work. A simplified version of the model description, including most references, is presented in:

Ginot, V., Gaba, S., Beaudouin, R., Aries, F., Monod, H. (in press). Combined use of local and ANOVA-based global sensitivity analyses for the investigation of a stochastic dynamic model: application to the case study of an Individual Based Model of a fish population. Ecological Modelling (in press).

Abstract: Global methods based on variance decomposition are increasingly being used for sensitivity analysis (SA). Of these, analysis of variance (ANOVA), is surprisingly rarely employed. Yet, it is a viable alternative to other model-free methods, as it gives comparable results and is readily available in most statistical packages. Furthermore, decomposing the input factors of ANOVA into orthogonal polynomial effects gives additional insights into the way a parameter impacts on model output (linear, quadratic, cubic). However, using global methods should not lead modellers to forego local methods which provide additional information, as for example time course analysis of local sensitivity coefficients. We illustrate the use of these techniques, particularly ANOVA, on a stochastic individual-based model of a mosquitofish (*Gambusia holbrooki*) population in experimental tanks. Local SA led to unexpected and counter-intuitive results, indicating that the model output (population size) was much more sensitive to the fecundity threshold (length at first parturition) than to the fecundity parameter (brood size). Time course analysis of local coefficients suggested that, as far as calibration is concerned, it would probably be impossible to determine more than two parameters on the sole records of the population size in time. Global SA (ANOVA) was targeted to assess which processes had an impact on the model outcome in our experimental conditions, by exploring the parameter space over the entire biological range of all parameters. It showed that parameters had mainly linear and additive effects (few interactions) on the output in a logarithmic scale, and that the main processes involved in population growth were individual growth and adult survival, followed by the breeding process. Juvenile survival had a lesser impact.

Modified model description written by: **Vincent Ginot**

Purpose

The model computes the early stages of the installation of a population of the mosquitofish (*Gambusia holbrooki*), a fast growing fish used in eco-toxicological experiments. Eco-toxicological experiments aim at estimating the concentration at which a given pesticide becomes harmful for the fish, supposed to represent non-target wild species. In these experiments, a few breeding couples are introduced in a set of 3 m³ outdoor tanks in May, and fishes can produce several reproduction cycles during the warm season. Tanks receive different concentrations of pesticide and experiments are halted in early October, before the onset of high fish densities and nutritive shortages that may alter population growth. The point is to assess if the population is affected by the pesticide. For this, data coming from the exposed tanks, namely fish length distribution at the end of the experiment, are compared to the non-treated tanks. But because of the low number of replications and of the high

variability of such experiments, statistical comparisons are difficult. In order to enhance the statistical power of these comparisons, we suggest to back up the non-treated tanks by a stochastic model of the fish population. The model is calibrated on independent experiments, and validated for the given experimental conditions on the data of the control tanks. It can then be used as an infinity of non-treated tanks (e.g. 10 000 stochastic replications of 'virtual' non-treated tanks), on which real data from treated tanks are compared. In particular, with such a model, it becomes possible to compute the likelihood of the treated tanks of being unaffected by the pesticide.

State variables and scales

An individual based model (IBM) was chosen, since we need to simulate realistic distributions of fish lengths. We have used the Mobidyc platform, a workbench we are currently developing to help non-computer experts (ecologists) in the IBM modelling process (Ginot *et al.*, 2002). Mosquitofish are ovoviviparous: embryos develop in the body of the mother, which drops juveniles already well equipped for life. Hence, the model includes three kinds of individuals only: juveniles, males and females. The tank is also modelled as an agent. It computes general information as environmental scenario or shared parameters. A last agent, the observer, saves the length distribution of the fish at the end of the simulation. The main state variables are the age and the length of each fish. But additional state variables are also computed, as female maturity or offspring. The full set of state variables (agents' state) and processes (agents' behaviour) is listed in Table 1. Time step is one day and the simulation lasts five months.

Process overview and scheduling

Time evolves in a 'clock' mode (discrete time simulation): the one day time step is fixed for all the simulation duration and each agent plays at each step of time. A step of time is scheduled as follows: 1- the tank agent plays, 2- the fish agents play, 3- the observer agent plays, 4- if activated, saving and displaying occurs. Amongst fish, scheduling is also sequential: each fish, whatever its stage or sex, plays in turn in a random order, and the next fish 'sees' the world just like the previous one has modified it. As fishes don't interact directly with each other, this sequential scheduling has no influence on simulations. At the beginning of each step of time, the tank agent updates the water temperature and the photoperiod according to the real environmental data recorded on the site. It also computes fish density. Then it computes the parameters that are temperature or density dependant, and that will be used by the fish. After the tank, fish can play. Each individual updates its age and length, and then challenges its survival. Then, if alive, it possibly produces offspring (for females) or undergoes metamorphosis (for juvenile) to step into the adult (male or female) stage. In order to represent the individual variability, most parameters include two components: a mean component representing the mean value of the parameter in the population, and an individual component (additive or multiplicative) representing the individual variability of the parameter. The mean component can be fixed for all the simulation duration, but it can also be computed by the tank agent at any step of time. The individual component is fixed for each fish, and usually drawn out normal laws centred on 1 (multiplicative) or 0 (additive), and with an empirical variance calibrated on experimental data. Processes are summarised in Table 1, equations are detailed in section 7, and parameters are listed in Table 2.

Design concepts

Fish individuals are purely reactive: they react to environmental stimuli (photoperiod, temperature, density), with no explicit aim, cognitive action (learning, choosing...), or other adaptive process. The individual growth pattern of each individual and the length distribution

of the whole population are the two emerging properties of the model, depending on water temperature, photoperiod and fish density. Fishes don't interact directly, but they are sensitive to overall density, computed by the tank agent (mediated interaction). The model is intrinsically stochastic: fish survival is a stochastic process and main parameters for fish growth and reproduction are randomly drawn for each initial or newborn individual. The environment is partly determinist, following the real daily temperature and photoperiod data, partly stochastic, since a "safety" parameter, representing the intensity of predation due to the aquatic predators of fish for a tank, is randomly drawn at the beginning of each simulation. For model testing, all state variables of all individuals (including the tank agent) are saved at each step of time. For model analysis, only the full length distribution of the fishes at the last step of time is recorded by the observer agent.

Initialization

In real experiments, 3 to 10 females, according to their length, and 3 to 6 males are introduced in each tank at the beginning of each trial. In the modelling, the same number of males and females is used, and the initial length is drawn from the real distribution of the initial fishes. Initial individual parameters are also set, using the same random laws than for reproduction and metamorphosis (Table 2). Hence, a random initial population is drawn at the beginning of each simulation, representing a possible real initial population of the simulated tank.

Input

The only inputs are the daily water temperature and photoperiod, the former recorded on the site, the later computed from the current Julian day.

Submodels

(Parameter values and units are listed in Table 2)

Fish growth

The common Von Bertalanffy (1938) relationship is used, where growth rate decreases linearly according to length. If $Length_{i,t}$ represents the length of fish i at day t , then the Length at day $t+1$ is:

$$(1) \quad Length_{i,t+1} = Length_{i,t} + a_{i,t} (1 - Length_{i,t} / K_i)$$

with $a_{i,t}$ the individual growth parameter and K_i the individual maximum length. $a_{i,t}$ varies in time according to water temperature ($Temp_t$) for juveniles, and according to water temperature and fish density ($Density_t$) for adults. a_i and K_i are both split in two components, a mean value shared by all individuals, and an individual component that slightly modifies this common value.

$$(2) \quad a_{i,t} = a * \omega a_i * f(Temp_t) \quad \text{for juveniles}$$

$$(3) \quad a_{i,t} = a * \omega a_i * f(Temp_t) * f(Density_t) \quad \text{for adults}$$

$$(4) \quad K_i = K * \omega K_i \quad \text{for all stages}$$

With a the mean growth rate of the population, ωa_i the individual variability of growth rate (drawn in a 95% truncated normal law, i.e. with the 2.5% extreme low and 2.5% extreme high values removed), $f(Temp_t)$ a tabulated function (figure 1) adapted from Wurtsbaugh & Cech (1983) and $f(Density)$ an empirical linear function derived from our experimental data:

$$(5) \quad f(\text{Density}_t) = \max (a - b * \text{Density}_t ; \text{threshold})$$

Temperature is read in the environmental scenario, while fish density is computed at the beginning of each step of time.

Fish survival

For each life stage, the survival rate ($Sr_{i,m,t}$) represents the probability of survival per days. Each day, each individual draws a random number between 0 and 1. If this number exceeds the survival rate the individual dies. $Sr_{i,m,t}$ depends on the length of the individual and on the "safety" m_m of its tank m . We use the expression adapted from DeAngelis & Goddout (1991):

$$(6) \quad Sr_{i,m,t} = 1 - m_m * a * \exp (-b * \text{Length}_{i,t})$$

The intensity of predation m_m represents the density of aquatic predators. This parameter is constant, and is determined for each tank at the start of the simulation. It is randomly drawn in a 95% truncated normal law empirically derived from our experiments.

Metamorphosis

If the length of a juvenile exceeds a threshold, different for male and female, it undergoes metamorphosis. The old individual is killed, and a new one is created, male or female according to the sex of the juvenile. The newcomer inherits the juvenile's state, in particular age and length, and the individual components ωa_i and ωK_i of the growth parameters.

Reproduction

First reproduction, for female, is conditioned by a minimum length, the length at first parturition (LengthFP). LengthFP decreases linearly with fish density but cannot fall under a threshold. It is computed daily by the tank agent.

$$(7) \quad \text{LengthFP} = \max (a - b * \text{Density} ; \text{threshold})$$

Subsequent reproductions are conditioned by the inter-parturition interval (IPI), which represents the time lag in days between two consecutive reproductions of a same female. IPI is linearly related to the mean temperature encountered by the female during the inter-parturition period. Hence this mean temperature is computed each day by each female. An individual variability ωIPI_i is added, drawn in a 95% truncated normal law. Value is rounded to the nearest integer. Expressions (7) and (9) are empirically drawn from our experimental data.

$$(8) \quad \text{IPI}_{i,t} = f(T_{\text{moy}_{i,t}}) + \omega \text{IPI}_i$$

$$(9) \quad f(T_{\text{moy}_{i,t}}) = a - b * T_{\text{moy}_{i,t}}$$

Offspring size is an exponential function of the female length (Bisazza, 1991), and of the individual variability ωOffSpr_i calibrated on our experimental data. Value is rounded to the nearest integer by a random drawing of the fractional part (e.g. a value of 10.2 juveniles gives 10 with a probability of 0.8 and 11 with a probability of 0.2).

$$(10) \quad \text{OffSpr}_i = \exp (a * \text{Length}_i + \omega \text{OffSpr}_i)$$

The newborns get a 1/1sex-ratio (Milton & Arthington, 1982). The initial length of the juveniles is drawn in a truncated normal law following Meffe (1990), and ωa_i and ωK_i , the two individual components of the growth parameters are drawn in truncated normal laws.

After reproduction, the female draws its next inter-parturition interval variability (ωIPI_i) in a truncated normal law.

Table 1. State variables (i.e. agents states) and processes (i.e. agents behaviours)

<i>Agent</i>	<i>State</i>	<i>Unit</i>	<i>Processes</i>
Tank	Photo-period	hours	Update photoperiod (scenario)
	Temperature	°C	Update temperature (scenario)
	Fish density	ind/m ³	Compute fish density
	Predation pressure	-	Compute parameters that depend on temperature or density (mean growth rates and length at first parturition)
	Mean growth rate for juveniles	-	
	Mean growth rate for males	-	
	Length at first parturition (female)	mm	
Juveniles	Age	day	Aging
	Length	mm	Growing
	Sex	-	Survival
Females			Metamorphosis
	Age	day	Aging
	Length	mm	Growing
	Maturity	day	Survival
	Inter-parturition interval (IPI)	day	Compute IPI
Males	Offspring	integer	Reproduction
	Age	day	Aging
	Length	mm	Growing
Observer			Survival
	Population length distribution	-	Compute population distribution

Table 2. Parameter values. N (μ ; σ) refers to a drawing in a normal law of mean μ and standard deviation σ , truncated to avoid the 2.5% upper and 2.5% lower values.

Parameter (Equation N°)		Unit	Value		Source
			Female	Male	
Growth					
Growth rate a (2)		mm.day ⁻¹	1.00		Vargas & Sostoa (1996)
Growth rate var. ωa _i (2)			N (1 ; 0.07)		Experiments (Rennes)
Maximal length K (4)		mm	60	35	Vargas & Sostoa (1996)
Max length var. ωK _i (4)			N (1 ; 2.39)		Experiments (Rennes)
Effect of density on growth rate (5)	a		1		Experiments (Rennes)
	b	m ³ .ind ⁻¹	0.005		
	threshold		0.35		
Effect of temperature on growth rate (3)			tabulated function		Wurtsbaugh & Cech (1983)
Survival					
Daily survival rate	a	days ⁻¹	0.016		Experiments (Rennes)
	b		0.0792		
mesocosm predation intensity			N(1,0.7)		Experiments (Rennes)
Metamorphosis (Puberty)					
Puberty threshold		mm	19	15	Experiments (Rennes)
Reproduction					
Length at first parturition (7)	a	mm	36,0	/	Camargue data (Crivelli)
	b	mm.ind. ⁻¹	0,106	/	
	threshold	mm	26	/	
Inter parturition interval (IPI) (9)	a	days	60	/	Camargue data (Crivelli)
	b	days.°C ⁻¹	- 1.2	/	
IPI variability (8)	ωIPI _i	days	N (0 ; 2.2)	/	
fecundity	a	ln(Alevin number).mm ⁻¹	0.1154	/	Experiments

		1			(Rennes)
	b	ln(Alevin number)	1.0532	/	
fecund.variability	ωOffSpr_i	ln(Alevin number)	N(0, 0.246)	/	Experiments (Rennes)
Juvenile length at birth		mm	N (7.9 ; 0.5)		Meffe (1990)

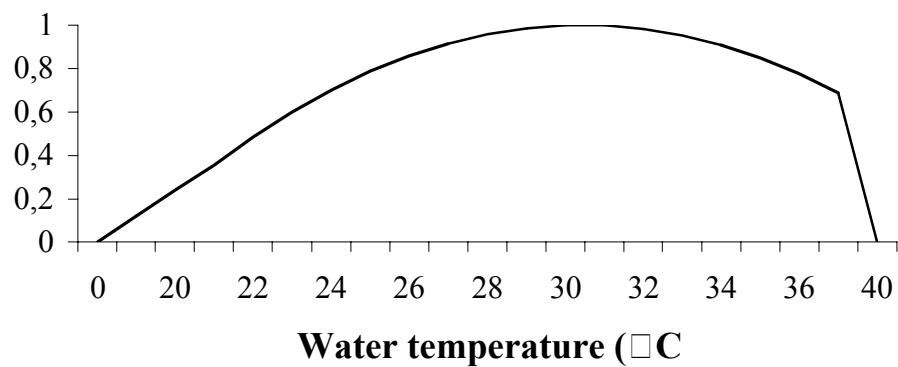


Figure 1. Relationship between water temperature and growth, adapted from the quadratic function of Wurtsbaugh & Cech (1983).

Example Biological Control

The following model description, including all full references, is presented in:

Visser U, Johst K, Köhler V, Wiegand K. Conservation biological control in fragmented landscapes – persistence and parasitism in a host-parasitoid model. (*unpublished manuscript*).

Abstract: Landscape structure and composition influence the persistence of parasitoid populations and parasitism rates. The maximization of both parasitoid persistence and parasitism rates is the crucial aim for conservation biological control through parasitoids in agricultural landscapes. With our study we contribute to the discussion on how the management of landscape structure could enhance conservation biological control.

We developed a spatially explicit simulation model of a host-parasitoid system with equal dispersal in host and parasitoid and simulated the spatial population dynamics of host and parasitoid in virtual landscapes. The landscapes consisted of suitable habitat and unsuitable matrix and differed in the degree of fragmentation, patch distance and amount of habitat. We determined the persistence of the parasitoid population and the parasitism rates on the landscape level.

We found that the impact of fragmentation on the host-parasitoid system depends on the total habitat amount in the landscape. If habitat was abundant persistence of the parasitoid population decreased with fragmentation and isolation. If habitat was scarce the persistence was highest at intermediate levels of fragmentation and isolation. The average parasitism rate, in turn, was negatively influenced by fragmentation and isolation regardless of the habitat amount available. The more fragmented and isolated habitat patches were the slower was the tracing of the hosts by the parasitoid even with equal dispersal distances. The decrease in parasitism rate was connected with an increase in the duration of host outbreaks. The results were robust for different dispersal and reproduction scenarios.

Our results suggest that habitat fragmentation and isolation may have a negative effect on the efficiency of conservation biological control in agricultural landscapes in terms of parasitism rates. However, the effect on the reliability of conservation biological control in terms of the persistence of the parasitoids deviates from the effect on parasitism rates if habitat is scarce. Thus, in landscapes where habitat is abundant high reliability and efficiency of biological control can be achieved by arranging habitat as clumped as possible, whereas in landscapes where habitat is scarce biological control has to consider a certain trade-off between efficiency and reliability: either a highly effective fragmentation scenario with high parasitism rates but high risk of extinction for parasitoid populations or a less efficient scenario with only moderate parasitism but high persistence.

Purpose

The aim of the modelling study was to identify basic mechanisms affecting persistence and parasitism rates in conservation biocontrol in heterogeneous landscapes. Therefore, we tested whether habitat loss, fragmentation, and isolation on different scales limits

conservation biocontrol in a host-parasitoid system without pronounced differences in the dispersal behaviour of host and parasitoid or a special searching behaviour of the parasitoid.

State variables and scales

We built a spatially-explicit grid-based model in which space is represented in the form of discrete cells. Each cell can contain a subpopulation of host and parasitoid of the size N_t and P_t , respectively.

One cell represents a 100 m × 100 m area of an agricultural landscape which can be either suitable (“habitat”) or unsuitable (“matrix”) for the host. We chose cell size according to the estimated searching range of a parasitoid. Adjacent habitat cells are grouped to habitat patches. This allows for emergent spatial dynamics within a patch. Thus, we could study a continuum of fragmentation and isolation levels. A landscape can consist of several habitat patches surrounded by different amounts of isolating matrix (for examples see Table 1 and Simulation experiments). Grid size is adjusted to encompass the entire area of all habitat patches and corresponds to landscapes of up to 100 by 100 square kilometres. Boundary conditions are absorbing. One time step corresponds to one year and the whole simulation period covers 600 time steps (see Simulation experiments).

Process overview and scheduling

Reproduction, parasitism, mortality, and dispersal are calculated in discrete annual time steps because both host and parasitoid reproduce once a year with non-overlapping generations. The density dependent reproduction of the host is characterized by the local carrying capacity K_H and the reproduction rate R_H . The specialized parasitoid reproduces with a maximal egg laying rate R_P .

Local subpopulations are linked by dispersing host and parasitoid individuals. Dispersal is characterized by mean dispersal distances, D_H and D_P which are equal for host and parasitoid. For an overview of the parameters and the standard parameter set see table 2.

At the beginning of the annual time step, hosts die due to parasitism of the former year. Then host and parasitoid individuals disperse and thereafter the size of the host and parasitoid subpopulations in the cells is updated. If a host individual lands in a habitat cell, it reproduces and dies afterwards. The offspring of the host can then be parasitized by egg laying parasitoids in the same cell, which die after laying the eggs. At the end of each time step, the data for the analysis are recorded.

Design concepts

Interaction. – We assumed that the size of a habitat cell corresponds to the size of the searching range of a parasitoid. In the model, parasitism in a local host population is limited by parasitoid fecundity (note that often parasitoids are assumed to be never egg-limited (e.g. {Hassell, 2000 HASSELL2000 /id})) and all available parasitoid eggs are randomly distributed over all hosts present in the same cell.

Stochasticity. – For dispersal, direction and distance are randomly chosen from a uniform and a negative exponential distribution, respectively. All other processes of the model are deterministic.

Emergence. – The interaction of host and parasitoid in the simulation model is locally unstable and exhibits oscillatory behaviour in time. Figure 1 shows the population dynamics of host and parasitoid in one cell for an exemplary landscape. When there are no parasitoids in the cell, host population size increases until population size reaches the carrying capacity. When a parasitoid reaches the host population, the parasitoid reproduces by parasitizing the

hosts and causes a reduction of host population size. These local oscillations of host and parasitoid densities lead to a wave-like spatial pattern (figure 2) with increasing local host populations at the wave front, followed by increasing parasitoid populations. The parasitoid populations cause the local extinction of host and parasitoid and leave a zone of empty cells behind. This wave of hosts and parasitoids moves across the landscape with time. This is in accordance with the fact that parasitoids and their hosts have been shown to be predisposed to locally unstable dynamics (e.g. {Bonsall, 2002 215 /id; Nachman, 1991 NACHMAN1991 /id} and travelling waves have been confirmed in a number of host-parasitoid systems (e.g. {Johnson, 2004 JOHNSON2004B /id}; {Blasius, 1999 BLASIUS1999 /id; Sherratt, 2003 SHERRATT2003 /id}).

Observation. –

Persistence. We estimated the persistence of the parasitoid population at the landscape level by calculating the proportion of simulation runs (out of 100) in which the parasitoid population survived for at least 600 years.

Parasitisation rate. The parasitisation rate is the average parasitoid-to-host ratio, calculated (if hosts are present) across all habitat cells and across the last 400 time steps.

Outbreak duration. To describe the spatiotemporal population dynamics, we chose an exemplary cell in the centre of a habitat patch. Within this cell and within the simulation period of 400 time steps, several outbreaks are possible. For each outbreak, we measured the average number of consecutive time steps a host population was present.

Initialization

Each simulation run was started by defining a landscape pattern according to the landscape scenarios described in the chapter Simulation experiments. In the new landscape, host and parasitoid populations were initialized by providing 0.2 % of the grid cells with a host and a parasitoid subpopulation of the size of K_H and $K_H/2$, respectively. In order to be independent of the initial conditions, we let the spatio-temporal dynamics develop for 200 time steps before recording data for the analysis.

Submodels

Host reproduction

We assumed that host reproduction is density dependent and that density dependence acts before parasitisation (compare e.g. {Nilsson, 1989 202 /id}). We modelled the female hosts only, which means that in the model one individual can start the growth of a population without reproduction partner (compare classical metapopulation and host-parasitoid models ({Levins, 1969 LEVINS1969A /id}; {Nicholson, 1935 NICHOLSON1935 /id}). We described density dependent logistic growth by the Ricker-function {Bellows, 1981 BELLOWS1981 /id}.

$$(1) \quad N_{t+1} = N_t \cdot R_H \cdot \exp\left(-\ln(R_H) \cdot \frac{N_t}{K_H}\right)$$

with N_t being the number of hosts in the cell at time t , a local maximum capacity K_H , and a maximal reproduction rate R_H .

Parasitoid reproduction

Based on the assumption that the size of a habitat cell corresponds to the size of the searching range of a parasitoid, in our model, the distribution of parasitoid eggs on hosts is random and limited by parasitoid fecundity (note that parasitoids are often assumed to be never egg-limited {Hassell, 2000 HASSELL2000 /id}). Thus, the probability that hosts escape parasitization is given by the zero-term of the Poisson-distribution. Thus, the number of parasitoids hatching in the next time step is then given by

$$(2) P_{t+1} = N_t \cdot (1 - \exp(-R_P \cdot \frac{P_t}{N_t}))$$

Here P_t and N_t are the population size of the parasitoid and the host at time t and R_P is the maximum number of eggs per parasitoid (compare {Thompson, 1929 273 /id}). Analogous to the hosts, we modelled female parasitoids only (with sex ratio 1:1).

Dispersal

We assumed that host and parasitoid have the same dispersal behaviour. Dispersing individuals fly in a randomly chosen direction and settle after covering a distance randomly chosen from a negative exponential distribution. The distribution is characterized by a mean dispersal distance D_H and D_P common to host and parasitoid. We did not include any movement response to the landscape structure.

Mortality

In the model, host and parasitoid are univoltine, which means that they live for one year and die after reproduction. Host and parasitoid individuals die when random dispersal ends in a matrix cell and host individuals die when being parasitized.

Parameterization

As reference for model parameterization, we chose the rape pollen beetle and its specific parasitoids in semi-natural habitat {Hokkanen, 2000 HOKKANEN2000 /id;Hokkanen, 1988 180 /id;Daebeler, 1990 DAEBELER1990 /id;Börjesdotter, 2000 116 /id;Fritzsche, 1956 184 /id}. To estimate the mean dispersal distance, we estimated that only a small proportion of a population (0.001 %) may be able to fly very far (6 km, the furthest estimated distance reported in the literature {Daebeler, 1990 DAEBELER1990 /id}; {Hokkanen, 1988 180 /id}.

The qualitative results of our simulation study are robust for a wide range of parameter variation. In this paper, we present characteristic results for one exemplary parameter set listed in Table 2.

Table 1. Parameter range and examples for the first and the second landscape scenario; Note that patch size describes the patch area and that patch isolation is the shortest distance between nearest neighbour-patches; dark grey: matrix, light grey: habitat.

	<i>Number of patches</i>	<i>patch size (cells)</i>	<i>patch isolation (cells)</i>




<i>Scenario 1</i>	<i>1</i>	<i>100 – 10000</i>	<i>0</i>
<i>Example scenario 1</i>			
<i>Scenario 2</i>	<i>1 – 100</i>	<i>25 - 2500</i>	<i>5 – 30</i>
<i>Example scenario 2</i>			

Table 2. Values of population model parameters used for simulation results. One cell corresponds to 100 m × 100 m.

Parameter	Value	Unit
K_H	500	individuals/cell
R_H	2.2	maximum number of offspring/adult
R_P	5	maximum number of offspring/adult
D_H	5	cells
D_P	5	Cells

Figure 1. Population density of adult hosts (black line) and parasitoids (red line) oscillating with time in one exemplary cell; simulation run with standard parameter set (see table 2) and landscape parameters as visualized in figure 2: patch size 100 cells, patch distance 10 cells.

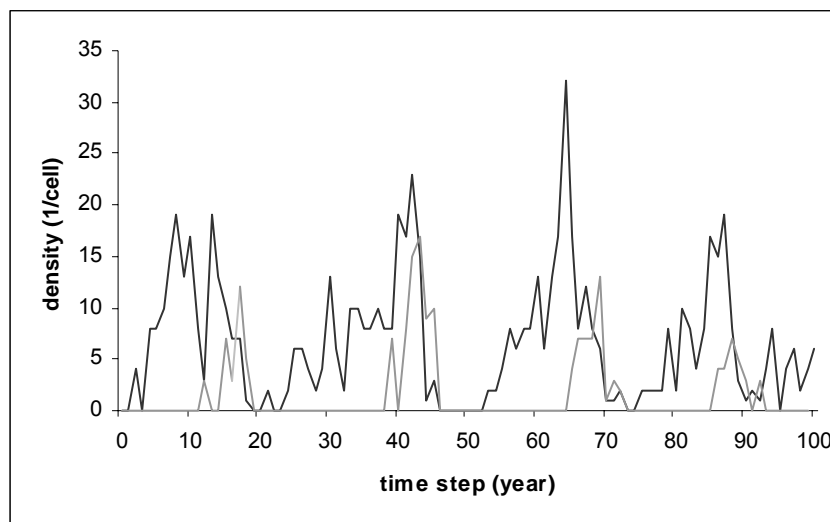
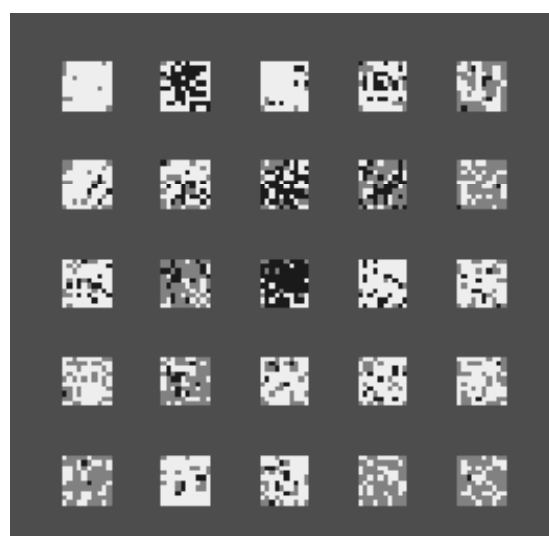


Figure 2. Snapshot of a virtual landscape of the second scenario set (patch size 100 cells, patch distance 10 cells) during a simulation run with standard parameter set (see table 2); white: cells with only host population, black: cells with host and parasitoid population, dark grey: matrix cells, light grey: empty habitat cells.



Example Species-rich Forest I

The original model description of FORMIND2.0, including the full references, is in:

Köhler, P. (2000). Modelling anthropogenic impacts on the growth of tropical rain forests. PhD thesis, University of Kassel, Kassel, Germany. Osnabrück: Der Andere Verlag.

Abstract: For answering questions concerning anthropogeneous impacts on tropical forest development the individual-oriented and process-based forest growth model Formind2.0 was developed. It simulates the spatio-temporal dynamics of uneven-aged mixed forest stands in areas of one hectare to several km². The model describes forest dynamics as a mosaic of interacting forest patches of 20 m² × 20 m² in size. Within these patches trees are not spatial-explicitly distributed, and thus all compete for light and space following the gap model approach. Tree species diversity is aggregated into 5-20 plant functional types (PFT) on the basis of species maximum tree height and successional status. The carbon balance of each individual tree incl. photosynthesis and respiration is modelled explicitly. Thus, we can match measured diameter increment for different PFT, size and light conditions accurately. Allometric relationships connect above-ground biomass, stem diameter, tree height and crown dimensions. Beside increasing mortality through self-thinning in dense plots one of the main processes of mortality is gap creation by falling of large trees. This process as well as seed dispersal from mature trees interlinks neighbouring plots with each other. The model was parametrised for three different sites in South-East Asia and South-America: Sabah (Malaysia), Venezuela, and French Guiana. Model accuracy is tested with growth data from permanent sampling plots in Sabah. Sensitivity of various result variables on variation of most parameter values is tested and gives important insights into general model behaviour. Two examples of anthropogeneous impacts on tropical forest dynamics are management practise and fragmentation, both of major concern. Following applications are performed: Growth and yield of Venezuelan rain forest under various logging methods, intensities and cycles are analysed for their sustainability; effects of logging (methods and cycles), fragmentation and recruitment assumptions on forest dynamics in Sabah are discussed. Finally, fragmentation impacts on mortality and recruitment are simulated and their effects on forest dynamic and biomass loss are evaluated for a forest site in French Guiana.

Modified model description written by: **Nadja Rüger**

Notes: In the following the actual version FORMIND2.3 is described which has been parameterised for Valdivian temperate evergreen rain forest (VTRF) in northern Chiloé Island, Chile (Rüger et al., unpublished manuscript).

Purpose

The individual-oriented forest growth model FORMIND was developed to study the long-term spatial and temporal dynamics of uneven-aged mixed species rain forest stands after natural or anthropogenic disturbances (e.g. wind throw, logging, fragmentation).

State variables and scales

FORMIND is a three-dimensional, grid-based, individual-oriented model. It comprises three hierarchical levels: tree cohorts, grid cells (below called patches) and hectares. To enable an individual-based simulation of the dynamics of species-rich forests, tree species that occur at the study sites are grouped into plant functional types (PFT) with similar shade-tolerance and maximum attainable height. In the case of relatively species-poor VTRF, the four PFTs correspond to three single species (*Aextoxicon punctatum*, *Eucryphia cordifolia*, *Laureliopsis philippiana*) and one species group that includes all species occurring at the study site that belong to the Myrtaceae family (*Amomyrtus luma*, *A. meli*, *Luma apiculata*, *Myrceugenia ovata*, *M. planipes*). All trees that belong to the same PFT, and that establish in the same year in the same patch are grouped into a cohort. All trees in one cohort are equal and tree growth is simulated for a representative individual. Trees with a diameter > 40 cm are usually simulated individually, because all other trees from their cohort have died. Each tree cohort is characterized by the state variables PFT, number of individuals, above-ground biomass of the representative individual and position (i.e. the patch where the cohort is located). From the biomass all other morphological variables of the tree are derived (e.g. diameter at breast height (dbh), height, crown diameter, crown depth, stem volume).

A patch is characterised by a list of tree cohorts present in the patch, and its coordinates within the hectare where the patch is located. The size of a patch corresponds to the crown size of mature trees (here 20 m × 20 m). To explicitly calculate the light climate, each patch is divided into vertical layers for each of which the leaf area, crown density, and available light is calculated. Neighbourhood relations link each patch to its four direct neighbours (across hectare boundaries) to allow dying trees to fall into another patch.

Finally, hectares are characterised by the list of patches they comprise, and they contain higher-level information on overall logging potential of all patches that belong to the hectare. Hectares are arranged spatially as a square, such that the simulation area necessarily is a square number of hectares. Minimum extent of the simulation area is one hectare, and several hundreds of hectares can be simulated. The simulation area is simulated as a torus (i.e. with periodic boundary conditions). The model simulates a forest in annual time steps and simulation runs usually comprise several hundred years.

Process overview and scheduling

It is assumed that light availability is the main driving force for individual tree growth and forest succession. Within each patch all trees compete for light and space following the distance-independent gap model approach (Shugart, 1998). The light climate in the forest interior of each patch is calculated via an extinction law depending on the vertical distribution of the leaf area of the trees (Monsi and Saeki, 1953). Depending on the resulting light climate, the light availability is determined for every tree. Annual growth of each tree is calculated on the basis of the main physiological processes photosynthesis and respiration, and litter fall. Growth process equations are partly taken from the model Formix3-Q (Ditzer et al., 2000). Allometric functions relate above-ground biomass, stem diameter, tree height, crown diameter and stem volume. Tree mortality can occur either through self-thinning in dense patches, stochastic mortality, gap creation by large falling trees, or medium-scale wind throws which are frequent in the study area. Recruitment occurs when the light intensity at forest floor exceeds a PFT-specific threshold. Recruitment rates describe the number of small trees growing over the dbh threshold of 1 cm per year.

The model proceeds in annual time steps. Within each year – or time step – six modules are processed in the following order: occurrence of medium-scale disturbances, establishment,

mortality, re-calculation of the light climate in the forest interior, growth, and logging. Disturbances act on the level of hectares; establishment, calculation of light climate and logging are executed for each patch, whereas growth and mortality are determined for each tree cohort.

Design concepts

Emergence. – Annual growth rates of trees are not directly built into the model but emerge from the competition for light between the trees in a patch due to shading. Recruitment rates depend on the light available at the forest floor, and mortality is composed of different processes. Hence, realised recruitment, growth and mortality rates are characteristics that emerge from the current tree assemblage of a patch (i.e. number, size and PFT of trees in the patch). Furthermore, all characteristics at higher levels (population level, patch level, stand level) emerge from the fate of and interactions between individual trees.

Sensing. – The current size of a tree affects both its potential biomass production (through the amount of leaf area) and its mortality rate which is elevated for small trees.

Interaction. – Interaction between single trees of the same patch occurs via competition for light and space (self-thinning). Direct interaction between trees of different patches occurs when dying large trees fall over and destroy a proportion of the trees in the patch where their crown hits the ground.

Stochasticity. – All facets of mortality are interpreted on the basis of probabilities. Mortality due to space competition affects randomly chosen trees. The observation that only some of the dying trees fall over and kill other trees is realised via a “falling probability”. Medium-scale disturbances affect a given hectare with a certain probability. Likewise, the number of disturbed patches per disturbance event is chosen randomly.

Collectives. – All trees that belong to the same PFT, and that establish in the same year in the same patch are grouped into a cohort. All trees in one cohort are equal and tree growth is simulated for one representative tree of the cohort. Trees with a dbh > 40 cm are usually simulated individually, because all other trees from their cohort have died.

Observation. – The individual-oriented approach allows us to compare model outcomes with field observations on the individual tree level, on the population level as well as on the level of the entire tree community. To test the model, we compare simulated and measured growth and mortality rates, as well as stem numbers and basal area for each PFT, or overall forest characteristics such as mean leaf area index (LAI) or size distributions. This wide range of possibilities to check the behaviour of the model ensures that the key processes are included and that the model is able to reproduce observed forest characteristics.

For an assessment and comparison of different logging scenarios we record several PFT-level and stand-level variables over time. These include stem numbers, basal area, biomass, and stem volume of the different PFTs, stem numbers in different diameter classes, stand LAI, harvested stem volume, logging damages, fraction of forest in gap, building or mature phase.

Initialisation

To study long-term forest dynamics after natural large-scale disturbance we start from a treeless area which is regarded to be suitable for establishment of all PFTs. For the logging scenarios we use inventory data of old-growth forest from the study site as initial situation. The inventory data are expanded to correspond to the simulation area and individual trees are randomly distributed among the different patches.

Input

Site conditions are assumed to be homogeneous and there is no inter-annual variability of environmental conditions.

Submodels

In the following the technical realisation of the submodels is described. Units of variables are given in Table 1 and a list of model parameters can be found in Table 2.

Disturbances. – Occasional wind throw events were modelled by killing all trees in an area comprising 2–4 neighbouring patches, thus creating gaps of 800–1600 m². The probability that a certain hectare is affected by a wind throw is 0.8 % per year. Disturbance size (i.e. 2, 3, or 4 patches) is drawn from a uniform distribution.

Establishment. – If irradiance at the forest floor (I_{floor}) matches light requirements for establishment of the given PFT (I_{min} , I_{max}), i.e.

$$I_{min} < I_{floor} < I_{max},$$

N_{max} small trees with a dbh of 1 cm establish. Additionally it is checked, that the height layer of seedling crowns is not completely crowded prior to establishment.

Mortality. – (1) Basic mortality: Each tree has a basic PFT-specific probability to die (m_B).

(2) Size-dependent mortality: Small trees experience additional mortality (m_D) depending on their actual dbh (D),

$$m_D = \begin{cases} m_{max} - m_{max} \frac{D}{D_{mort}}, & \text{if } D < D_{mort} \\ 0, & \text{else} \end{cases}$$

where m_{max} is the maximum size-dependent mortality of small trees and D_{mort} is the dbh up to which mortality is increased. Basic and size-dependent mortality are added,

$$m = m_B + m_D.$$

For cohorts with > 100 individuals and a dbh < 10 cm, the number of dying trees (N_d) is

$$N_d = m \cdot N_t,$$

where N_t is the number of trees in the cohort; for the non-integral part of N_d it is stochastically determined if an additional tree dies. Likewise, for cohorts with < 100 individuals or dbh \geq 10 cm it is stochastically determined if a tree dies.

(3) Self-thinning: In dense patches mortality is increased due to competition for space among the trees. When the sum of the crown area of all trees (which have their crown in this height layer) in a given height layer exceeds the patch area, trees are randomly removed until the crowns of all trees “fit” into the patch.

(4) Gap creation: Large falling trees kill a proportion of the trees in the patch where their crown hits the ground. Trees with a dbh > D_{fall} fall over with the probability p_{fall} . The probability that a tree in the target patch is killed (p_k) is proportional to the ratio between the crown projection area of the falling tree (CA) and patch size (a),

$$p_k = \min\left(\frac{CA}{a}, 1\right).$$

Again, for cohorts with > 100 individuals and a dbh < 10 cm, the number of dying trees is calculated deterministically, otherwise it is stochastically determined if a tree dies. Only trees that do not overtop the falling tree by > 1 m can be killed.

Light competition. – The vertical distribution of leaf area determines the light climate in each patch. This is accounted for by dividing each patch into vertical layers of the width Δh . The crowns of most trees span over several height layers, and thus contribute to the leaf area index (LAI) in each height layer i that contains a part of the tree crown (LAI_i),

$$LAI_i = \sum_{t \text{ with crown in } i} \left(N_t \cdot \frac{CA_t}{a} \right) \cdot \left(LAI_t \frac{\Delta h}{CL_t} \right),$$

with N_t being the number of trees, CA_t crown area, CL_t crown depth, LAI_t LAI of cohort t , and a patch area. When crowns of large trees exceed the patch area, “overhanging” crown and leaf area is distributed evenly to the corresponding height layers of the four neighbouring patches.

The cumulative LAI ($LAIC_i$) adds up the LAI in all height layers above layer i ,

$$LAIC_i = \sum_{j>i} LAI_j.$$

The available light at the crown of each tree (I_t) is calculated via an extinction law

$$I_t = I_0 \cdot e^{-k \cdot LAIC_t},$$

with I_0 being the average irradiance above the forest canopy, $LAIC_t$ the cumulative LAI in all height layers above the crown of the tree and k the light extinction coefficient of the forest.

Growth. – The calculation of light extinction within the forest canopy and leaf-level rates of photosynthesis follows Thornley and Johnson (1990). Both, incident irradiance and rate of photosynthesis need to be considered on the level of single leaves (i.e. per unit leaf area) and the level of an entire tree crown (per unit crown projection area), denoted by l and t respectively. The rate of single-leaf photosynthesis (P_l) is modelled as a saturating function of the incident light on the leaf (I_l),

$$P_l(I_l) = \frac{\alpha I_l p_{\max}}{\alpha I_l + p_{\max}},$$

with p_{\max} being the maximum rate of photosynthesis and α the initial slope of the light-response curve. The irradiance incident on the surface of a leaf within the canopy of a tree is

$$I_l = \frac{k}{1-m} I_t,$$

with I_t being the irradiance incident on the tree crown, k the light extinction coefficient of the forest, and m the light transmission coefficient of leaves. Self-shading of the tree canopy is accounted for by integrating P_l over the total LAI of tree t (LAI_t) and the resulting instantaneous rate of photosynthesis of the tree (P_t , per unit crown projection area) is

$$P_t = \int_0^{LAI_t} P_t(I_t(L)) dL,$$

where L is the cumulative LAI of the tree. Solving the integral leads to

$$P_t(I_t) = \frac{p_{\max}}{k} \ln \frac{\alpha \cdot k \cdot I_t + p_{\max}(1-m)}{\alpha \cdot k \cdot I_t \cdot e^{-k \cdot LAI_t} + p_{\max}(1-m)}$$

(Thornley and Johnson, 1990).

To calculate total gross biomass production of the tree (PB), the rate of photosynthesis is multiplied by the length of the photosynthetic active period per year (S), the crown area of the tree (CA) and a conversion coefficient ($codm$) from absorbed CO_2 to organic dry mass,

$$PB = P_t(I_t) \cdot S \cdot CA \cdot codm.$$

S is calculated as

$$S = 365 \cdot s_d \cdot 60 \cdot 60,$$

where s_d is the average daily photosynthetic active period,

Respiration processes can be divided into growth respiration during the build-up of new biomass (parameter r_g) and maintenance respiration of living biomass (parameters r_0 , r_1 , r_2). Growth respiration is assumed to be a fixed fraction of net biomass production, whereas maintenance respiration is assumed to be non-linearly dependent on the living biomass (B) of the tree. Thus, biomass increment B_{inc} of the tree is calculated as

$$B_{inc} = (1 - r_g)(PB - (r_0 B + r_1 B^2 + r_2 B^3)).$$

Maintenance respiration parameters are fitted such that measured maximum diameter increment values for each PFT are reproduced. Additionally it is assured that $B_{inc}(B(D_{\max})) = 0$. The new biomass ($B_{new} = B_{old} + B_{inc}$) is then translated into the new dbh of the tree via a table function. The table is filled once at the beginning of a simulation for each PFT and assigns each possible dbh (in steps of one mm) the corresponding biomass on the basis of the equation

$$B(D) = \frac{\pi}{4} D^2 \cdot H(D) \cdot \frac{f \cdot \rho}{sw},$$

with D being tree dbh, H being the height of the tree, f the form factor that corrects the deviation of the stem from the idealised conical shape, ρ the wood density and sw the fraction of stem wood biomass from total tree biomass. Between tabulated values linear interpolation is applied.

From the new dbh all other variables describing the geometry of the tree are derived. Height (H) is calculated as

$$H(D) = \frac{D \cdot 100}{\frac{1}{h_0} + \frac{D \cdot 100}{h_1}}.$$

Crown depth (CL) is a constant fraction of height,

$$CL(H) = c \cdot H.$$

Crown diameter (CD) is assumed to be proportional to the stem diameter,

$$CD(D) = cd \cdot D \cdot 100.$$

The crown is assumed to be a cylinder, hence crown area (CA) is

$$CA(CD) = \frac{\pi}{4} CD^2.$$

LAI of a tree (LAI) is fixed to L_{max} . Stem volume (SV) is

$$SV(D) = \frac{\pi}{4} D^2 \cdot H(D) \cdot f.$$

Bole volume (stem volume below the crown, BV) is derived from geometrical properties of the frustum of a cone (Bronstein and Semendjajew, 1991; Ditzer, 1999)

$$BV(D) = \frac{1}{3f} (1 + x + x^2) \cdot (1 - CL(D)) \cdot SV(D),$$

with x being

$$x(D) = 1 - (1 - CL(D)) \left(\frac{3}{2} - \sqrt{3f - \frac{3}{4}} \right).$$

Logging. – (1) Selective logging: The program keeps track of harvestable trees that comply with defined criteria of the logging scenarios (e.g. commercial PFTs, minimum and maximum allowed dbh thresholds for harvesting). Before the logging module is applied, it is evaluated whether the minimum criterion (i.e. minimum number of trees to be extracted per hectare) can be fulfilled taking potential logging damages into account. If the minimum criterion is met, a logging operation takes place; otherwise logging is omitted in the respective hectare. Patches are visited randomly and the largest harvestable tree of the patch is logged, until all patches have been visited at least once or the harvest target has been met. Then, patches are visited randomly until the harvest target is met. (2) Logging in bands: Each hectare is divided into five 20 m wide bands which are recurrently clear-cut. All trees from the logged band are removed, regardless of their PFT or dbh.

For both logging strategies, reduced impact logging is assumed. This means, that falling logged trees are directed to previously damaged patches, if possible, to reduce logging damages by falling trees. Vegetation damage in the patch where the crown of the logged tree hits the ground is simulated in the same way as described for naturally falling trees (see *Mortality* (4) Gap creation), except that harvestable trees in the target patch are prevented

from being damaged. When a tree is directed to a previously damaged patch, only the difference between potential damage caused by its crown and the previously damaged proportion of the trees is damaged. Additional logging damages due to skidding apply to the entire hectare, independently of the location of logged trees. The intensity of this global damage is defined for each logging scenario depending on the logging intensity.

Table 1. Variables of FORMIND2.3.

Variable	Description	Unit
Variables of tree cohorts		
N	Number of individuals	[1]
D	Tree diameter	[m]
H	Tree height	[m]
CD	Crown diameter	[m]
CA	Crown area	[m ²]
CL	Crown depth	[m]
B	Tree biomass	[t organic dry mass]
PB	Gross tree biomass production	[t organic dry mass]
B_{inc}	Net tree biomass production	[t organic dry mass]
SV	Tree stem volume	[m ³]
BV	Tree bole volume (volume below crown)	[m ³]
LAI	Tree leaf area index	[m ² leaf m ⁻² ground]
P_l	Rate photosynthesis per unit leaf area	[$\mu\text{mol}(\text{CO}_2)$ m ⁻² leaf s ⁻¹]
P_t	Rate photosynthesis per unit ground area	[$\mu\text{mol}(\text{CO}_2)$ m ⁻² ground s ⁻¹]
I_l	Irradiance incident on leaf surface	[$\mu\text{mol}(\text{photons})$ m ⁻² leaf s ⁻¹]
I_t	Irradiance incident on tree crown	[$\mu\text{mol}(\text{photons})$ m ⁻² ground s ⁻¹]
Variable of height layers		
$LAIC$	Cumulative leaf area index in height layers	[m ² leaf m ⁻² ground]
Variable of patches		
I_{floor}	Irradiance at forest floor	[% of I_0]
Environmental variable		
S	Length of photosynthetic active period per year	[s]

Table 2. Parameters of FORMIND2.3 for Valdivian temperate evergreen rain forest in northern Chiloé Island, Chile. AP = *Aextoxicon punctatum*, EC = *Eucryphia cordifolia*, LP = *Laureliopsis philippiana*, MY = myrtaceous species. References can be found in Rüger, N., A.G. Gutiérrez, W.D. Kissling, J.J. Armesto, and A. Huth. Identifying ecological impacts of potential harvesting strategies for temperate rain forest in southern Chile – a simulation experiment. (unpublished manuscript).

Parameter	Description	Unit	AP	EC	LP	MY	Reference
Environmental parameters							
k	Light extinction coefficient	[m ² ground m ⁻² leaf]			0.5		estimated
I_0	Average irradiance above canopy	[μmol(photons) m ⁻² s ⁻¹]			700		C. Lovengreen (unpubl. data)
s_d	Mean sunshine hours per day	[h]			12		estimated
Recruitment parameters							
D_s	Diameter of ingrowing trees	[m]			0.01		technical parameter
I_{min}	Minimum light intensity for establishment	[% of I_0]	1	70	3	1	Lusk and Kelly, 2003
I_{max}	Maximum light intensity for establishment	[% of I_0]	90	100	70	95	estimated
N_{max}	Maximum recruitment rates of small trees	[ha ⁻¹ y ⁻¹]	100	75	250	150	estimated
Mortality parameters							
m_B	Basic mortality	[y ⁻¹]	0.0045	0.005	0.0035	0.0025	estimated
m_{max}	Maximum mortality of small trees	[y ⁻¹]			0.055		estimated
D_{mort}	Diameter up to which mortality is increased	[m]			0.15		estimated
D_{fall}	Minimum diameter of falling trees	[m]			0.45		estimated
p_{fall}	Probability of dying trees to fall	[%]			30		estimated
Tree geometry parameters							
h_0	Parameter of diameter-height relationship	[cm m ⁻¹]			1.2		Brun 1969

h_l	Parameter of diameter-height relationship	[m ⁻¹]	41.6	48.7	40.1	27.7	Brun 1969
f	Form factor	[-]	0.4	0.4	0.4	0.35	Brun 1969
cd	Parameter of diameter-crown diameter relationship	[m cm ⁻¹]			0.12		estimated
H_{max}	Maximum height	[m]	30	40	30	20	e.g. Brun, 1969;
D_{max}	Maximum diameter	[m]	1	2	1	0.7	Lusk and del Pozo, 2002
c	Crown depth fraction	[-]			0.25		estimated
L_{max}	Maximum leaf area index per tree	[m ² leaf m ⁻² ground]			4		Saldaña and Lusk, 2003
sw	Fraction of stem wood biomass to total biomass	[-]			0.7		estimated
Biomass production parameters							
p_{max}	Maximum rate of photosynthesis	[μmol(CO ₂) m ⁻² s ⁻¹]	5.6	10	6.4	7	C. Lusk (unpubl. data) and estimated
		[μmol(CO ₂)					estimated
α	Slope of light-response-curve	μmol(photons) ⁻¹]	0.25	0.2	0.2	0.35	
ρ	Wood density	[t m ⁻³]	0.59	0.72	0.55	1.15	Pérez-Galaz, 1983; Diaz-vaz et al., 2002
r_g	Parameter of growth respiration	[-]			0.2		Ryan 1991
r_0	Parameter of maintenance respiration	[-]	0.1	0.11	0.13	0.1	estimated using diameter increment data (Gutiérrez et al., in prep.)
r_1	Parameter of maintenance respiration	[-]	0.0	0.0	0.0008	0.003	
r_2	Parameter of maintenance respiration	[-]	0.0001	0.0	0.0	0.0	
m	Transmission coefficient of leaves	[-]			0.1		Larcher, 2001
$codm$	Parameter for conversion in organic dry matter	[t μmol(CO ₂) ⁻¹]			0.63 44e ⁻¹²		Larcher, 2001
Technical parameters							
a	Patch size	[m ²]			400		technical parameter
Δh	Step width of vertical discretization	[m]			0.5		technical parameter

Example Species-rich Forest II

The original model description of FORMIND2.0, including the full references, is in:

Huth, A., Ditzer, T. (2000) Simulation of the growth of a lowland Dipterocarp rain forest with FORMIX3. Ecological Modelling 134: 1-25.

Abstract: In this paper a new model for simulation of the growth of tropical rain forest is presented (FORMIX3). The model describes growth, mortality, recruitment of trees and competition between trees. The calculation of tree growth is based on a carbon balance. The carbon gain of a tree depends on the photo production of its leaves, respiration and other losses. Trees compete for light and space. Dying large trees fall down and create gaps in the forest. Based on an extensive field data review a parametrisation was developed for the simulation of lowland Dipterocarp rain forest at Deramakot, Malaysia.

28 variables describing different aspects of forest structure and growth were compared with field data. The model reproduces most parts of the forest dynamics well. A new concept for sensitivity analysis is presented: 46 model parameter were varied and analysed in respect to their influence on 26 variables describing the forest state. The influence of the different processes on forest structure is complex. Some general trends can be observed: The growth characteristics of the two Dipterocarp species groups strongly influences species composition in the forest, but not general forest structure (biomass, leaf area, production, leaf area, tree size distribution).

Modified model description written by: **Andreas Huth**

Notes: In this example, all details are skipped.

Purpose

FORMIX3 is a model for analysing the dynamics of disturbed and undisturbed tropical rain forests. The model mainly describes development of biomass, species composition, tree sizes for forest of different sizes in different landscape matrixes. The impact of forest management scenarios can be analysed model.

State variables and scales

State variables of model are the stem diameter (at breast height) of every tree. Trees are grouped in different plant functional types. The location of trees is described using a patch grid, which divides the forest in a mosaic of small patches of similar size.

FORMIX3 can simulate forests from one ha up to several thousand hectares. Typical simulation periods are a hundreds of years.

Process overview and scheduling

The model includes the following main processes: growth, photosynthetic production, respiration, tree geometry, mortality, regeneration, light climate, competition and gap building. Main processes for management scenarios are: logging cycle, logging intensity, logging damages.

The model simulates a forest of several hectares as a mosaic of interacting patches, corresponding to the crown size of mature trees (e.g. 0.04 ha). Tree growth is calculated using a carbon balance. This balance is modelled for each individual tree explicitly, including the main physiological processes (photosynthesis, respiration). Allometric functions relate the above-ground biomass, the stem diameter, the tree height, the crown diameter and the stem volume. Tree mortality can occur either through self-thinning in dense patches, senescence, or gap formation by large falling trees. Gap formation and seed dispersal by mature trees link neighbouring patches together. Trees compete for light and space in a patch using the gap model approach (Shugart 1998). Light climate directly influence tree growth.

The seed production rates of mature trees are effective rates regarding the recruitment of seedlings with seed loss through mortality, predation and other processes already being implicitly incorporated. Seed germination depends from the light climate on the ground.

Time is modelled using fixed time steps. A typical time step is one month or year. Processes are scheduled in the following order: calculation of light climate in the forest, photoproduction of leaves, respiration, mortality, regeneration, falling down of large trees, biomass growth, and diameter growth, extraction of trees due to logging or disturbances, damages due to logging.

Design concepts

Emergence

All analysed forest attributes like forest biomass and species composition directly emerge from the interactions of the individual trees.

Adaptation/ Fitness/ Prediction

Height growth and diameter growth strategy of an individual trees are fixed and do not change. The fitness of an individual tree is mainly described by its size (stem diameter). Larger trees obtain more light and thus grow faster. There are no processes included which to estimate future fitness consequences of different growth strategy.

Interaction /Sensing /Stochasticity

The processes growth, mortality and regeneration of a tree directly depend on other individuals. Growth of a tree is strongly influenced by the light climate, which is determined by the crown distribution of the local tree population. Mortality depends also on the density of the local tree population and the falling down of neighbouring dying trees. Regeneration of trees is mainly a function of the light climate on the ground.

Trees sense other individual only indirectly through the local light climate or crowding of the canopy. Mortality and Regeneration are modelled as stochastic processes.

Collectives

Trees in the same height layer and of the same species group are grouped to simplify the model calculations.

Observation

The following variables are mainly analysed (from an omniscient perspective):

forest biomass, wood volume, productivity, stem numbers, canopy cover, heterogeneity of forest structure (e.g. gap area size), species composition, diameter and height growth, tree size distribution, yield and damaged wood (for analysis of logging strategies).

Initialization, Input, Submodels

[Not included here. This information can be found in

Huth,A., Ditzer,T., Bossel,H., 1998. The rain forest growth model FORMIX3; Model description and analysis of forest growth and logging scenarios for the deramakot forest reserve (Malaysia). Verlag Erich Goltze, Göttingen.

Huth, A., Ditzer, T. (2000) Simulation of the growth of a lowland Dipterocarp rain forest with FORMIX3. Ecological Modelling 134: 1-25.]

Example Range Management

The following model description, including the full references, is in:

B. Müller, A. Linstädter, K. Frank, M. Bollig & C. Wissel (2005): Learning from indigenous knowledge: Modelling the pastoral-nomadic range management of the Ova-Himba (*unpublished manuscript*)

Abstract: It is widely accepted that successful grazing management strategies in semi-arid ecosystems need to be adapted to the highly temporally and spatially heterogeneous forage production. Nevertheless, a full understanding of the key factors and processes for sustainable adaptive management is far to be reached. The investigation of existing, successful range management systems by simulation models may help to derive general understanding and basic principles.

The semi-nomadic Ova-Himba in northern Namibia have applied till the mid-nineties of last century a sophisticated management system which combined season-dependent pasture use (resulting in rainy season pastures and dry season pastures), preservation of reserves for drought and sanctions for rule breaking. A stochastic ecological simulation model is constructed which represents the main aspects of this management system. With this model we analyse (i) which components of the traditional Ova-Himba strategy are essential for sustainability and (ii) what happens to the state of the rangeland system under socio-economic changes.

The study shows that temporally and spatially heterogeneous pasture use yields higher productivity and quality of a pasture area than a homogeneous, permanent grazing pressure. Two aspects are of importance: (a) intra-annual heterogeneous use: resting of the dry season pastures during the rainy season and (b) inter-annual heterogeneous use: spatial extension of grazing in years of drought. This management system leads to an effective build up and use of a buffer in the system – the reserve biomass (the non-photosynthetic reserve organs of the plants), an indicator for grazing and management history.

Analysing exemplarily purchase as one form of socio-economic changes, we demonstrate that relieved market access to purchase livestock may lead to a decline in vegetation quality. However, cattle production increases as long as resting on parts of the pasture during the rainy season is granted.

Methodically, we underline that simulation models offer an excellent framework to analyse and depict basic principles in sustainable range management derived from indigenous knowledge. They offer the opportunity to test whether these basic principles are also valid under different ecological and socio-economic settings.

Modified model description written by: **Birgit Müller**

Notes: Here a model is described that is not individual-based. It is noteworthy that the ODD protocol nevertheless can be used, although some of the Design concepts do not apply.

Purpose

The model was developed to analyse the ecological and economic implications of the traditional range management practised by the pastoral-nomadic Ova-Himba. In particular,

we ask which components of the traditional management regime are essential for sustainability and should be maintained under changing socio-economic circumstances.

Structure and scales

The model is based on central rules of the traditional range management and on ecological consequences of cattle grazing for pasture productivity. The pasture utilised by the user group of the village Omuramba in north-western Kunene Region with an area of 40x40km is modelled. The area under investigation is represented by a grid of 6400 cells with a cell size of 25 ha.

A habitat cell is characterised by its soil type and vegetation state (Table 1). Three soil types are distinguished: (1) “deep soil”, (2) “shallow soil” and (3) “unsuitable soil”. For the grass layer vegetation, two functional components are distinguished: firstly annual grasses and forbs, and secondly perennial grasses. Both annual and perennial grasses are therefore characterized (1) by the amount of palatable “green biomass” produced within a particular vegetation period, which serves as forage for livestock and the perennials by (2) the reserve biomass (termed after {Noy-Meir, 1982 NOYMEIR1982 /id}). This characteristic is measured via the ground cover of perennial grasses and represents vegetation vitality and hence the rain and grazing management history ({O'Connor, 1991 OCONNOR1991 /id}). And finally both plant functional types have (3) a status of the soil seed bank for each grid cell. Seed bank could also be seen as a part of the reserve biomass.

The livestock is modelled as herd and characterized by its size.

Table 1. Full set of state variables in the model

		Name of variable		Units
Habitat		Soil type of cell i	st_i	three types (deep, shallow, unsuitable)
Precipitation		Amount per year	$r(t)$	4 classes
Vegetation	Grass layer (1): Fodder production	Green biomass per cell i	$b_i^{per}(t)$ $b_i^{ann}(t)$	t/ha
	Grass layer (2): Reserve biomass of perennial grasses	Perennial ground cover per cell i	$c_i(t)$	4 classes [%]
	Grass layer (3): Status of seed bank	Depletion level of soil seed bank per cell i	$sb_i^{per}(t)$ $sb_i^{ann}(t)$	0,1,..., sl_{per} 0,1,..., sl_{ann}
Pasture (4 types)		Available biomass for livestock	$b_{av}^{past}(t)$	t
		Required biomass for livestock	$b_{req}^{past}(t)$	t
		Grazing pressure	$gp^{past}(t)$	5 classes
Management		Traditional Strategy/ Alternative Strategy	T, A1, A2, A3	4 types
		Purchase	no, P ₁ , P ₂	3 types
Livestock		Number	$n(t)$	number in TLU

	Purchased number of animals	$n_{purch}(t)$	number in TLU
--	-----------------------------	----------------	---------------

Notes: For the specification of the alternative strategies and the purchase strategies, it is referred to the submodels section
Abbreviations: “ann” – Annual grasses and forbs, “per” – perennial grasses, TLU – Tropical Livestock Unit

The grazing management strategy maintained during the whole modelled time span is indicated by two components: (1) by the time of pasture use (all year round; only in dry season; no use) and (2) to which extent purchase of livestock is allowed.

Pastures are characterised by a fixed proportion of habitat cells with a similar soil type. In this spatially implicit model, the location of the cell on the grid is not considered. In each cell of one pasture the same grazing strategy is applied. Four pasture types are differentiated: “rainy season pasture” (RSP), “dry season pasture” (DSP), “reserve for drought” (RFD) and “area unsuitable for grazing” (UFG). One time step represents one year, starting in November with the onset of the rainy season. In reality the presented traditional grazing strategy was only applied up to 40 years. Hence it can not be judged, whether this strategy was sustainable. The modelled time span was chosen to be longer than the planning horizon of the pastoralists and at a scale, where grazing impacts on the vegetation are visible. Hence 100 years after beginning of grazing are modelled.

Process overview and scheduling

In this paragraph the processes of the model are shortly specified to allow a general overview of the model and the dynamics. For a detailed description of each of the processes, see section “Submodels”. The processes are presented according to their sequence proceeding within one time step. For the causal relations between the processes, see also Figure 2.

Process 1: Rainfall

The precipitation of a rainy season is randomly chosen according to the underlying rainfall distribution.

Process 2: Production of green biomass (= usable forage)

The green biomass of both functional types of the grass layer (annual and perennial grasses) is determined by three factors: precipitation, soil type, and in case of perennials its previous ground cover (cf. Figure 1.). Firstly biomass growth of perennial grasses is modelled. Annual grasses produce biomass according to the space left by perennial grass tufts, and according to precipitation and seed bank status.

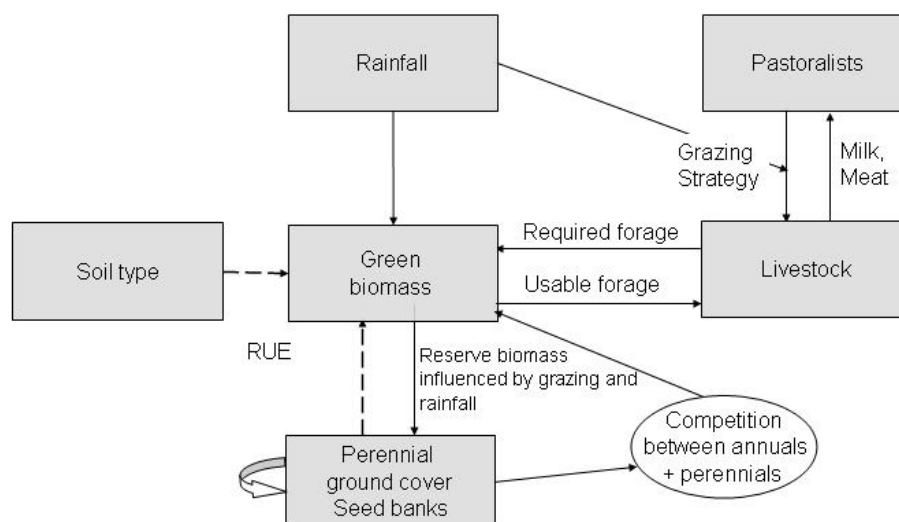


Figure 1. Causal diagram indicating the influential factors on vegetation and livestock dynamics in the model (RUE=Rain Use Efficiency)

Process 3: Livestock demographics

Livestock demographics in dependence of the availability of usable forage and the grazing strategy are modelled: A constant birth rate is assumed. The ratio between available and required biomass determines the grazing pressure. If available biomass is insufficient on a pasture the next pastures are used earlier. If the total available forage is insufficient animals die/ are sold / are swapped to other herds with a certain rate.

Process 4: Feedback of grazing and rainfall on perennial ground cover (reserve biomass)

At the end of a time step the perennial ground cover (representing the reserve biomass) is adjusted. The perennial ground cover depends on (1) current rainfall, (2) grazing pressure, (3) time of grazing (in dry season or all year round) and (4) on perennial ground cover of the previous year. Finally the degree of seed bank depletion per cell is adjusted in dependence of precipitation and the probability of seed entry.

Initialization

The proportion of the pasture types with different soil properties correspond to the pastures of the households of the village Omuramba: rainy season pasture 10%, dry season pasture 45 %, reserves for drought 18% and the rest 27% is unsuitable to grazing. Rainy season pasture (RSP) consists of cells with “deep soil”. Dry season pastures (DSP), reserves for drought (RFD) and area unsuitable for grazing (UFG) consist of cells with “shallow soil”.

The perennial ground cover of all cells was set to “middle”. In order to minimise the effect of initial conditions forty years without grazing are simulated, before livestock number is initialised according to the available forage.

Submodels

Rainfall

The highly stochastic precipitation is modelled using four classes, with r_{mean} indicating the long-term mean of the annual rainfall. As no sufficient data are available on Omuramba the frequency distribution of the relative deviations are taken from Ombulantu, a site 200 km east.

The mean annual rainfall of Omuramba is about 280mm/a. As rain value associated to each class the mid-point of the class (Table 2, column 4) is used.

Table 2. Rainfall classes used in the model and underlying frequency distribution of rainfall derived from the data set of Ombalantu. Classification based on unpublished data from the Weather Bureau Windhoek, Namibia. For an optical presentation of rain frequency distributions in the Kunene Region, see {Sander, 2002 SANDER2002 /id}, p. 63

Class		Range	Rain values	Frequency
-2	Drought	$r(t) < 0.5 * r_{mean}$	$0.25 * r_{mean}$	12 %
-1	Below average	$0.5 * r_{mean} \leq r(t) < 0.75 * r_{mean}$	$0.625 * r_{mean}$	16 %
0	Average	$0.75 * r_{mean} \leq r(t) < 1.25 * r_{mean}$	r_{mean}	43 %
1	Above average	$1.25 * r_{mean} \leq r(t)$	$1.375 * r_{mean}$	29 %

Growth of green biomass

As simplest case, a linear relationship between biomass and precipitation is assumed with intercept equals zero ({Lauenroth, 1992 LAUENROTH1992 /id}, {O'Connor, 2001 OCONNOR2001 /id}). The slope of this function represents the Rain-Use-Efficiency (RUE). In our model, the parameter depends on habitat type (deep vs. shallow soil) and for perennial grasses on the reserve biomass of the plants represented by ground cover $c(t)$ (see Table 3). The values for annual grasses are based on empirical data of *Schmidtia kalahariensis* (A. Linstädter *unpublished data*). For perennial grasses expert knowledge and specifications found in the literature are used ({Le Houérou, 1988 LEHOUEROU1988 /id}, p.1, {Le Houérou, 1984 LEHOUEROU1984 /id}, p.221). The used classification of perennial cover $c(t)$ depends on the soil type (Table 4).

Table 3. Rain use efficiencies RUE [t/(ha*mm)] for perennial and annual grasses in dependence of soil type and ground cover $c(t)$ in time step t (in case of perennials)

	Perennials				Annals
	$c(t) = 0$	$c(t) = 1$	$c(t) = 2$	$c(t) = 3$	
deep	0	3	4	4.8	2.78
shallow	0	1.5	2	2.4	1.35

Table 4. Classification of perennial ground cover $c(t)$ [%] for deep and shallow soils. For shallow soil the perennial ground cover is assumed to be half of the ranges of deep soil. A perennial ground cover higher than 90 % does not occur under natural circumstances.

Class		$c(t) = 0$	$c(t) = 1$	$c(t) = 2$	$c(t) = 3$
		no	low	middle	high
Perennial ground cover [%]	deep soil	0	1-30	31-60	61-90
	shallow soil	0	1-15	16-30	31-45

It is assumed that no green biomass is taken over from the previous year, by doing so natural decay is included implicitly in the model.

The biomass of perennials at time t is calculated by

$$b_i^{per}(t) = RUE(st_i, c_i(t)) * r(t)$$

and the biomass of annuals at time t by

$$b_i^{ann}(t) = RUE(st_i) * r(t)$$

for all cells i , $i=1, \dots, 1600$. $c_i(t)$ indicates the current perennial ground cover on i and st_i the soil type.

The interspecific competition between annual and perennial grasses is modelled implicitly. It is assumed that perennial grasses outcompete the annuals, since they occupy the available place first. Hence annuals may only occupy the space left. We assume that green biomass has an upper limit due to restricted abiotic resources such as water, nutrients, and sunlight. If the sum of annual and perennial grass biomass exceeds this limit, the biomass of the annuals is correspondingly diminished. The limit is assumed to be $cap_{dp} = 1.5$ t/ha on deep soil and $cap_{sh} = 1$ t/ha on shallow soil ({Schulte, 2002 SCHULTE2002 /id}).

For annuals holds, if the seed bank is empty on a grid cell, no green biomass is produced.

Only a portion of the whole green biomass serves as forage. The causes are: grazing efficiency (the proportion of total herbage livestock can harvest) and forage loss (due to trampling, decomposition, etc.). Mostly in literature the proper use factor pf is used to cover all three aspects. Different values for pf are proposed: 0.45 {de Leeuw, 1993 DELEEUEW1993A /id}, 0.25-0.3 {Guevara, 1996 GUEVARA1996 /id}, p. 350, 0.5 {Le Hou  rou, 1984 LEHOUE  ROU1984 /id} p. 233 and 0.25-0.3 - {Le Hou  rou, 1989 LEHOUE  ROU1989 /id} p. 110). We use firstly $pf_{per} = pf_{ann} = 0.45$ in the model, not distinguishing between annuals and perennials. However in a later part of the study the influence of different grazing values for annuals and perennials on the assessment of the grazing strategies is investigated carrying out a sensitivity analysis.

In a next step, the available palatable biomass - $b_{av}^{past}(t)$, $past=RSP, DSP, RFD$ - is calculated by summing up the biomass of annuals b_i^{ann} and perennials b_i^{per} on all cells i belong to pasture $past$:

$$b_{av}^{past}(t) = \sum_{i \in past} b_i^{per} * pf_{per} + b_i^{ann} * pf_{ann}.$$

Demographics of livestock

Only cattle demographics are included in the model analysis. Calving rates are 0.4 per year and cow ({Bollig, 2000 BOLLIG2000B /id}). Since just under 50 percent of the livestock are females, a total constant cattle growth rate of $g_c=0.2$ is used ({Bollig, 1999 BOLLIG1999A /id}). A decrease of livestock numbers is caused either by drought-induced mortality, by the consumption of meat or by renting to relatives. All these processes are summarized and modelled by a constant mortality rate $prob_{mort}$. For a detailed description under which circumstances mortality takes place in the model, it is referred to the next section.

Movement and grazing of livestock

The grazing strategy applied from 1960-1995 (traditional strategy) is compared to three alternative strategies. The three alternative strategies are constructed in such a ways that in each case a certain aspect of the traditional strategy is altered. Hence let us look first at the

Characteristics of the traditional strategy T:

1. **Seasonal Resting on Dry Season Pastures (DSP)** (including its division in three parts (DSP1, DSP2, DSP3))
 - Use of RSP by the whole herd in the rainy season, by lactating animals in the dry season (portion of lactating animals: $p_l = 0.2$ of the herd ({Bollig, 1999 BOLLIG1999A /id}, p. 85))
 - Resting of dry season pastures DSP in rainy season, grazing in dry season by non-lactating animals (If the forage is insufficient on RSP, then DSP1 is used already in the rainy season)
2. **Spatial extension**, with respect to two different aspects
 - a. Use of dry season pastures DSP2, DSP3 only if DSP 1 (DSP2 respectively) is used up, otherwise these pastures are rested the whole year
 - b. Reserves for drought RFD are used only if all DSP are used up, otherwise they are rested the whole year

Applying alternative strategies (A1), (A2) seasonal resting for DSP is dropped and both pastures (rainy and dry season pastures) are used all year round. Reserves for drought are granted with (A1), but not with (A2). Alternative strategy (A3) maintains seasonal resting of DSP and RFD, but involves a complete utilisation of the total pasture in each year (cf. Table 5 for a short overview of the 4 strategies).

Table 5. Overview about the four compared strategies (T, A1, A2, A3)

		Traditional Strategy	Alternative Strategies		
		T	A1	A2	A3
1. Seasonal Resting		yes	No	no	yes
2. Spatial extension	a) DSP	yes	No	no	no
	b) RFD	yes	Yes	no	no

The explicit translation of these different management strategies in model rules is made by some intermediate steps. Brief description before detailed outline: Firstly for each pasture its required biomass $b_{req}^{past}(t)$, is calculated (i). Here the specific grazing strategy comes into play.

Afterwards the grazing pressure $gp^{past}(t)$ per pasture can be calculated straightforward (ii). If grazing pressure it too high a certain action is undertaken (

Table 6).

Table 6. For each pasture it is indicated which action is undertaken, if the available biomass is insufficient and hence the quotient of available and required biomass does not a reach threshold.

Biomass insufficient on	Action
Rainy season pasture	Early Movement to DSP1

Dry season pasture 1 (DSP1)	Use of DSP2
Dry season pasture 2 (DSP2)	Use of DSP3
Dry season pasture 3 (DSP3)	Use of Reserve of Drought
Reserves for drought	Dying/Sale/Renting of Livestock

In detail: Ad i) The **required biomass per pasture** $b_{req}^{past}(t)$ is determined by livestock number $n(t)$, amount of dry matter d , in tonnes, per TLU and year and the pasture proportion of total required biomass, $pp_{req}^{past}(t)$:

$$b_{req}^{past}(t) = d * pp_{req}^{past}(t) * n(t), \quad \text{past} = \text{RSP, DSP1, DSP2, DSP3, RFD}$$

The amount of dry matter d required to maintain the diet and to produce milk for one TLU per year depends on different factors (for instance on nutritive value of the forage during the seasons, and on animal race). We assumed a constant requirement of $d=2.5$ t for one TLU per year (cf. 2.3-2.7t/a {de Leeuw, 1993 DELEEUEW1993A /id}, p.78, 2.3t/a - {Guevara, 1996 GUEVARA1996 /id}).

The proportion per pasture of total required biomass, $pp_{req}^{past}(t)$ depends for the two strategies which include seasonal resting (T, A3) on the length of the rainy season (4 months, cf. {Bollig, 2002 BOLLIG2002C /id}). For the two strategies with continuous resting (A1, A2), the proportion depends on the amount of required biomass on the considered pasture in relation to total required biomass ($d * n(t)$) (see Table 7 for details).

Table 7. Formula to calculate the portion of fodder required $pp_{req}^{past}(t)$ for each pasture (past=RSP, DSP1, DSP2, DSP3, RFD) and each grazing strategy (T-traditional, A1, A2, A3 alternatives), p_l indicates the portion of lactating animals, $b_{av}^{past}(t)$ the biomass available on the pasture at time step t .

	T	A1	A2	A3
$pp_{req}^{RSP}(t)$	$4/12 \cdot (1 - p_l(t)) + p_l(t)$	$\frac{b_{av}^{RSP}(t)}{b_{av}^{RSP}(t) + b_{av}^{DSP}(t)}$	$\frac{b_{av}^{RSP}(t)}{b_{av}^{RSP}(t) + b_{av}^{DSP}(t) + b_{av}^{RFD}(t)}$	$4/12 \cdot (1 - p_l(t)) + p_l(t)$
$pp_{req}^{DSP1}(t)$	$8/12 \cdot (1 - p_l(t))$	$\frac{b_{av}^{DSP}(t)}{b_{av}^{RSP}(t) + b_{av}^{DSP}(t)} / 3$	$\frac{b_{av}^{DSP}(t)}{b_{av}^{RSP}(t) + b_{av}^{DSP}(t) + b_{av}^{RFD}(t)} / 3$	$\frac{b_{av}^{DSP}(t)}{b_{av}^{DSP}(t) + b_{av}^{RFD}(t)} / 3 \cdot 8/12 \cdot (1 - p_l(t))$
$pp_{req}^{DSP2}(t)$	0	$\frac{b_{av}^{DSP}(t)}{b_{av}^{RSP}(t) + b_{av}^{DSP}(t)} / 3$	$\frac{b_{av}^{DSP}(t)}{b_{av}^{RSP}(t) + b_{av}^{DSP}(t) + b_{av}^{RFD}(t)} / 3$	$\frac{b_{av}^{DSP}(t)}{b_{av}^{DSP}(t) + b_{av}^{RFD}(t)} / 3 \cdot 8/12 \cdot (1 - p_l(t))$
$pp_{req}^{DSP3}(t)$	0	$\frac{b_{av}^{DSP}(t)}{b_{av}^{RSP}(t) + b_{av}^{DSP}(t)} / 3$	$\frac{b_{av}^{DSP}(t)}{b_{av}^{RSP}(t) + b_{av}^{DSP}(t) + b_{av}^{RFD}(t)} / 3$	$\frac{b_{av}^{DSP}(t)}{b_{av}^{DSP}(t) + b_{av}^{RFD}(t)} / 3 \cdot 8/12 \cdot (1 - p_l(t))$
$pp_{req}^{RFD}(t)$	0	0	$\frac{b_{av}^{RFD}(t)}{b_{av}^{RSP}(t) + b_{av}^{DSP}(t) + b_{av}^{RFD}(t)}$	$\frac{b_{av}^{RFD}(t)}{b_{av}^{DSP}(t) + b_{av}^{RFD}(t)} \cdot 8/12 \cdot (1 - p_l(t))$

Ad ii) The **grazing pressure** $gp^{past}(t)$ depends on how much biomass is available, $b_{av}^{past}(t)$, compared to the required biomass $b_{req}^{past}(t)$. Hence, the ratio of both factors is calculated and compared to a threshold th_1 (this procedure is applied in the same way independent of the strategy).

Three cases may occur:

$$(1) \quad gp^{past}(t) = \text{“heavy”}, \quad \text{if } \frac{b_{av}^{past}(t)}{b_{req}^{past}(t)} \leq th_1$$

$$(2) \quad gp^{past}(t) = \text{“moderate”}, \quad \text{if } \frac{b_{av}^{past}(t)}{b_{req}^{past}(t)} > th_1$$

$$(3) \quad gp^{past}(t) = \text{“no”}, \quad \text{if } b_{req}^{past}(t) = 0$$

In order to decide when the biomass on a pasture is insufficient and the cattle herd has to move to the next pasture, a second threshold th_2 , $th_2 < th_1$, is defined. Hence, if the ratio between available and required biomass falls below this threshold th_2 , an action is undertaken (cf.

Table 6). In reality the level of milk production is used as an indicator. If too less milk is gained per cow a new grazing area is looked for.

The required biomass on the next pasture is newly calculated by adding the amount of forage missing on the previous pasture. If the herd is already on the reserves for drought, a certain portion $prob_{mort}=0.8$ of the herd is assumed to die (or, seen equivalently, to be sold or to be rented). That implies that a portion $(1 - prob_{mort})$ of the cattle herd is able to cope with shortages of forage by other means (e.g. browsing seeds and leaves of trees and using fat reserves).

The status variable grazing pressure is determined, apart from strength of grazing, by the time of grazing: If a pasture is used already in the rainy season the status of grazing pressure is set to “grazing in rainy and dry season”. This holds, even if the time span the pasture is used during the rainy season is short. If the pasture is grazed exclusively in the dry season the status of grazing pressure is set to “grazing only in dry season”. Hence combined with the strength of grazing, $gp^{past}(t)$ may take five values: (1) “no grazing pressure”, (2) “moderate (only in dry season)”, (3) “heavy (only in dry season)”, (4) “moderate (rainy + dry season)”, (5) “heavy (rainy + dry season)”.

Alternative scenarios are modelled, where purchase of livestock is part of the management strategy.

Two **purchase strategies** are compared:

(P₁) Purchase, but without using the reserves for drought.

(P₂) Purchase, with using the reserves for drought.

The number of animals purchased is determined according to the following rule: Animals are purchased as long as the mean pressure on the whole territory stays moderate. That means that the purchase of animals $n_{purch}(t)$ is carried out as long as ratio of total available and total

required biomass is higher than threshold th_l . For strategy (P_1) the total biomass without RFD is used, for (P_2) the total biomass with RFD.

Long term condition of perennials

The ground cover of the perennial grasses $c(t)$ depends on four factors: (1) current precipitation, (2) grazing pressure, (3) time of grazing (only in dry season or all year round) and (4) perennial ground cover of the previous year $c(t-1)$ (cf. Figure 1.).

In Table 8 the dynamics of perennial ground cover in dependence on these four factors is listed. They are assumed to be the same for deep and shallow soil. The values originate from either empirical investigation (A. Linstädter *unpublished data*) or from expert knowledge.

Seed bank dynamics

We assume that the seed bank of perennials decrease either by germination or by natural decay of seeds. Replenishment from inside the habitat cell i can only take place if the perennial ground cover $c(t)$ in cell i is not zero. If $c(t)$ is zero, a counter, reflecting the depletion of the seed bank in cell i , is incremented by one. If the counter passes a certain threshold sl_{per} , the seed bank of the cell is assumed to be empty. Only if the seed bank is not empty (counter $< sl_{per}$) and rainfall high enough, the perennial ground cover may rise from class 0 to class 1, if (cf. Table 8). In this case the seed bank is assumed to be refilled and the counter is reset to zero.

Table 8. Adjustment of perennial ground cover $c(t)$ for each cell at time t in dependence on previous ground cover states (0,1,2,3) $c(t-1)$, current precipitation, grazing pressure (including time of grazing). Five types of grazing pressures are differentiated (no grazing (1); grazing the whole year: moderate (2) / heavy (3); grazing only during dry season moderate (4)/ heavy (5))

		Grazing pressure (grazing in rainy season+ dry season)											
		No				Moderate				Heavy			
Previous ground cover $c(t-1)$		0	1	2	3	0	1	2	3	0	1	2	3
Precipitation	Drought	0	0	1	2	0	0	0	1	0	0	0	0
	Below average	0	1	2	3	0	0	1	1	0	0	0	0
	Average	1	1	2	3	0	0	1	1	0	0	1	1
	Above average	1	2	3	3	1	1	2	2	0	1	1	1
		Grazing pressure (grazing only in dry season)											
		No				Moderate				Heavy			
Previous ground cover $c(t-1)$		0	1	2	3	0	1	2	3	0	1	2	3
Precipitation	Drought	0	0	1	2	0	0	1	2	0	0	0	1
	Below average	0	1	2	3	0	0	1	2	0	0	1	1
	Average	1	1	2	3	0	1	2	3	0	1	1	2
	Above average	1	2	3	3	1	2	2	3	1	1	2	3

The dynamics of the seed bank of the annuals is modelled in a corresponding manner. But here holds that only under high grazing pressure and low rainfall at the same time, the seed

bank decreases. However already one year with at least average rainfall or only “moderate” grazing pressure resets the counter to zero. Here again, if the counter passes a certain threshold sl_{ann} , the seed bank is assumed to be empty for that cell.

Recolonisation of prior empty cells is modelled in a very simple manner. Whenever one cell exists somewhere on the grid, where the perennials /annuals are not extinct, each empty cell may be recolonised with a certain probability $prob_{per}^{entry}$, $prob_{ann}^{entry}$ for both plant functional types respectively in years with at least average rainfall.

Parameter set

In Table 9 the names of all parameters of the model, their values and their ranges in the sensitivity analysis are displayed.

Table 9. List of parameters, default parameter set and parameter ranges for sensitivity analysis

Parameter	Abbreviation	Value	Parameter range for sensitivity analysis
Total pasture size in km ²	s	1600	1600
Portion of RSP	a^{RSP}	0.18	0-0.55
Portion of DSP	a^{DSP}	0.37	0-0.55
Portion of RFD	a^{RFD}	0.18	0-0.55
Portion of UFG	a^{UFG}	0.27	0.27
Recolonisation probability for perennials	$prob_{per}^{entry}$	0.5	0-1
Recolonisation probability for annuals	$prob_{ann}^{entry}$	0.5	0-1
Seed bank longevity of the perennials in years	sl_{per}	10	1-10
Seed bank longevity of the annuals in years	sl_{ann}	10	1-10
Threshold 1 (respective ratio between available and required biomass)	th_1	1.5	0.5-3
Threshold 2 (respective ratio between available and required biomass)	th_2	0.9	$th_1 * 0.75$
Dry matter intake in tonnes per TLU (Tropical Livestock Unit) and year	d	2.5	1-4
Proper use factor for perennial grasses	pf_{per}	0.45	0-1
Proper use factor for annual grasses	pf_{ann}	0.45	0-1
Mean annual precipitation in mm	r_{mean}	280	280
Mortality rate of livestock	$prob_{mort}$	0.8	0.4-1
Cattle growth rate	g_c	0.2	0-1
Capacity limit of grass biomass per cell in t/ha on deep soil	cap_{dp}	2	1-4
Capacity limit of grass biomass per cell in t/ha on shallow soil	cap_{sh}	1	$cap_{dp}/2$
Portion of lactating animals	p_l	0.2	0.2

Example Epidemiology

The following model description is taken from:

Bastiansen, F. Urbi et Echi – The urban cycle of the fox tapeworm in the city of Zürich, Switzerland. PhD thesis, UFZ Leipzig-Halle (Centre of Environmental Research, Department of Ecological Modelling), in preparation.

Abstract: The model describes the urban cycle of the fox tapeworm *Echinococcus multilocularis*. This parasite has an indirect life cycle, i.e. there is more than one stage (two in this case) which develop in different hosts. Adult individuals live in the gut of the red fox (*Vulpes vulpes*) and other canids. They produce eggs that are released into the environment by the definite host's faeces. The eggs are taken up by small rodents of the family Arvicolidae (mainly *Microtus arvalis* and *Arvicola terrestris* in central Europe, mainly *A.t.* in Zürich). In the intermediate host's liver, the eggs develop to larvae and reproduce asexually. The cycle is closed by foxes feeding on infectious voles and taking up larvae this way. In the fox these develop into adult tapeworms (Eckert et al., 1996).

Humans can get infected with the eggs of *Echinococcus multilocularis* as well, leading to a chronic disease which is mostly lethal if left untreated (Stieger et al., 2002).

In recent years (since the 1980s in continental Europe, already since the 1930s in the United Kingdom) foxes invaded cities, where they occur in much higher densities than in rural areas (Harris et al., 2001). With higher numbers and lower distance to humans the public health risk increases.

This phenomenon is studied in Zürich, Switzerland, since 1996 from a parasitological and epidemiological perspective as well as regarding the spatial and behavioural ecology of the red fox. Among other things, a high prevalence of the fox tapeworm in the definite host (47% in the central urban area, 67% in the border area) and in the intermediate host *Arvicola terrestris* (up to 20% locally) was observed (Hofer et al., 2000). Due to high amounts of anthropogenic food and behavioural adaptations a high fox density is observed (10 individuals/km² compared to 1-2 individuals/km² in rural areas; Gloor et al., 2002). The population density is still rising while foxes' dread declines.

To study the spread of the fox tapeworm, an individual-based, spatially explicit ecological model is created that simulates the fox tapeworm dynamics in the city of Zürich. This way areas of high risk for humans can be identified. Additionally, future control measures can be tested to increase baiting efficiency.

Furthermore, the model is aimed at becoming a general simulation framework of the fox tapeworm cycle for usage in different urban scenarios.

Model description written by: **Finn Bastiansen**

Purpose

This is a spatially and temporally explicit, individual-based model. Its purpose is to investigate the spatial and temporal dynamics of fox tapeworm (*Echinococcus multilocularis*)

infections in an urban context. The model is grid-based, the model world represents the urban habitats in the city of Zürich. Grid cells represent the home ranges of female water voles (*Arvicola terrestris*).

The model is, where available, calibrated with field data from the city of Zürich, Switzerland. The temporal and spatial dynamics of the definite host, *Vulpes vulpes*, and the intermediate host, *Arvicola terrestris*, are simulated. The hosts are represented as individuals. The transmission dynamics of the tapeworm stages is modelled spatially explicit.

This study examines the question if we could create a model in which the epidemiological situation in Zürich - as observed in field studies - emerges from simulation of the ecological processes.

State variables and scales

Entities

Red fox (*Vulpes vulpes*):

Variable	States (if applicable)
Sex	male or female
Age	
infection state	uninfected or infected
Territoriality	territorial or floater
dispersal state	has dispersed / has not dispersed
number of protoscolices	
number of adult tapeworms	

Water vole (*Arvicola terrestris*):

Variables	States (if applicable)
Sex	male or female
Age	
infection state	uninfected or infected
time till release of next offspring	0-12 weeks
number of past reproductions	0-4
dispersal state	has dispersed / has not dispersed

Fox tapeworm (*Echinococcus multilocularis*):

E. multilocularis eggs in the environment are described by their number within a single grid cell (see the description of the grid's state variables). *E. multilocularis* infections in voles are described by the infection state of the vole individual.

Grid:

The model world is composited of grid cells representing territories of female voles. A grid cell is described by the following state variables:

Variables	States (if applicable)
habitat type	urban meadows / non-meadow urban habitat / urban

	water / rural
number of tapeworm eggs	

Fox territories:

Fox individuals live within quadratic territories. Each territory contains 0 to 5 adult foxes as well as juvenile foxes. Foxes share the territory with other individuals in respect to reproduction, hunting and defecation (see 2.1.3.2).

Variables	States (if applicable)
suitability for foxes	yes/no
consisting mainly of urban area	yes/no
consisting mainly of water	yes/no

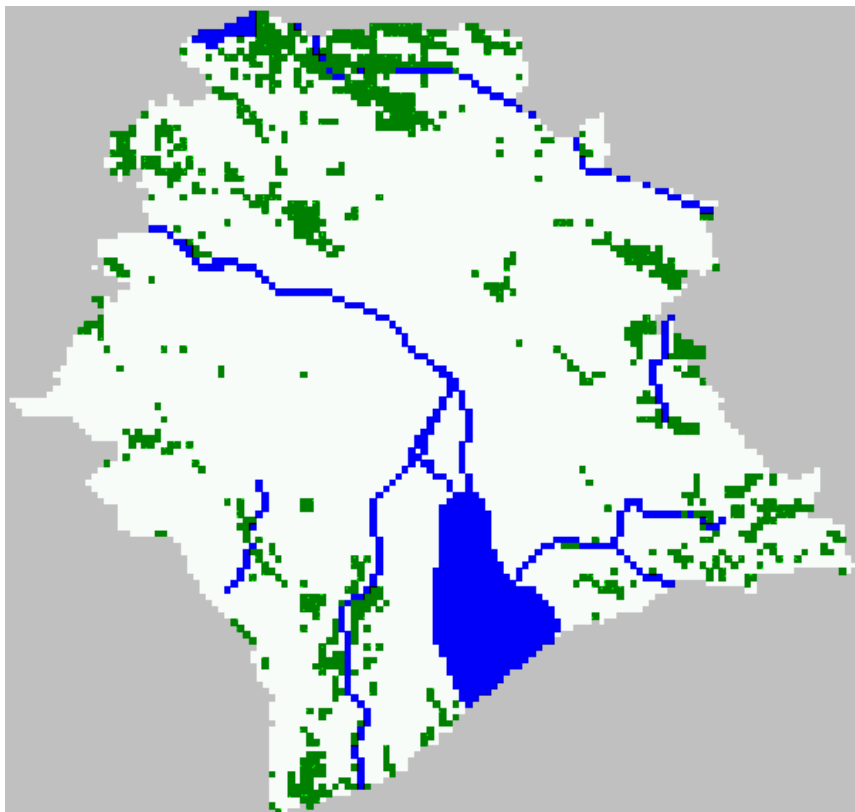


Figure 1. Model area. White: Urban area; Green: Habitats suitable for voles; Blue: Water; Grey: Rural area

System state variables:

A time step represents the period of one week.

Male voles, whose home ranges cover several female home ranges, are assumed not to spread infections over their territory. Thus the home range of a female vole is regarded as the smallest homogeneous unit and defined as the content of a single grid cell.

The size of the home range of a female *Arvicola terrestris* is 43-70 m² (Reichstein 1987). Therefore a cell of the *Arvicola* grid was defined to represent an area of 8m*8m, which equals to 0.0064 ha.

In the study site Zürich, Switzerland, a mean of 10 fox individuals per km² are found (D. Hegglin, pers. comm.); the mean size of a family group is 3.13 individuals (Gloor, 2002). Thus the average size of a fox territory in the urban area of Zürich is assumed to be 30 ha. As an *Arvicola terrestris* home range covers 0.0064 ha, this leads to a number of $(68,4)^2$ vole territories in a fox territory, which was rounded to 70*70 territories.

The model world has a range of 1120x1120 cells of the *Arvicola* grid containing ca. 55,000 vole territories and 111 fox territories. It represents the area of the city of Zürich, Switzerland. The habitat information was interpolated from a habitat map with a cell size of 1 ha.

Process overview and scheduling

In each time step foxes feed on voles, defecate and are subjected to mortality. Tapeworms in foxes age and are subjected to mortality. Feeding on infectious voles leads to infection with the fox tapeworm. Infectious foxes place tapeworm eggs in the vole cells within their territory. In spring, reproduction takes place; from September to January of the following year dispersal happens.

Voles are subjected to a season-dependent mortality and potentially get infected from tapeworm eggs in their territory. Between March and October they reproduce several times. Dispersal takes place at the age of four months (males) or in the spring of their second year (females). A density regulation function acting on territory scale kills voles independent of their state if the number exceeds the carrying capacity (1000 individuals/ha; Reichstein 1987).

Tapeworm eggs in grid cells die with a season-dependent probability.

Time is modelled in discrete time steps, representing one week. In each step, first the vole processes are carried out, followed by the fox processes and the egg mortality (which is the only process acting on grid cell scale).

Order of vole processes: Reproduction (during reproduction period); Infection; Dispersal (during dispersal period); Mortality.

Order of fox processes: Tapeworm aging and mortality, Reproduction (during reproduction period); Feeding on voles; Defecation; Dispersal(during dispersal period); Mortality.

Due to the time delay (> 1 week) from infection to infectivity in the intermediate host as well as the definite host, the order of transmission processes within a time step does not make a difference.

Design concepts

Emergence

Population dynamics emerge from the processes of reproduction, dispersal and mortality in both voles and foxes. Transmission dynamics, however, only partially emerges from the processes: The number of larvae does not depend on the time since the respective vole was infected but is drawn from an exponential distribution that was observed in field studies. Additionally, the number of eggs released by a fox with the faeces depends on the number of worms the fox carries, but the number of eggs per worm is assumed to be constant in each time step.

Stochasticity

“Noise“ is introduced into most ecological processes by including stochasticity:

Fox processes:

- Tapeworm mortality

- Reproduction (ratio of subordinate females reproducing, litter size, week of birth, offspring sex determination)
- Predation (choice of grid cell from which individual is taken)
- Dispersal (main dispersal direction, deviation from that direction, dispersal distance)
- Defecation (placement of faeces within the fox territory)
- Mortality

Vole processes:

- Reproduction (litter size, period between reproduction events, number of litters per female)
- Infection (infection probability)
- Dispersal (choice among aequidistant dispersal destinations)
- Mortality

Observation

The observations are done from an omniscient perspective (a-d) as well as from a virtual ecologist point of view (e). The following parameters are observed:

a) Abundances of voles

b) Abundance of foxes

c) Dispersal distances of foxes

d) Tapeworm prevalences in foxes, recorded separately for the city centre area and the border area of Zürich, as defined in Stieger et al. (2002)

e) Prevalences in voles, investigated following exactly the sampling regime used in the field studies (D. Hegglin., pers. comm.)

Initialization

- A habitat map with a cell size of 1 ha defines the habitat type of the grid cells. Each grid cell is initialized being free of tapeworm eggs.
- In each grid cell suitable for voles, one male and one female are placed, marked as having dispersed and being uninfected.
- Urban fox territories are filled with 3 fox individuals each, one female and one male (both marked as having dispersed) plus one more individual with random sex. That last fox is marked as not having dispersed; this individual did not leave during its first year but might disperse in the following year (“helper”). Among these three individuals, a certain ratio is already infected, the ratio depending on the particular simulation experiment.

Input

Water vole mortality and egg mortality are calculated based on average monthly temperatures from Zürich of the years 1991-2000.

Table 1. Average temperatures [°C] (based on data from 1991-2000; D. Hegglin, pers. comm.) from the city of Zürich, Switzerland

Jan	Feb	Mar	April	May	June	July	Aug	Sep	Oct	Nov	Dec
0.77	1.85	5.88	8.77	13.51	16.13	18.42	18.62	14.04	9.44	4.21	1.63

Submodels

In the following, only a short description of the submodels is given. For a full description, see Appendix [not included].

Processes determining foxes' individual fates

Tapeworm aging and mortality. – Protoscolices in foxes die with $p=0.035$. Adult (infectious) tapeworms die with $p=0.64$.

Reproduction. – Reproduction takes place once a year in April. The dominant female of a group produces a litter of 4 to 6 juveniles, 56% of the subordinate females produce offspring as well (Baker et al. 2004).

Dispersal. – Between October and the following February (White et al., 1996) 50% / 40% (males/females) of the individuals born in the current year and 60% / 1/6 (males/females) of those that hadn't dispersed in the previous year disperse, leading to an overall dispersal rate of 80% / 50% (overall rate after Harris & Baker, 2001). Males disperse within the range of 18 territories, females within the range of 6 territories (calculated after Trehwella's equation; Trehwella et al., 1988). Apart from these two parameters, the dispersal algorithm is in structure and parametrization in accordance with the one described in Eisinger et al. (2005), i.e. the probability of settlement in an evaluated territory depends on individual density and distance from the original territory.

Floater. – Individuals that do not succeed in finding a new territory during dispersal become "floaters". A floater's home range covers the area of territories of 3-11 neighbouring foxes (Gloor 2002). A floater becomes resident if there is a free space (< 5 adult foxes) in one of the territories within its home range.

Predation/Infection. – Foxes feed on 20 random individuals of the intermediate hosts from within their territory and get infected with the tapeworm larvae if the prey was infectious. The number of larvae is drawn from an exponential distribution between 0 and 244,400 based on observations from Zürich (described in Stieger et al., 2002; fig. 4 there). A fox becomes infectious in the fifth week after infection.

$$\text{numLarvae} = 10^i ; 2.0 < i < 5.388$$

Defecation/Egg release. – Foxes defecate randomly within their territory 47 to 60 times per step (Webbon et al., 2004), thereby placing tapeworm eggs within the respective grid cells if they are infectious. The number of eggs depends on the number of adult tapeworms in the fox, each of which is assumed to produce always the same number of eggs per step.

Mortality. – Adult foxes die with $p=0.011$; juvenile foxes die with $p=0.02$. Foxes are considered as juvenile until after dispersal (Eisinger et al., 2005). Additionally, the dispersing foxes die during dispersal with $p=0.22$ (Eisinger et al., 2005).

Processes determining voles' individual fates

Reproduction. – After reaching fertility at an age of 9 weeks, reproduction takes place every 6 to 12 weeks. Females can only become pregnant 4 to 5 times. Offspring is between 4 and 6 individuals. Reproduction happens between beginning of March and mid of October (Reichstein 1987).

Dispersal. – *Arvicola terrestris* individuals disperse (females in the spring of their second year, males at the age of 4 months; Macdonald et al., 1997) within an area of 500 m. Within this area, the nearest free space is occupied.

Infection. – Voles get infected with a constant probability ($p=0.4$) if the number of eggs in the grid cell is >1 . A vole becomes infectious six weeks after infection (Eckert et al., 1996).

Mortality. – Voles die with a season-dependent mortality (see 2.1.6). Mortality fluctuates between a maximum value in winter and a minimum value in summer.

M: effective mortality

$M_{\min} = 0.054$ (minimum mortality)

$M_{\max} = 0.072$ (maximum mortality)

$M = M_{\min} + (M_{\max} - M_{\min}) * ((30 - \text{Temp}) * 0.025)$

With Temp being the current temperature. This way M_{\min} is applied for a temperature of 30°C, M_{\min} is applied for -10°C, intermediate mortalities for temperatures between -10 and 30°C.

Processes acting on tapeworms eggs in grid cells

Mortality. – Eggs die with a season-dependent mortality (Veit et al. 1995).

$M = (\text{Temp}/1.5)$

For the time being this simple function gives a fair approximation of the egg viability in the field.

References

- Baker PJ, Funk SM, Bruford MW, Harris S (2004) "Polygynandry in a red fox population: implications for the evolution of group living in canids?" *Journal of Animal Behaviour* 15(5):766-778
- Eckert J (1996) "The "dangerous fox tapeworm" (*Echinococcus multilocularis*) and alveolar echinococcosis of humans in central Europe" *Berliner und Münchner Tierärztliche Wochenschrift* 109(6-7):202-210
- Eisinger D, Thulke HH, Selhorst T, Müller T (2005) "Emergency vaccination of rabies under limited resources – combating or containing?" *BMC Infectious Diseases* 5:10
- Gloor S (2002) "The Rise of Urban Foxes (*Vulpes vulpes*) in Switzerland and Ecological and Parasitological Aspects of a Fox Population in the Recently Colonised City of Zurich" PhD Thesis, University of Zürich
- Harris S, Baker PJ (2001) "Urban Foxes" Whittet Books, Suffolk
- Hofer S, Gloor S, Müller U, Mathis A, Heglin D, Deplazes P (2000) "High prevalence of *Echinococcus multilocularis* in urban red foxes (*Vulpes vulpes*) and voles (*Arvicola terrestris*) in the city of Zürich, Switzerland" *Parasitology* 120:135-142
- Macdonald DW, Mace GM, Rushton S (1997) "Proposals for Future Monitoring of British Mammals" Department of the Environment Transport and Regions, London, UK
- Reichstein H (1987) „*Arvicola terrestris* - Schermaus“ In: Niethammer J, Krapp F: „Handbuch der Säugetiere Europas, Band 2/1, Nagetiere II“, Akademische Verlagsanstalt Wiesbaden
- Stieger C, Hegglin D, Schwarzenbach G, Mathis A, Deplazes P (2002) "Spatial and temporal aspects of urban transmission of *Echinococcus multilocularis*" *Parasitology* 124:631-640
- Trehwella WJ, Harris S (1988) "A Simulation Model of the pattern of dispersal in urban fox (*Vulpes vulpes*) populations and its application for rabies control" *Journal of Applied Ecology* 25:435-450
- Veit P et al. (1995) "Influence of environmental factors on the infectivity of *Echinococcus multilocularis* eggs" *Parasitology* 110:79-86
- Webbon C, Baker PJ, Harris S (2004) "Faecal density counts for monitoring changes in red fox numbers in rural Britain" *Journal of Applied Ecology* 41:768-779
- White PCL, Saunders G, Harris S (1996) "Spatio-temporal patterns of home range use by foxes (*Vulpes vulpes*) in urban environments" *Journal of Animal Ecology* 65(1):121-125

Example Lesser Spotted Woodpecker

The original model description, including the full references, is in:

Rossmannith, E. (2005) Breeding biology, mating system and population dynamics of the Lesser Spotted Woodpecker (*Picoides minor*): combining empirical and model investigations. PhD thesis, University of Potsdam, Germany.

and in:

Rossmannith E, Grimm V, Blaum N, Jeltsch F (2006) Behavioural flexibility in the mating system buffers population persistence: lessons from the Lesser Spotted Woodpecker (*Picoides minor*). Journal of Animal Ecology 75: 540-548.

Abstract:

1. In most stochastic models addressing the persistence of small populations, environmental noise is included by imposing a synchronized effect of the environment on all individuals. However, buffer mechanisms are likely to exist which may counteract this synchronization to some degree.
2. We have studied whether the flexibility in the mating system, which has been observed in some bird species, is a potential mechanism counteracting the synchronization of environmental fluctuations. Study organism is the Lesser Spotted Woodpecker (*Picoides minor*, Linnaeus), a generally monogamous species. However, facultative polyandry, where one female mates with two males with separate nests, was observed in years with male-biased sex ratio.
3. We constructed an individual-based model, which is based on observations and data of a population in Taunus, Germany. We tested the impact of three behavioural scenarios on population persistence: (i) strict monogamy, (ii) polyandry without costs and (iii) polyandry assuming costs for polyandry in terms of lower survival and reproductive success for secondary males. We assumed that polyandry occurs only in years with male-biased sex ratio and only in females with favoured breeding conditions.
4. Even low rates of polyandry had a strong positive effect on population persistence. The increase of persistence with carrying capacity was flat in the monogamous scenario, indicating strong environmental noise. In the polyandrous scenarios, the increase of persistence was stronger, indicating a buffer mechanism. In the polyandrous scenarios, populations had a higher mean population size, a lower variation in number of individuals, and recovered faster after a population breakdown. Presuming a realistic polyandry rate and costs for polyandry, there was still a strong effect of polyandry on persistence.
5. The results show that polyandry and in general flexibility in mating systems are buffer mechanisms and can significantly reduce the impact of environmental and demographic noise in small populations. Consequently, we suggest that even behaviour that seems to be exceptional should be considered explicitly when predicting the persistence of populations.

Notes: This model contains numerous probabilistic rules, so that the “Submodels” part of the model description mainly consists of a list of rules, which are numbered consecutively.

Purpose

The purpose of the model is to assess the risk of extinction of small populations of the Lesser Spotted Woodpecker using parameter values drawn from a field study (Rossmann 2005). In particular, it aims to understand how occasional social polyandry (i.e., one female has two separate nests with two different males) affects population persistence.

State variables and scales

Individuals are characterised by the state variables age, sex, mating status (unpaired/old paired/newly paired/polyandrous paired) as well as breeding start (early/late). Moreover, the identity of its current partner and its characteristics are known to the breeding individuals. Annual time steps are considered, and the model is run for several decades or until extinction of the population. Spatial relationships are not considered.

Process overview and scheduling

Each time step begins in spring and includes the processes of mating, reproduction and deaths, which are described by ten rules in the section „Submodels“ below.

Design concepts

Emergence. – Population dynamics emerge from the behaviour of the individuals, but the individual's life cycle and behaviour is represented entirely by empirical rules describing, for example, mortality and dispersal rates as probabilities. Adaptation and fitness-seeking are thus not modelled explicitly, but are included in the empirical rules.

Sensing. – Decision making of individuals is not modelled explicitly, so no explicit assumptions about what the individuals know are made. However, implicitly we assume that the birds know the identity of their current partner and the nature of their relationship (unpaired/old paired/new paired/polyandrous paired).

Stochasticity. – All demographic and behavioural parameters are represented as probabilities, or are drawn from empirical probability distributions. This was done to include demographic noise and because the focus of the model is on population-level phenomena, not on individual behaviour *per se*. In processes that are supposed to be strongly influenced by environmental fluctuations between years (predation and survival), parameter-values were drawn from a normal distribution (truncated at 0 and 1) with given mean and standard deviation at the beginning of each time-step (Table 2).

Observation. – For each parameter set, the model was run 2000 times for 6000 time steps or until the population became extinct. For model analysis, only population-level variables were recorded, e.g. time to extinction and fraction of polyandrous females. From the distribution of extinction times, we calculated the intrinsic mean time to extinction T_m (in years) by using the “ $\ln(1-P_0)$ plot” described by Grimm & Wissel (2004). From T_m we also calculated the risk of extinction, $P_0(100)$, after 100 years. As viability criterion for the population, we here defined a $P_0(100)$ that does not exceed 5%.

Initialization

Each population was initialised with 200 individuals of random sex and age (between 1 and 6 years) and run for 15 time steps before the actual model analysis started. Earlier statistical analysis on the model proved that this time span is sufficient to exclude initialisation effects.

In simulation experiments aiming to test the effect of different carrying capacities, the size of the start population was 2/3 of the assumed carrying capacity.

Input

There is no input.

Submodels

Rule 1: If both partners from the previous breeding season are still alive, they re-establish their old pairing. With a small probability $pDivorce$, they split up and mating status becomes unpaired. Unpaired males mate with unpaired females and establish a new pair. If there is no unpaired female available, the mating opportunities of the unpaired male depend on the mating system scenario (monogamy/polygamy, see below).

Rule 2: All old pairs have an early breeding start, while new pairs have an early breeding start with the probability $pStartEarly$, otherwise their breeding start is late. The breeding start is an attribute that influences the number of fledglings (see rule 6).

Rule 3: The probability of failing because eggs do not hatch is $pFailure$. Additionally, mechanisms described in rule 4 and 5 can cause failure in reproduction.

Rule 4: Nest predation occurs with the probability $pPredation$ and results in the death of all nestlings.

Rule 5: When an individual dies (probabilities to survive $pSurvBreed_{male}$ and $pSurvBreed_{female}$), its brood fails and its mate remains unpaired until the next breeding time.

Rule 6: In successful nests – i.e. when eggs have hatched, parents have survived the breeding season and no predation has occurred – nestlings fledge. The probabilities for a certain number of fledglings were chosen according to empirically observed distributions of brood sizes in the field; these probabilities were distinguished between broods of early and late pairs (Table 2). Based on the observed sex ratio of fledglings in the field, the probability for a fledgling to be male is $pYoungMale$, otherwise it is a female.

Rule 7: Fledglings have a certain probability of surviving ($pSurvWinter_{juvenile}$) the time between fledging and first breeding time.

Rule 8: There is a maximum number of territories, i.e. a maximum number of individuals that can exist in the area, given in the parameter carrying capacity. Only if the number of birds is below the carrying capacity can fledglings stay in the area, otherwise they emigrate. Since adult birds do not emigrate, an occupied territory only becomes available when an individual dies.

Rule 9: If an individual exceeds maximum age (=10 years), it dies. Otherwise it has the probability of $pSurvWinter_{male}$ and $pSurvWinter_{female}$ to survive winter.

Rule 10: At the end of the simulation year, the age of all individuals is updated.

Except for pre-breeding survival and its annual variation ($pSurvWinter_{juvenile} + \text{s.d.}$), all parameter values were derived from data collected in our field study (Table 2). Pre-breeding survival was estimated by pattern-oriented parameterisation (Wiegand *et al.* 2004) using the model presented here, i.e. the model was simultaneously fitted to a set of four empirically observed patterns (adult sex ratio, ratio of old and new pairs, proportion of nest producing at least one fledgling, number of fledglings per successful nest, see Rossmanith 2005).

Table 2. Default parameter set of the woodpecker model. Quality of the parameters: values based on empirical investigations with large (++) and small (+) sample sizes, parameter estimation by pattern-oriented modelling (+/-) and assumptions (-). A sensitivity analysis was conducted for the monogamous (mono) and the high cost polyandrous (poly) scenario (after Rossmanith, 2005). As all stochastic parameters are dimensionless probabilities, we do not provide a column for dimensions

Stochastic parameters	Value	Quality	Sensitivity		Description: Probability...
			mono	poly	
pDivorce	0.03	+	<1	-1	for old pairs to split up
pStartEarly	0.46	+	3	3	for new pairs to start early
pFailure	0.03	++	-2	-1	to fail in reproduction
pPredation	0.16	++	-6	5	to lose brood to predators
(\pm s.d.)	± 0.02	+	-4	6	
pSurvBreed _{male}	0.969	++	-3	-3	to survive during breeding time
pSurvBreed _{female}	0.966	++	-3	<1	
p(x)Fledg _{early pairs}	0.09 [x=2]	+	57	27	for successful pairs with early breeding start to produce x fledglings
	0.33 [x=3]				
	0.33 [x=4]				
	0.25 [x=5]				
p(x)Fledg _{late pairs}	0.20 [x=1]	+	16	14	for successful pairs with late breeding start to produce x fledglings
	0.20 [x=2]				
	0.40 [x=3]				
	0.00 [x=4]				
	0.20 [x=5]				
pYoungMale	0.54	++	8	28	for young to become male
pSurvWinter _{male}	0.582	+	-62	-97	to survive during non-breeding season
(\pm s.d.)	± 0.060	+	<1	-3	
pSurvWinter _{female}	0.621	+	-7	-4	
(\pm s.d.)	± 0.207	+	-6	-6	
pSurvWinter _{juvenile}	0.50	+/-	-49	-54	to survive before first breeding
(\pm s.d.)	± 0.03	-	<1	-1	
Parameters for polyandrous broods					
pFailure	0.15	-		<1	for secondary broods to fail because eggs do not hatch
pSurvBreed	0.845	-		-4	for secondary males to survive during breeding time
p(2)Fledg	1.0	-		1	for successful secondary males to produce x fledglings
pPolyandry	Varied between 0 and 1	-		<1	for unpaired male and early breeding, paired female to mate
Other parameters					
Capacity	250		6		Max. number of territories

StartSize	200	<1	Number of individuals at initialization
MaxAge	10	<1	Maximum age [years]